DEPARTMENT OF PHYSICS
UNIVERSITY OF JYVÄSKYLÄ
RESEARCH REPORT No. 4/2010

Shape evolution in even-even N≤126, Z≥82 nuclei

by

Panu Rahkila

Academic Dissertation
for the Degree of
Doctor of Philosophy

To be presented, by permission of the
Faculty of Mathematics and Science
of the University of Jyväskylä,
for public examination in Auditorium FYS-1 of the
University of Jyväskylä on April 30, 2010
at 12 o'clock noon

Jyväskylä, Finland
April 2010

Abstract

Rahkila, Panu
Shape evolution in even-even N≤126, Z≥82 nuclei
Jyväskylä: University of Jyväskylä, 2010, 111 p.
Department of Physics Research Report No. 4/2010
ISSN: 0075-465X; 4/2010
ISBN: 978-951-39-3857-4 (paper version)
ISBN: 978-951-39-3858-1 (electronic version)
Diss.

The shape evolution in the neutron-deficient lead, polonium and radium nuclei has been investigated via in-beam and delayed γ-ray and conversion electron spectroscopy. The lead isotope ^{180}Pb is found to still exhibit prolate excited structure, related to the known intruder structures in the heavier isotopes. The production cross-section of ^{180}Pb was only 10 nb, one of the lowest ever employed in an in-beam experiment. A candidate for an excited prolate band was found in ^{192}Po, making it the first polonium isotope for which both oblate and prolate rotational bands have been established. Contrary to the previous results, the current experiments indicate that the onset of deformation in the radium isotopic chain seems not to take place yet in ^{206}Ra. Based on the very similar decay patterns obtained in several in-beam experiments on the neutron-deficient nuclei in the region and on the statistical limits of detection, three possible further cases for experiments are proposed. Methods developed for the data analysis, specially aimed at the studies of exotic nuclei, are presented.

Keywords: Shape coexistence, Recoil Decay Tagging, Total Data Readout, Data analysis methods, Exotic nuclei

Author's address Panu Rahkila
Department of Physics
University of Jyväskylä
Finland

Supervisors Prof. Rauno Julin
Department of Physics
University of Jyväskylä
Finland

Reviewers Dr. Araceli Lopez-Martens
CSNSM Orsay
IN2P3-CNRS
France

Dr. David Cullen
Schuster Laboratory
School of Physics and Astronomy
University of Manchester
United Kingdom

Opponents Prof. Rolf-Dietmar Herzberg
Oliver Lodge Laboratory
Department of Physics
University of Liverpool
United Kingdom

Preface

This work has been carried out at the Acclerator Laboratory of the Department of Physics, University of Jyväskylä, Finland from 1996 to 2010. Financial support from the European Union, the Academy of Finland and the University of Jyväskylä is gratefully acknowledged.

The supervisor of a post-grad student, especially in a project this long, always requires a big amount of kudos. My supervisor, Professor Rauno Julin is known to be a very patient man and I have probably exploited this fact quite close to the limit. In any case, his support has always been there and, equally importantly, also the freedom to pursue time consuming off-the-beaten-track projects, which hopefully in the end have contributed to this work or at least helped others.

There are many, many people who have contributed to this work over the years. Even if it is impossible to name you all, current and past colleagues, short and long term visitors, collaborators in the experiments at Jyväskylä and abroad, I would like to thank you for the extremely valuable contributions to this work. At least the same gratitude has to be extended to all the people who skied, rowed, ran, biked, kayaked, hiked, orienteered and went to Sauna in the end. And for those who maybe had some pints afterwards. The person that needs to be thanked individually is Dr. Paul Greenlees, for peaceful coexistence in the same office space for about a decade now.

Kiitokset isälle ja äidille kaikesta. Tämän työn kannalta tärkeitä ovat olleet erityisesti oppitunnit Hellaakoskimaisessa hiihdossa jo nuorelta iältä alkaen. Ja Pyrylle kiitokset vierellähiihtämisestä.

And last, thanks to Cath for being a colleague, friend, companion, partner and soon a mother.

Panu Rahkila
Jyväskylä, April 2010

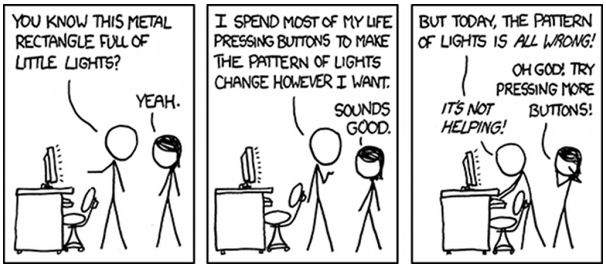

http://xkcd.com/722/

List of Publications

The contents of papers 1 and 2 are discussed in chapters 2 and 3, respectively. Methods described in chapter 2 and paper 1 have been used in the data analysis for papers 2-29, 31-37, 40-45, 47-50, 52 and 55. Papers 11, 12, 22, 25, 32, 37, 41, 50, 51, 66, 71, 78, 81, 82, 90, 92 and 94 present results on the shape evolution and shape coexistence in the even-even, Z$\geq$82, N$\leq$126 nuclei. Only peer-reviewed journal articles, excluding all conference proceedings have been listed.

1. **P. Rahkila**
   Grain–A Java data analysis system for Total Data Readout
   Nucl.Instrum.Methods Phys.Res. A **595**, 637 (2008)
   arXiv:0711.3364 [nucl-ex]
2. **P. Rahkila**, D. G. Jenkins, J. Pakarinen, C. Gray-Jones, P. T. Greenlees, U. Jakobsson, P. Jones, R. Julin, S. Juutinen, S. Ketelhut, H. Koivisto, M. Leino, P. Nieminen, M. Nyman, P. Papadakis, S. Paschalis, M. Petri, P. Peura, O. J. Roberts, T. Ropponen, P. Ruotsalainen, J. Sarén, C. Scholey, J. Sorri, A. G. Tuff, J. Uusitalo, R. Wadsworth, M. Bender and P.-H. Heenen
   Shape coexistence at the proton drip-line: First identification of excited states in ^{180}Pb
   Submitted to Phys.Rev. C.
   arXiv:1003.0452 [nucl-ex]
3. E. Ideguchi, B. Cederwall, E. Ganioğlu, B. Hadinia, K. Lagergren, T. Bäck, A. Johnson, R. Wyss, S. Eeckhaudt, T. Grahn, P. Greenlees, R. Julin, S. Juutinen, H. Kettunen, M. Leino, A. P. Leppänen, P. Nieminen, M. Nyman, J. Pakarinen, **P. Rahkila**, C. Scholey, J. Uusitalo, D. T. Joss, E. S. Paul, D. R. Wiseman, R. Wadsworth and A. V. Afanasjev
   High-spin intruder band in ^{107}In
   Phys. Rev. C **81**, 034303 (2010)
   arXiv:1002.2298 [nucl-ex]

4. P. Mason, D. Cullen, C. Scholey, A. Dewald, O. Möller, H. Iwasaki, T. Pissulla, W. Rother, J. Dare, P. Greenlees, U. Jakobsson, P. Jones, R. Julin, S. Juutinen, S. Ketelhut, M. Leino, N. Lumley, B. Niclasen, M. Nyman, P. Peura, A. Puurunen, **P. Rahkila**, P. Ruotsalainen, J. Sorri, J. Sarén, J. Uusitalo and F. Xu
Isomer-tagged differential-plunger measurements in proton-unbound ^{144}Ho
Phys.Lett. B **683**, 17 (2010)
5. P. J. R. Mason, D. M. Cullen, C. Scholey, P. T. Greenlees, U. Jakobsson, P. M. Jones, R. Julin, S. Juutinen, S. Ketelhut, M. Leino, M. Nyman, P. Peura, A. Puurunen, **P. Rahkila**, P. Ruotsalainen, J. Sorri, J. Sarén, J. Uusitalo and F. R. Xu
Spectroscopy of ^{144}Ho *using recoil-isomer tagging*
Phys. Rev. C **81**, 024302 (2010)
6. C. Scholey, K. Andgren, L. Bianco, B. Cederwall, I. G. Darby, S. Eeckhaudt, S. Ertürk, M. B. Gómez Hornillos, T. Grahn, P. T. Greenlees, B. Hadinia, E. Ideguchi, P. Jones, D. T. Joss, R. Julin, S. Juutinen, S. Ketelhut, M. Leino, A. P. Leppänen, P. Nieminen, M. Niikura, M. Nyman, D. O'Donnell, R. D. Page, J. Pakarinen, **P. Rahkila**, J. Sarén, M. Sandzelius, J. Simpson, J. Sorri, J. Thomson, J. Uusitalo and M. Venhart
Isomeric and ground-state properties of $^{171}_{78}Pt$, $^{167}_{76}Os$, *and* $^{163}_{74}W$
Phys.Rev. C **81**, 014306 (2010)
7. M. Scheck, T. Grahn, A. Petts, P. A. Butler, A. Dewald, L. P. Gaffney, M. B. Gómez Hornillos, A. Görgen, P. T. Greenlees, K. Helariutta, J. Jolie, P. Jones, R. Julin, S. Juutinen, S. Ketelhut, T. Kröll, R. Krücken, M. Leino, J. Ljungvall, P. Maierbeck, B. Melon, M. Nyman, R. D. Page, J. Pakarinen, E. S. Paul, T. Pissulla, **P. Rahkila**, J. Sarén, C. Scholey, A. Semchenkov, J. Sorri, J. Uusitalo, R. Wadsworth and M. Zielińska
Lifetimes of odd-spin yrast states in ^{182}Hg
Phys.Rev. C **81**, 014310 (2010)
8. J. Thomson, D. T. Joss, E. S. Paul, C. Scholey, J. Simpson, S. Ertürk, L. Bianco, B. Cederwall, I. G. Darby, S. Eeckhaudt, M. B. Gómez Hornillos, T. Grahn, P. T. Greenlees, B. Hadinia, P. Jones, R. Julin, S. Juutinen, S. Ketelhut, M. Leino, M. Nyman, D. O'Donnell, R. D. Page, J. Pakarinen, **P. Rahkila**, N. Rowley, M. Sandzelius, P. J. Sapple, J. Sarén, J. Sorri and J. Uusitalo
Competing quasiparticle configurations in ^{163}W
Phys.Rev. C **81**, 014307 (2010)
9. D. M. Cullen, P. J. R. Mason, S. V. Rigby, C. Scholey, S. Eeckhaudt, T. Grahn, P. T. Greenlees, U. Jakobsson, P. M. Jones, R. Julin, S. Juutinen, S. Ketelhut, A. M. Kishada, M. Leino, A. P. Leppänen, K. Mäntyniemi, P. Nieminen, M. Nyman, J. Pakarinen, P. Peura, **P. Rahkila**, J. Sarén, J. Sorri, J. Uusitalo, B. J. Varley and M. Venhart
20 μs isomeric state in doubly odd $^{134}_{61}Pm$
Phys.Rev. C **80**, 024303 (2009)

10. M. B. Gómez Hornillos, D. O'Donnell, J. Simpson, D. T. Joss, L. Bianco, B. Cederwall, T. Grahn, P. T. Greenlees, B. Hadinia, P. Jones, R. Julin, S. Juutinen, S. Ketelhut, M. Labiche, M. Leino, M. Nyman, R. D. Page, E. S. Paul, M. Petri, P. Peura, **P. Rahkila**, P. Ruotsalainen, M. Sandzelius, P. J. Sapple, J. Sarén, C. Scholey, J. Sorri, J. Thomson and J. Uusitalo
γ-ray spectroscopy approaching the limits of existence of atomic nuclei: A study of the excited states of ^{168}Pt and ^{169}Pt
Phys.Rev. C **79**, 064314 (2009)

11. T. Grahn, A. Dewald, P. T. Greenlees, U. Jakobsson, J. Jolie, P. Jones, R. Julin, S. Juutinen, S. Ketelhut, T. Kröll, R. Krücken, M. Leino, P. Maierbeck, B. Melon, M. Nyman, R. D. Page, P. Peura, T. Pissulla, **P. Rahkila**, J. Sarén, C. Scholey, J. Sorri and J. Uusitalo
Lifetime measurement in ^{195}Po
Eur.Phys.J. A **39**, 291 (2009)

12. T. Grahn, A. Dewald, P. T. Greenlees, U. Jakobsson, J. Jolie, P. Jones, R. Julin, S. Juutinen, S. Ketelhut, T. Kröll, R. Krücken, M. Leino, P. Maierbeck, B. Melon, M. Nyman, R. D. Page, P. Peura, T. Pissulla, **P. Rahkila**, J. Sarén, C. Scholey, J. Sorri, J. Uusitalo, M. Bender and P. H. Heenen
Collectivity of ^{196}Po at low spin
Phys.Rev. C **80**, 014323 (2009)

13. T. Grahn, A. Petts, M. Scheck, P. A. Butler, A. Dewald, M. B. Gómez Hornillos, P. T. Greenlees, A. Görgen, K. Helariutta, J. Jolie, P. Jones, R. Julin, S. Juutinen, S. Ketelhut, R. Krücken, T. Kröll, M. Leino, J. Ljungvall, P. Maierbeck, B. Melon, M. Nyman, R. D. Page, T. Pissulla, **P. Rahkila**, J. Sarén, C. Scholey, A. Semchenkov, J. Sorri, J. Uusitalo, R. Wadsworth and M. Zielińska
Evolution of collectivity in ^{180}Hg and ^{182}Hg
Phys.Rev. C **80**, 014324 (2009)

14. B. Hadinia, B. Cederwall, R. D. Page, M. Sandzelius, C. Scholey, K. Andgren, T. Bäck, E. Ganioğlu, M. B. Gómez Hornillos, T. Grahn, P. T. Greenlees, E. Ideguchi, U. Jakobsson, A. Johnson, P. M. Jones, R. Julin, J. Juutinen, S. Ketelhut, A. Khaplanov, M. Leino, M. Niikura, M. Nyman, I. Özgür, E. S. Paul, P. Peura, **P. Rahkila**, J. Sarén, J. Sorri, J. Uusitalo and R. Wyss
Identification of γ rays from ^{172}Au and α decays of ^{172}Au, ^{168}Ir, and ^{164}Re
Phys.Rev. C **80**, 064310 (2009)

15. S. Ketelhut, P. T. Greenlees, D. Ackermann, S. Antalic, E. Clément, I. G. Darby, O. Dorvaux, A. Drouart, S. Eeckhaudt, B. J. P. Gall, A. Görgen, T. Grahn, C. Gray-Jones, K. Hauschild, R. D. Herzberg, F. P. Heßberger, U. Jakobsson, G. D. Jones, P. Jones, R. Julin, S. Juutinen, T. L. Khoo, W. Korten, M. Leino, A. P. Leppänen, J. Ljungvall, S. Moon, M. Nyman, A. Obertelli, J. Pakarinen, E. Parr, P. Papadakis, P. Peura, J. Piot, A. Pritchard, **P. Rahkila**, D. Rostron, P. Ruotsalainen, M. Sandzelius, J. Sarén, C. Scholey, J. Sorri, A. Steer, B. Sulignano, C. Theisen, J. Uusitalo, M. Venhart, M. Zielińska, M. Bender and P. H. Heenen
γ-Ray Spectroscopy at the Limits: First Observation of Rotational Bands in ^{255}Lr
Phys.Rev.Lett. **102**, 212501 (2009)

16. P. J. R. Mason, D. M. Cullen, C. Scholey, S. Eeckhaudt, T. Grahn, P. T. Greenlees, U. Jakobsson, P. M. Jones, R. Julin, S. Juutinen, S. Ketelhut, A. M. Kishada, M. Leino, A. P. Leppänen, K. Mäntyniemi, P. Nieminen, M. Nyman, J. Pakarinen, P. Peura, **P. Rahkila**, S. V. Rigby, J. Sarén, J. Sorri, J. Uusitalo, B. J. Varley and M. Venhart
Prompt and delayed spectroscopy of ^{142}Tb using recoil-isomer tagging
Phys.Rev. C **79**, 024318 (2009)

17. D. O'Donnell, J. Simpson, C. Scholey, T. Bäck, P. T. Greenlees, U. Jakobsson, P. Jones, D. T. Joss, D. S. Judson, R. Julin, S. Juutinen, S. Ketelhut, M. Labiche, M. Leino, M. Nyman, R. D. Page, P. Peura, **P. Rahkila**, P. Ruotsalainen, M. Sandzelius, P. J. Sapple, J. Sarén, J. Thomson, J. Uusitalo and H. V. Watkins
First observation of excited states in $^{175}Hg_{95}$
Phys.Rev. C **79**, 051304 (2009)

18. D. O'Donnell, T. Grahn, D. T. Joss, J. Simpson, C. Scholey, K. Andgren, L. Bianco, B. Cederwall, D. M. Cullen, A. Dewald, E. Ganioğlu, M. B. Gómez Hornillos, P. T. Greenlees, B. Hadinia, H. Iwasaki, U. Jakobsson, J. Jolie, P. Jones, D. S. Judson, R. Julin, S. Juutinen, S. Ketelhut, M. Labiche, M. Leino, N. M. Lumley, P. J. R. Mason, O. Möller, P. Nieminen, M. Nyman, R. D. Page, J. Pakarinen, E. S. Paul, M. Petri, A. Petts, P. Peura, N. Pietralla, T. Pissulla, **P. Rahkila**, P. Ruotsalainen, M. Sandzelius, P. J. Sapple, J. Sarén, J. Sorri, J. Thomson, J. Uusitalo and H. V. Watkins
Spectroscopy of the neutron-deficient nucleus $^{167}Os_{91}$
Phys.Rev. C **79**, 064309 (2009)

19. J. Pakarinen, A. N. Andreyev, R. Julin, S. Juutinen, S. Antalic, L. Bianco, I. G. Darby, S. Eeckhaudt, T. Grahn, P. T. Greenlees, D. G. Jenkins, P. Jones, P. Joshi, H. Kettunen, M. Leino, A. P. Leppänen, P. Nieminen, M. Nyman, R. D. Page, J. Perkowski, P. M. Raddon, **P. Rahkila**, D. Rostron, J. Sarén, C. Scholey, J. Sorri, B. Streicher, J. Uusitalo, K. Van de Vel, M. Venhart, R. Wadsworth and D. R. Wiseman
Evidence for prolate structure in light Pb isotopes from in-beam γ-ray spectroscopy of ^{185}Pb
Phys.Rev. C **80**, 031303 (2009)

20. M. Sandzelius, E. Ganioğlu, B. Cederwall, B. Hadinia, K. Andgren, T. Bäck, T. Grahn, P. Greenlees, U. Jakobsson, A. Johnson, P. M. Jones, R. Julin, S. Juutinen, S. Ketelhut, A. Khaplanov, M. Leino, M. Nyman, P. Peura, **P. Rahkila**, J. Sarén, C. Scholey, J. Uusitalo and R. Wyss
First observation of excited states in ^{172}Hg
Phys.Rev. C **79**, 064315 (2009)

21. M. Sandzelius, B. Cederwall, E. Ganioğlu, J. Thomson, K. Andgren, L. Bianco, T. Bäck, S. Eeckhaudt, S. Ertürk, M. B. Gómez Hornillos, T. Grahn, P. T. Greenlees, B. Hadinia, A. Johnson, P. M. Jones, D. T. Joss, R. Julin, S. Juutinen, S. Ketelhut, A. Khaplanov, M. Leino, M. Nyman, R. D. Page, **P. Rahkila**, J. Sarén, C. Scholey, J. Simpson, J. Sorri, J. Uusitalo and R. Wyss
γ-ray spectroscopy of ^{163}Ta
Phys.Rev. C **80**, 054316 (2009)

22. K. Andgren, B. Cederwall, J. Uusitalo, A. N. Andreyev, S. J. Freeman, P. T. Greenlees, B. Hadinia, U. Jakobsson, A. Johnson, P. M. Jones, D. T. Joss, S. Juutinen, R. Julin, S. Ketelhut, A. Khaplanov, M. Leino, M. Nyman, R. D. Page, **P. Rahkila**, M. Sandzelius, P. Sapple, J. Sarén, C. Scholey, J. Simpson, J. Sorri, J. Thomson and R. Wyss
Excited states in the neutron-deficient nuclei $^{197,199,201}Rn$
Phys.Rev. C **77**, 054303 (2008)

23. K. Andgren, U. Jakobsson, B. Cederwall, J. Uusitalo, T. Bäck, S. J. Freeman, P. T. Greenlees, B. Hadinia, A. Hugues, A. Johnson, P. M. Jones, D. T. Joss, S. Juutinen, R. Julin, S. Ketelhut, A. Khaplanov, M. Leino, M. Nyman, R. D. Page, **P. Rahkila**, M. Sandzelius, P. Sapple, J. Sarén, C. Scholey, J. Simpson, J. Sorri, J. Thomson and R. Wyss
γ-ray spectroscopy of ^{197}At
Phys.Rev. C **78**, 044328 (2008)

24. L. Bianco, R. D. Page, D. T. Joss, J. Simpson, B. Cederwall, M. B. Gómez Hornillos, P. T. Greenlees, B. Hadinia, U. Jakobsson, P. M. Jones, R. Julin, S. Ketelhut, M. Labiche, M. Leino, M. Nyman, E. S. Paul, M. Petri, P. Peura, A. Puurunen, **P. Rahkila**, P. Ruotsalainen, M. Sandzelius, P. J. Sapple, J. Sarén, C. Scholey, J. Thomson and J. Uusitalo
α-Decay branching ratios measured by γ-ray tagging
Nucl.Instrum.Methods Phys.Res. A **597**, 189 (2008)

25. T. Grahn, A. Dewald, O. Möller, R. Julin, C. W. Beausang, S. Christen, I. G. Darby, S. Eeckhaudt, P. T. Greenlees, A. Görgen, K. Helariutta, J. Jolie, P. Jones, S. Juutinen, H. Kettunen, T. Kröll, R. Krücken, Y. Le Coz, M. Leino, A. P. Leppänen, P. Maierbeck, D. A. Meyer, B. Melon, P. Nieminen, M. Nyman, R. D. Page, J. Pakarinen, P. Petkov, **P. Rahkila**, B. Saha, M. Sandzelius, J. Sarén, C. Scholey, J. Uusitalo, M. Bender and P. H. Heenen
Lifetimes of intruder states in ^{186}Pb, ^{188}Pb *and* ^{194}Po
Nucl.Phys. **A801**, 83 (2008)

26. P. T. Greenlees, R. D. Herzberg, S. Ketelhut, P. A. Butler, P. Chowdhury, T. Grahn, C. Gray-Jones, G. D. Jones, P. Jones, R. Julin, S. Juutinen, T. L. Khoo, M. Leino, S. Moon, M. Nyman, J. Pakarinen, **P. Rahkila**, D. Rostron, J. Sarén, C. Scholey, J. Sorri, S. K. Tandel, J. Uusitalo and M. Venhart
High-K structure in ^{250}Fm and the deformed shell gaps at N=152 andZ=100
Phys.Rev. C **78**, 021303 (2008)

27. S. V. Rigby, D. M. Cullen, P. J. R. Mason, D. T. Scholes, C. Scholey, **P. Rahkila**, S. Eeckhaudt, T. Grahn, P. Greenlees, P. M. Jones, R. Julin, S. Juutinen, H. Kettunen, M. Leino, A. P. Leppänen, P. Nieminen, M. Nyman, J. Pakarinen and J. Uusitalo
Decay of a $\pi h_{11/2}$ (X) $\nu h_{11/2}$ microsecond isomer in $^{136}_{61}Pm_{75}$
Phys.Rev. C **78**, 034304 (2008)

28. A. Chatillon, C. Theisen, E. Bouchez, P. A. Butler, E. Clément, O. Dorvaux, S. Eeckhaudt, B. J. P. Gall, A. Görgen, T. Grahn, P. T. Greenlees, R. D. Herzberg, F. Heßberger, A. Hürstel, G. D. Jones, P. Jones, R. Julin, S. Juutinen, H. Kettunen, F. Khalfallah, W. Korten, Y. Le Coz, M. Leino, A. P. Leppänen, P. Nieminen, J. Pakarinen, J. Perkowski, **P. Rahkila**, M. Rousseau, C. Scholey, J. Uusitalo, J. N. Wilson, P. Bonche and P. H. Heenen
Observation of a Rotational Band in the Odd-Z Transfermium Nucleus $^{251}_{101}Md$
Phys.Rev.Lett. **98**, 132503 (2007)

29. B. Hadinia, B. Cederwall, D. T. Joss, R. Wyss, R. D. Page, C. Scholey, A. Johnson, K. Lagergren, E. Ganioğlu, K. Andgren, T. Bäck, D. E. Appelbe, C. J. Barton, S. Eeckhaudt, T. Grahn, P. Greenlees, P. Jones, R. Julin, S. Juutinen, H. Kettunen, M. Leino, A. P. Lepanen, R. J. Liotta, P. Nieminen, J. Pakarinen, J. Perkowski, **P. Rahkila**, M. Sandzelius, J. Simpson, J. Uusitalo, K. Van de Vel, D. D. Warner and D. R. Wiseman
In-beam γ-ray and α-decay spectroscopy of ^{170}Ir
Phys.Rev. C **76**, 044312 (2007)

30. A. P. Leppänen, J. Uusitalo, M. Leino, S. Eeckhaudt, T. Grahn, P. T. Greenlees, P. Jones, R. Julin, S. Juutinen, H. Kettunen, P. Kuusiniemi, P. Nieminen, J. Pakarinen, **P. Rahkila**, C. Scholey and G. Sletten
α decay studies of the nuclides ^{218}U and ^{219}U
Phys.Rev. C **75**, 054307 (2007)

31. B. S. Nara Singh, A. N. Steer, D. G. Jenkins, R. Wadsworth, M. A. Bentley, P. J. Davies, R. Glover, N. S. Pattabiraman, C. J. Lister, T. Grahn, P. T. Greenlees, P. Jones, R. Julin, S. Juutinen, M. Leino, M. Nyman, J. Pakarinen, **P. Rahkila**, J. Sarén, C. Scholey, J. Sorri, J. Uusitalo, P. A. Butler, M. Dimmock, D. T. Joss, J. Thomson, B. Cederwall, B. Hadinia and M. Sandzelius
Coulomb shifts and shape changes in the mass 70 region
Phys.Rev. C **75**, 061301 (2007)
arXiv:0706.3365 [nucl-ex]

32. J. Pakarinen, V. Hellemans, R. Julin, S. Juutinen, K. Heyde, P. H. Heenen, M. Bender, I. G. Darby, S. Eeckhaudt, T. Enqvist, T. Grahn, P. T. Greenlees, F. Johnston-Theasby, P. Jones, H. Kettunen, M. Leino, A. P. Leppänen, P. Nieminen, M. Nyman, R. D. Page, P. M. Raddon, **P. Rahkila**, C. Scholey, J. Uusitalo and R. Wadsworth
Investigation of nuclear collectivity in the neutron mid-shell nucleus ^{186}Pb
Phys.Rev. C **75**, 014302 (2007)

33. R. D. Page, L. Bianco, I. G. Darby, J. Uusitalo, D. T. Joss, T. Grahn, R. D. Herzberg, J. Pakarinen, J. Thomson, S. Eeckhaudt, P. T. Greenlees, P. M. Jones, R. Julin, S. Juutinen, S. Ketelhut, M. Leino, A. P. Leppänen, M. Nyman, **P. Rahkila**, J. Sarén, C. Scholey, A. Steer, M. B. Gómez Hornillos, J. S. Al-Khalili, A. J. Cannon, P. D. Stevenson, S. Ertürk, B. Gall, B. Hadinia, M. Venhart and J. Simpson
α decay of ^{159}Re *and proton emission from* ^{155}Ta
Phys.Rev. C **75**, 061302 (2007)

34. M. Petri, E. S. Paul, B. Cederwall, I. G. Darby, M. R. Dimmock, S. Eeckhaudt, E. Ganioğlu, T. Grahn, P. T. Greenlees, B. Hadinia, P. Jones, D. T. Joss, R. Julin, S. Juutinen, S. Ketelhut, A. Khaplanov, M. Leino, L. Nelson, M. Nyman, R. D. Page, **P. Rahkila**, M. Sandzelius, J. Sarén, C. Scholey, J. Sorri, J. Uusitalo and R. Wadsworth
Nuclear levels in proton-unbound ^{109}I*: Relative single-particle energies beyond the proton drip line*
Phys.Rev. C **76**, 054301 (2007)

35. M. Sandzelius, C. Scholey, B. Cederwall, E. Ganioğlu, K. Andgren, D. E. Appelbe, C. J. Barton, T. Bäck, S. Eeckhaudt, T. Grahn, P. T. Greenlees, B. Hadinia, A. Johnson, P. M. Jones, D. T. Joss, R. Julin, S. Juutinen, H. Kettunen, K. Lagergren, M. Leino, A. P. Leppänen, P. Nieminen, R. D. Page, J. Pakarinen, J. Perkowski, **P. Rahkila**, J. Simpson, J. Uusitalo, K. Van de Vel, D. D. Warner, D. R. Wiseman and R. Wyss
First identification of excited states in ^{169}Ir
Phys.Rev. C **75**, 054321 (2007)

36. M. Sandzelius, B. Hadinia, B. Cederwall, K. Andgren, E. Ganioğlu, I. G. Darby, M. R. Dimmock, S. Eeckhaudt, T. Grahn, P. T. Greenlees, E. Ideguchi, P. M. Jones, D. T. Joss, R. Julin, S. Juutinen, A. Khaplanov, M. Leino, L. Nelson, M. Niikura, M. Nyman, R. D. Page, J. Pakarinen, E. S. Paul, M. Petri, **P. Rahkila**, J. Sarén, C. Scholey, J. Sorri, J. Uusitalo, R. Wadsworth and R. Wyss
Identification of Excited States in the T_z=1 Nucleus ^{110}Xe*: Evidence for Enhanced Collectivity near the N=Z=50 Double Shell Closure*
Phys.Rev.Lett. **99**, 022501 (2007)

37. D. R. Wiseman, A. N. Andreyev, R. D. Page, M. B. Smith, I. G. Darby, S. Eeckhaudt, T. Grahn, P. T. Greenlees, P. Jones, R. Julin, S. Juutinen, H. Kettunen, M. Leino, A. P. Leppänen, M. Nyman, J. Pakarinen, **P. Rahkila**, M. Sandzelius, J. Sarén, C. Scholey and J. Uusitalo
In-beam gamma-ray spectroscopy of $^{190,197}Po$
Eur.Phys.J. A **34**, 275 (2007)

38. J. E. Bastin, R. D. Herzberg, P. A. Butler, G. D. Jones, R. D. Page, D. G. Jenkins, N. Amzal, P. M. T. Brew, N. J. Hammond, R. D. Humphreys, P. J. C. Ikin, T. Page, P. T. Greenlees, P. M. Jones, R. Julin, S. Juutinen, H. Kankaanpää, A. Keenan, H. Kettunen, P. Kuusiniemi, M. Leino, A. P. Leppänen, M. Muikku, P. Nieminen, **P. Rahkila**, C. Scholey, J. Uusitalo, E. Bouchez, A. Chatillon, A. Hürstel, W. Korten, Y. Le Coz, C. Theisen, D. Ackermann, J. Gerl, K. Helariutta, F. P. Heßberger, C. Schlegel, H. J. Wollersheim, M. Lach, A. Maj, W. Meczynski, J. Styczen, T. L. Khoo, C. J. Lister, A. V. Afanasjev, H. J. Maier, P. Reiter, P. Bednarczyk, K. Eskola and K. Hauschild
In-beam gamma ray and conversion electron study of ^{250}Fm
Phys.Rev. C **73**, 024308 (2006)

39. F. Becker, A. Petrovici, J. Iwanicki, N. Amzal, W. Korten, K. Hauschild, A. Hürstel, C. Theisen, P. A. Butler, R. A. Cunningham, T. Czosnyka, G. de France, J. Gerl, P. Greenlees, K. Helariutta, R. D. Herzberg, P. Jones, R. Julin, S. Juutinen, H. Kankaanpää, M. Muikku, P. Nieminen, O. Radu, **P. Rahkila** and C. Schlegel
Coulomb excitation of ^{78}Kr
Nucl.Phys. **A770**, 107 (2006)

40. A. Chatillon, C. Theisen, P. T. Greenlees, G. Auger, J. E. Bastin, E. Bouchez, B. Bouriquet, J. M. Casandjian, R. Cee, E. Clément, R. Dayras, G. de France, R. de Tourreil, S. Eeckhaudt, A. Görgen, T. Grahn, S. Grevy, K. Hauschild, R. D. Herzberg, P. J. C. Ikin, G. D. Jones, P. Jones, R. Julin, S. Juutinen, H. Kettunen, A. Korichi, W. Korten, Y. Le Coz, M. Leino, A. Lopez-Martens, S. M. Lukyanov, Y. E. Penionzhkevich, J. Perkowski, A. Pritchard, **P. Rahkila**, M. Rejmund, J. Sarén, C. Scholey, S. Siem, M. G. Saint-Laurent, C. Simenel, Y. G. Sobolev, C. Stodel, J. Uusitalo, A. Villari, M. Bender, P. Bonche and P. H. Heenen
Spectroscopy and single-particle structure of the odd-Z heavy elements ^{255}Lr, ^{251}Md *and* ^{247}Es
Eur.Phys.J. A **30**, 397 (2006)

41. T. Grahn, A. Dewald, O. Möller, R. Julin, C. W. Beausang, S. Christen, I. G. Darby, S. Eeckhaudt, P. T. Greenlees, A. Görgen, K. Helariutta, J. Jolie, P. Jones, S. Juutinen, H. Kettunen, T. Kröll, R. Krücken, Y. Le Coz, M. Leino, A. P. Leppänen, P. Maierbeck, D. A. Meyer, B. Melon, P. Nieminen, M. Nyman, R. D. Page, J. Pakarinen, P. Petkov, **P. Rahkila**, B. Saha, M. Sandzelius, J. Sarén, C. Scholey and J. Uusitalo
Collectivity and Configuration Mixing in $^{186,188}Pb$ *and* ^{194}Po
Phys.Rev.Lett. **97**, 062501 (2006)

42. R. D. Herzberg, P. T. Greenlees, P. A. Butler, G. D. Jones, M. Venhart, I. G. Darby, S. Eeckhaudt, K. Eskola, T. Grahn, C. Gray-Jones, F. P. Heßberger, P. Jones, R. Julin, S. Juutinen, S. Ketelhut, W. Korten, M. Leino, A. P. Leppänen, S. Moon, M. Nyman, R. D. Page, J. Pakarinen, A. Pritchard, **P. Rahkila**, J. Sarén, C. Scholey, A. Steer, Y. Sun, C. Theisen and J. Uusitalo
Nuclear isomers in superheavy elements as stepping stones towards theisland of stability
Nature(London) **442**, 896 (2006)

43. D. T. Joss, J. Simpson, D. E. Appelbe, C. J. Barton, D. D. Warner, K. Lagergren, B. Cederwall, B. Hadinia, S. Eeckhaudt, T. Grahn, P. T. Greenlees, P. M. Jones, R. Julin, S. Juutinen, H. Kettunen, M. Leino, A. P. Leppänen, P. Nieminen, J. Pakarinen, J. Perkowski, **P. Rahkila**, C. Scholey, J. Uusitalo, K. Van de Vel, R. D. Page, E. S. Paul, D. R. Wiseman and M. A. Riley
Yrast states and band crossings in the neutron-deficient platinum isotopes $^{169-173}Pt$
Phys.Rev. C **74**, 014302 (2006)

44. D. T. Joss, I. G. Darby, R. D. Page, J. Uusitalo, S. Eeckhaudt, T. Grahn, P. T. Greenlees, P. M. Jones, R. Julin, S. Juutinen, S. Ketelhut, M. Leino, A. P. Leppänen, M. Nyman, J. Pakarinen, **P. Rahkila**, J. Sarén, C. Scholey, A. Steer, A. J. Cannon, P. D. Stevenson, J. S. Al-Khalili, S. Ertürk, M. Venhart, B. Gall, B. Hadinia and J. Simpson
Probing the limit of nuclear existence: Proton emission from ^{159}Re
Phys.Lett. B **641**, 34 (2006)

45. K. Lagergren, D. T. Joss, R. Wyss, B. Cederwall, C. J. Barton, S. Eeckhaudt, T. Grahn, P. T. Greenlees, B. Hadinia, P. M. Jones, R. Julin, S. Juutinen, D. Karlgren, H. Kettunen, M. Leino, A. P. Leppänen, P. Nieminen, M. Nyman, R. D. Page, J. Pakarinen, E. S. Paul, **P. Rahkila**, C. Scholey, J. Simpson, J. Uusitalo and D. R. Wiseman
High-spin states in the proton-unbound nucleus ^{161}Re
Phys.Rev. C **74**, 024316 (2006)

46. A. P. Leppänen, J. Uusitalo, P. T. Greenlees, R. D. Herzberg, N. Amzal, F. Becker, P. A. Butler, A. J. C. Chewter, J. F. C. Cocks, O. Dorvaux, S. Eeckhaudt, K. Eskola, J. Gerl, T. Grahn, N. J. Hammond, K. Hauschild, K. Helariutta, F. P. Heßberger, M. Houry, G. D. Jones, P. M. Jones, R. Julin, S. Juutinen, H. Kankaanpää, H. Kettunen, T. L. Khoo, W. Korten, P. Kuusiniemi, Y. Le Coz, M. Leino, C. J. Lister, R. Lucas, M. Muikku, P. Nieminen, M. Nyman, R. D. Page, J. Pakarinen, **P. Rahkila**, P. Reiter, J. Sarén, C. Schlegel, C. Scholey, O. Stezowski, C. Theisen, W. H. Trzaska and H. J. Wollersheim
Recoil-fission tagging of the transfermium nucleus ^{252}No
Eur.Phys.J. A **28**, 301 (2006)

47. A. N. Steer, D. G. Jenkins, R. Glover, B. S. Nara Singh, N. S. Pattabiraman, R. Wadsworth, S. Eeckhaudt, T. Grahn, P. T. Greenlees, P. Jones, R. Julin, S. Juutinen, M. Leino, M. Nyman, J. Pakarinen, **P. Rahkila**, J. Sarén, C. Scholey, J. Sorri, J. Uusitalo, P. A. Butler, I. G. Darby, R. D. Herzberg, D. T. Joss, R. D. Page, J. Thomson, R. Lemmon, J. Simpson and B. Blank
Recoil-beta tagging: A novel technique for studying proton-drip-line nuclei
Nucl.Instrum.Methods Phys.Res. A **565**, 630 (2006)

48. S. Eeckhaudt, P. T. Greenlees, N. Amzal, J. E. Bastin, E. Bouchez, P. A. Butler, A. Chatillon, K. Eskola, J. Gerl, T. Grahn, A. Görgen, R. D. Herzberg, F. P. Heßberger, A. Hürstel, P. J. C. Ikin, G. D. Jones, P. Jones, R. Julin, S. Juutinen, H. Kettunen, T. L. Khoo, W. Korten, P. Kuusiniemi, Y. Le Coz, M. Leino, A. P. Leppänen, P. Nieminen, J. Pakarinen, J. Perkowski, A. Pritchard, P. Reiter, **P. Rahkila**, C. Scholey, C. Theisen, J. Uusitalo, K. Van de Vel and J. Wilson
Evidence for non-yrast states in ^{254}*No*
Eur.Phys.J. A **26**, 227 (2005)

49. B. Hadinia, B. Cederwall, J. Blomqvist, E. Ganioğlu, P. T. Greenlees, K. Andgren, I. G. Darby, S. Eeckhaudt, E. Ideguchi, P. M. Jones, D. T. Joss, R. Julin, S. Juutinen, S. Ketelhut, K. Lagergren, A. P. Leppänen, M. Leino, M. Nyman, J. Pakarinen, E. S. Paul, M. Petri, **P. Rahkila**, M. Sandzelius, J. Sarén, C. Scholey, J. Uusitalo, R. Wadsworth and R. Wyss
First identification of excited states in ^{106}*Te and evidence for isoscalar-enhanced vibrational collectivity*
Phys.Rev. C **72**, 041303 (2005)

50. J. Pakarinen, I. G. Darby, S. Eeckhaudt, T. Enqvist, T. Grahn, P. T. Greenlees, V. Hellemans, K. Heyde, F. Johnston-Theasby, P. Jones, R. Julin, S. Juutinen, H. Kettunen, M. Leino, A. P. Leppänen, P. Nieminen, M. Nyman, R. D. Page, P. M. Raddon, **P. Rahkila**, C. Scholey, J. Uusitalo and R. Wadsworth
Evidence for oblate structure in ^{186}*Pb*
Phys.Rev. C **72**, 011304 (2005)

51. J. Uusitalo, M. Leino, T. Enqvist, K. Eskola, T. Grahn, P. T. Greenlees, P. Jones, R. Julin, S. Juutinen, A. Keenan, H. Kettunen, H. Koivisto, P. Kuusiniemi, A. P. Leppänen, P. Nieminen, J. Pakarinen, **P. Rahkila** and C. Scholey
α decay studies of very neutron-deficient francium and radium isotopes
Phys.Rev. C **71**, 024306 (2005)

52. B. Hadinia, B. Cederwall, K. Lagergren, J. Blomqvist, T. Bäck, S. Eeckhaudt, T. Grahn, P. Greenlees, A. Johnson, D. T. Joss, R. Julin, S. Juutinen, H. Kettunen, M. Leino, A. P. Leppänen, R. J. Liotta, P. Nieminen, M. Nyman, J. Pakarinen, E. S. Paul, **P. Rahkila**, C. Scholey, J. Uusitalo, R. Wadsworth and D. R. Wiseman
First identification of γ-ray transitions in ^{107}*Te*
Phys.Rev. C **70**, 064314 (2004)

53. R. D. Humphreys, P. A. Butler, J. E. Bastin, P. T. Greenlees, N. J. Hammond, R. D. Herzberg, D. G. Jenkins, G. D. Jones, H. Kankaanpää, A. Keenan, H. Kettunen, T. Page, **P. Rahkila**, C. Scholey, J. Uusitalo, N. Amzal, P. M. T. Brew, K. Eskola, J. Gerl, K. Hauschild, K. Helariutta, F. P. Heßberger, A. Hürstel, P. M. Jones, R. Julin, S. Juutinen, T. L. Khoo, W. Korten, P. Kuusiniemi, Y. Le Coz, M. Leino, A. P. Leppänen, M. Muikku, P. Nieminen, S. W. Ødegård, J. Pakarinen, P. Reiter, G. Sletten, C. Theisen and H. J. Wollersheim
In-beam electron spectroscopy of ^{226}U *and* ^{254}No
Phys.Rev. C **69**, 064324 (2004)

54. A. Hürstel, Y. Le Coz, E. Bouchez, A. Chatillon, A. Görgen, P. T. Greenlees, K. Hauschild, S. Juutinen, H. Kettunen, W. Korten, P. Nieminen, M. Rejmund, C. Theisen, J. Wilson, A. N. Andreyev, F. Becker, T. Enqvist, P. M. Jones, R. Julin, H. Kankaanpää, A. Keenan, P. Kuusiniemi, M. Leino, A. P. Leppänen, M. Muikku, J. Pakarinen, **P. Rahkila** and J. Uusitalo
Prolate deformation in the $^{187,189}Bi$ *isotopes*
Eur.Phys.J. A **21**, 365 (2004)

55. D. T. Joss, K. Lagergren, D. E. Appelbe, C. J. Barton, J. Simpson, B. Cederwall, B. Hadinia, R. Wyss, S. Eeckhaudt, T. Grahn, P. T. Greenlees, P. M. Jones, R. Julin, S. Juutinen, H. Kettunen, M. Leino, A. P. Leppänen, P. Nieminen, J. Pakarinen, **P. Rahkila**, C. Scholey, J. Uusitalo, R. D. Page, E. S. Paul and D. R. Wiseman
Recoil decay tagging of γ *rays in the extremely neutron-deficient nucleus* ^{162}Os
Phys.Rev. C **70**, 017302 (2004)

56. H. Kankaanpää, P. Butler, P. Greenlees, J. Bastin, R. Herzberg, R. Humphreys, G. Jones, P. Jones, R. Julin, A. Keenan, H. Kettunen, M. Leino, L. Miettinen, T. Page, **P. Rahkila**, C. Scholey and J. Uusitalo
In-beam electron spectrometer used in conjunction with a gas-filled recoil separator
Nucl.Instrum.Methods Phys.Res. A **534**, 503 (2004)

57. H. Kettunen, T. Enqvist, T. Grahn, P. T. Greenlees, P. Jones, R. Julin, S. Juutinen, A. Keenan, P. Kuusiniemi, M. Leino, A. P. Leppänen, P. Nieminen, J. Pakarinen, **P. Rahkila** and J. Uusitalo
Decay studies of $^{170,171}Au$, $^{171-173}Hg$, *and* ^{176}Tl
Phys.Rev. C **69**, 054323 (2004)

58. P. Nieminen, S. Juutinen, A. N. Andreyev, J. F. C. Cocks, O. Dorvaux, K. Eskola, P. T. Greenlees, K. Hauschild, K. Helariutta, M. Huyse, P. M. Jones, R. Julin, H. Kankaanpää, H. Kettunen, P. Kuusiniemi, Y. Le Coz, M. Leino, T. Lonnroth, M. Muikku, **P. Rahkila**, A. Savelius, J. Uusitalo, N. Amzal, N. J. Hammond, C. Scholey and R. Wyss
γ*-ray spectroscopy of* $^{191,193}Bi$
Phys.Rev. C **69**, 064326 (2004)

59. P. M. Raddon, D. G. Jenkins, C. D. O'Leary, A. J. Simons, R. Wadsworth, A. N. Andreyev, R. D. Page, M. P. Carpenter, F. G. Kondev, T. Enqvist, P. T. Greenlees, P. M. Jones, R. Julin, S. Juutinen, H. Kettunen, M. Leino, A. P. Leppänen, P. Nieminen, J. Pakarinen, **P. Rahkila**, J. Uusitalo and D. T. Joss
α decay and recoil decay tagging studies of ^{183}Tl
Phys.Rev. C **70**, 064308 (2004)

60. T. Bäck, B. Cederwall, K. Lagergren, R. Wyss, A. Johnson, D. Karlgren, P. Greenlees, D. Jenkins, P. Jones, D. T. Joss, R. Julin, S. Juutinen, A. Keenan, H. Kettunen, P. Kuusiniemi, M. Leino, A. P. Leppänen, M. Muikku, P. Nieminen, J. Pakarinen, **P. Rahkila** and J. Uusitalo
First observation of gamma-rays from the proton emitter ^{171}Au
Eur.Phys.J. A **16**, 489 (2003)

61. T. Bäck, B. Cederwall, K. Lagergren, R. Wyss, A. Johnson, P. Greenlees, D. Jenkins, P. Jones, D. T. Joss, R. Julin, S. Juutinen, A. Keenan, H. Kettunen, P. Kuusiniemi, M. Leino, A. P. Leppänen, M. Muikku, P. Nieminen, J. Pakarinen, **P. Rahkila** and J. Uusitalo
Spectroscopy of the neutron-deficient nuclide ^{171}Pt
Eur.Phys.J. A **17**, 1 (2003)

62. E. Bouchez, I. Matea, W. Korten, F. Becker, B. Blank, C. Borcea, A. Buta, A. Emsallem, G. de France, J. Genevey, F. Hannachi, K. Hauschild, A. Hürstel, Y. Le Coz, M. Lewitowicz, R. Lucas, F. Negoita, F. de Oliveira Santos, D. Pantelica, J. Pinston, **P. Rahkila**, M. Rejmund, M. Stanoiu and C. Theisen
New Shape Isomer in the Self-Conjugate Nucleus ^{72}Kr
Phys.Rev.Lett. **90**, 082502 (2003)

63. H. Kettunen, T. Enqvist, M. Leino, K. Eskola, P. T. Greenlees, K. Helariutta, P. Jones, R. Julin, S. Juutinen, H. Kankaanpää, H. Koivisto, P. Kuusiniemi, M. Muikku, P. Nieminen, **P. Rahkila** and J. Uusitalo
Investigations into the alpha-decay of ^{195}At
Eur.Phys.J. A **16**, 457 (2003)

64. H. Kettunen, T. Enqvist, T. Grahn, P. T. Greenlees, P. Jones, R. Julin, S. Juutinen, A. Keenan, P. Kuusiniemi, M. Leino, A. P. Leppänen, P. Nieminen, J. Pakarinen, **P. Rahkila** and J. Uusitalo
Alpha-decay studies of the new isotopes ^{191}At and ^{193}At
Eur.Phys.J. A **17**, 537 (2003)

65. A. Melerangi, D. Appelbe, R. D. Page, H. J. Boardman, P. T. Greenlees, P. Jones, D. T. Joss, R. Julin, S. Juutinen, H. Kettunen, P. Kuusiniemi, M. Leino, M. H. Muikku, P. Nieminen, J. Pakarinen, **P. Rahkila** and J. Simpson
Shape isomerism and spectroscopy of ^{177}Hg
Phys.Rev. C **68**, 041301 (2003)

66. K. Van de Vel, A. N. Andreyev, R. D. Page, H. Kettunen, P. T. Greenlees, P. Jones, R. Julin, S. Juutinen, H. Kankaanpää, A. Keenan, P. Kuusiniemi, M. Leino, M. Muikku, P. Nieminen, **P. Rahkila**, J. Uusitalo, K. Eskola, A. Hürstel, M. Huyse, Y. Le Coz, M. B. Smith, P. Van Duppen and R. Wyss
In-beam γ-ray spectroscopy of ^{190}Po: First observation of a low-lying prolate band in Po isotopes
Eur.Phys.J. A **17**, 167 (2003)

67. A. N. Andreyev, M. Huyse, K. Van de Vel, P. Van Duppen, O. Dorvaux, P. Greenlees, K. Helariutta, P. Jones, R. Julin, S. Juutinen, H. Kettunen, P. Kuusiniemi, M. Leino, M. Muikku, P. Nieminen, **P. Rahkila**, J. Uusitalo, R. Wyss, K. Hauschild and Y. Le Coz
In-Beam and α-Decay Spectroscopy of ^{191}Po and Evidence for TripleShape Coexistence at Low Energy in the Daughter Nucleus ^{187}Pb
Phys.Rev. C **66**, 014313 (2002)

68. D. E. Appelbe, J. Simpson, M. Muikku, H. J. Boardman, A. Melarangi, R. D. Page, P. T. Greenlees, P. M. Jones, R. Julin, S. Juutinen, A. Keenan, H. Kettunen, P. Kuusiniemi, M. Leino, P. Nieminen, J. Pakarinen, **P. Rahkila**, J. Uusitalo and D. T. Joss
First Observation of Excited States in the Very Neutron Deficient Nucleus $^{165}_{76}$Os and the Yrast Structure of $^{166}_{76}$Os
Phys.Rev. C **66**, 014309 (2002)

69. P. A. Butler, R. D. Humphreys, P. T. Greenlees, R. D. Herzberg, D. G. Jenkins, G. D. Jones, H. Kankaanpää, H. Kettunen, **P. Rahkila**, C. Scholey, J. Uusitalo, N. Amzal, J. E. Bastin, P. M. T. Brew, K. Eskola, J. Gerl, N. J. Hammond, K. Hauschild, K. Helariutta, F. P. Heßberger, A. Hürstel, P. M. Jones, R. Julin, S. Juutinen, A. Keenan, T. L. Khoo, W. Korten, P. Kuusiniemi, Y. Le Coz, M. Leino, A. P. Leppänen, M. Muikku, P. Nieminen, S. W. Ødegård, T. Page, J. Pakarinen, P. Reiter, G. Sletten, C. Theisen and H. J. Wollersheim
Conversion Electron Cascades in $^{254}_{102}$No
Phys.Rev.Lett. **89**, 202501 (2002)

70. D. M. Cullen, L. K. Pattison, R. S. Chakrawarthy, D. Dobson, J. L. Durell, S. J. Freeman, D. T. Scholes, C. Scholey, E. S. Paul, P. T. W. Choy, P. T. Greenlees, P. M. Jones, R. Julin, S. Juutinen, A. Keenan, H. Kettunen, P. Kuusiniemi, M. Leino, A. P. Leppänen, P. Nieminen, J. Pakarinen, **P. Rahkila**, J. Uusitalo, M. A. Bentley and D. T. Joss
Identification of Excited States in Doubly Odd $^{140}_{63}Eu_{77}$ by Recoil-Isomer Tagging
Phys.Rev. C **66**, 034308 (2002)

71. D. J. Dobson, S. J. Freeman, P. T. Greenlees, A. N. Qadir, S. Juutinen, J. L. Durell, T. Enqvist, P. Jones, R. Julin, A. Keenan, H. Kettunen, P. Kuusiniemi, M. Leino, P. Nieminen, **P. Rahkila**, S. D. Robinson, J. Uusitalo and B. J. Varley
Low-lying structure of light radon isotopes
Phys.Rev. C **66**, 064321 (2002)

72. N. J. Hammond, G. D. Jones, P. A. Butler, R. D. Humphreys, P. T. Greenlees, P. M. Jones, R. Julin, S. Juutinen, A. Keenan, H. Kettunen, P. Kuusiniemi, M. Leino, M. Muikku, P. Nieminen, **P. Rahkila**, J. Uusitalo and S. V. Khlebnikov
Observation of K = 1 / 2 Octupole Deformed Bands in ^{227}Th
Phys.Rev. C **65**, 064315 (2002)

73. R. D. Herzberg, N. Amzal, F. Becker, P. A. Butler, A. J. C. Chewter, J. F. C. Cocks, O. Dorvaux, K. Eskola, J. Gerl, P. T. Greenlees, N. J. Hammond, K. Hauschild, K. Helariutta, F. Heßberger, M. Houry, G. D. Jones, P. M. Jones, R. Julin, S. Juutinen, H. Kankaanpää, H. Kettunen, T. L. Khoo, W. Korten, P. Kuusiniemi, Y. Le Coz, M. Leino, C. J. Lister, R. Lucas, M. Muikku, P. Nieminen, R. D. Page, **P. Rahkila**, P. Reiter, C. Schlegel, C. Scholey, O. Stezowski, C. Theisen, W. H. Trzaska, J. Uusitalo and H. J. Wollersheim
Spectroscopy of Transfermium Nuclei: $^{252}_{102}No$
Phys.Rev. C **65**, 014303 (2002)

74. A. Hürstel, M. Rejmund, E. Bouchez, P. T. Greenlees, K. Hauschild, S. Juutinen, W. Korten, Y. Le Coz, P. Nieminen, C. Theisen, A. N. Andreyev, F. Becker, T. Enqvist, P. M. Jones, R. Julin, H. Kankaanpää, A. Keenan, P. Kuusiniemi, M. Leino, A.-P. Leppänen, M. Muikku, J. Pakarinen, **P. Rahkila** and J. Uusitalo
Isomeric states in proton-unbound $^{187,189}Bi$ *isotopes*
Eur.Phys.J. A **15**, 329 (2002)

75. D. G. Jenkins, A. N. Andreyev, R. D. Page, M. P. Carpenter, R. V. F. Janssens, C. J. Lister, F. G. Kondev, T. Enqvist, P. T. Greenlees, P. M. Jones, R. Julin, S. Juutinen, H. Kettunen, P. Kuusiniemi, M. Leino, A. P. Leppänen, P. Nieminen, J. Pakarinen, **P. Rahkila**, J. Uusitalo, C. D. O'Leary, P. Raddon, A. Simons, R. Wadsworth and D. T. Joss
Confirmation of Triple Shape Coexistence in ^{179}Hg*: Focal plane spectroscopy of the* α *decay of* ^{183}Pb
Phys.Rev. C **66**, 011301 (2002)

76. D. M. Cullen, C. Scholey, C. Fox, A. J. Boston, E. S. Paul, H. C. Scraggs, S. L. Shepherd, O. Stezowski, T. Enqvist, P. A. Butler, A. M. Bruce, P. M. Walker, M. Caamano, J. Garces Narro, M. A. Bentley, D. T. Joss, P. T. Greenlees, K. Helariutta, P. M. Jones, R. Julin, S. Juutinen, H. Kettunen, M. Leino, M. Muikku, O. Dorvaux, **P. Rahkila**, J. Uusitalo and P. Nieminen
Recoil-Isomer Tagging Near the Mass 140 Proton Drip Line
Nucl.Phys. **A682**, 264c (2001)

77. K. Hauschild, M. Rejmund, H. Grawe, E. Caurier, F. Nowacki, F. Becker, Y. LeCoz, W. Korten, J. Doring, M. Gorska, K. Schmidt, O. Dorvaux, K. Helariutta, P. Jones, R. Julin, S. Juutinen, H. Kettunen, M. Leino, M. Muikku, P. Nieminen, **P. Rahkila**, J. Uusitalo, F. Azaiez and M. Belleguic
Isomer Spectroscopy in $^{216}_{90}Th^{126}$ *and the Magicity of* $^{218}_{92}U_{126}$
Phys.Rev.Lett. **87**, 072501 (2001)

78. H. Kettunen, J. Uusitalo, M. Leino, P. Jones, K. Eskola, P. T. Greenlees, K. Helariutta, R. Julin, S. Juutinen, H. Kankaanpää, P. Kuusiniemi, M. Muikku, P. Nieminen and **P. Rahkila**
α Decay Studies of the Nuclides ^{195}Rn and ^{196}Rn
Phys.Rev. C **63**, 044315 (2001)

79. M. Muikku, P. T. Greenlees, K. Hauschild, K. Helariutta, D. G. Jenkins, P. Jones, R. Julin, S. Juutinen, H. Kankaanpää, N. S. Kelsall, H. Kettunen, P. Kuusiniemi, M. Leino, C. J. Moore, P. Nieminen, C. D. O'Leary, R. D. Page, **P. Rahkila**, W. Reviol, M. J. Taylor, J. Uusitalo and R. Wadsworth
Shape Coexistence in ^{183}Tl
Phys.Rev. C **64**, 044308 (2001)

80. C. Scholey, D. M. Cullen, E. S. Paul, A. J. Boston, P. A. Butler, T. Enqvist, C. Fox, H. C. Scraggs, S. L. Shepherd, O. Stezowski, A. M. Bruce, P. M. Walker, M. Caamano, J. Garces Narro, M. A. Bentley, D. T. Joss, O. Dorvaux, P. T. Greenlees, K. Helariutta, P. M. Jones, R. Julin, S. Juutinen, H. Kankaanpää, H. Kettunen, P. Kuusiniemi, M. Leino, M. Muikku, P. Nieminen, **P. Rahkila** and J. Uusitalo
Recoil Isomer Tagging in the Proton-Rich Odd-Odd $N = 77$ Isotones, $^{142}_{65}Tb$ and $^{144}_{67}Ho$
Phys.Rev. C **63**, 034321 (2001)

81. A. P. Byrne, A. M. Baxter, G. D. Dracoulis, S. M. Mullins, T. Kibedi, T. R. McGoram, K. Helariutta, J. F. C. Cocks, P. Jones, R. Julin, S. Juutinen, H. Kankaanpää, H. Kettunen, P. Kuusiniemi, M. Leino, M. Muikku, P. Nieminen, **P. Rahkila** and A. Savelius
Microsecond Isomers in ^{187}Tl and ^{188}Pb
Eur.Phys.J. A **7**, 41 (2000)

82. D. G. Jenkins, M. Muikku, P. T. Greenlees, K. Hauschild, K. Helariutta, P. M. Jones, R. Julin, S. Juutinen, H. Kankaanpää, N. S. Kelsall, H. Kettunen, P. Kuusiniemi, M. Leino, C. J. Moore, P. Nieminen, C. D. O'Leary, R. D. Page, **P. Rakhila**, W. Reviol, M. J. Taylor, J. Uusitalo and R. Wadsworth
First Observation of Excited States in ^{182}Pb
Phys.Rev. C **62**, 021302 (2000)

83. M. Lach, P. Bednarczyk, P. T. Greenlees, K. Helariutta, P. Jones, R. Julin, S. Juutinen, H. Kankaanpää, H. Kettunen, P. Kuusiniemi, M. Leino, W. Meczynski, M. Muikku, P. Nieminen, **P. Rahkila**, J. Styczen and J. Uusitalo
Identification of the $13^- / 2^+$ Isomer in ^{199}At
Eur.Phys.J. A **9**, 307 (2000)

84. E. S. Paul, H. C. Scraggs, A. J. Boston, O. Dorvaux, P. T. Greenlees, K. Helariutta, P. Jones, R. Julin, S. Juutinen, H. Kankaanpää, H. Kettunen, M. Muikku, P. Nieminen, **P. Rahkila** and O. Stezowski
High-Spin Study of Neutron-Deficient ^{114}Xe
Nucl.Phys. **A673**, 31 (2000)

85. E. S. Paul, K. Starosta, A. J. Boston, C. J. Chiara, M. Devlin, O. Dorvaux, D. B. Fossan, P. T. Greenlees, K. Helariutta, P. Jones, R. Julin, S. Juutinen, H. Kankaanpää, H. Kettunen, D. R. LaFosse, G. J. Lane, I. Y. Lee, A. O. Macchiavelli, M. Muikku, P. Nieminen, **P. Rahkila**, D. G. Sarantites, H. C. Scraggs, J. M. Sears, A. T. Semple, J. F. Smith and O. Stezowski
High-Spin Study of ^{111}I
Phys.Rev. C **61**, 064320 (2000)

86. H. C. Scraggs, E. S. Paul, A. J. Boston, C. J. Chiara, M. Devlin, O. Dorvaux, D. B. Fossan, P. T. Greenlees, K. Helariutta, P. Jones, R. Julin, S. Juutinen, H. Kankaanpää, H. Kettunen, D. R. LaFosse, G. J. Lane, I. Y. Lee, A. O. Macchiavelli, M. Muikku, P. Nieminen, **P. Rahkila**, D. G. Sarantites, J. M. Sears, A. T. Semple, J. F. Smith, K. Starosta and O. Stezowski
High-Spin Study of ^{113}Xe*: Smooth band termination in valence space*
Phys.Rev. C **61**, 064316 (2000)

87. M. B. Smith, R. Chapman, J. F. C. Cocks, K. M. Spohr, O. Dorvaux, K. Helariutta, P. M. Jones, R. Julin, S. Juutinen, H. Kankaanpää, H. Kettunen, P. Kuusiniemi, Y. Le Coz, M. Leino, D. J. Middleton, M. Muikku, P. Nieminen, **P. Rahkila** and A. Savelius
Isomeric State in the Doubly Odd ^{196}At *Nucleus*
J.Phys.(London) G **26**, 787 (2000)

88. R. A. Bark, S. Törmänen, T. Bäck, B. Cederwall, S. W. Ødegård, J. F. C. Cocks, K. Helariutta, P. Jones, R. Julin, S. Juutinen, H. Kankaanpää, H. Kettunen, P. Kuusiniemi, M. Leino, M. Muikku, **P. Rahkila** and A. Savelius
Bandcrossings in ^{171}Os
Nucl.Phys. **A646**, 399 (1999)

89. R. A. Bark, S. Törmänen, T. Bäck, B. Cederwall, S. W. Ødegård, J. F. C. Cocks, K. Helariutta, P. Jones, R. Julin, S. Juutinen, H. Kankaanpää, H. Kettunen, P. Kuusiniemi, M. Leino, M. Muikku, **P. Rahkila**, A. Savelius, M. Bergström, F. Ingebretsen, A. Maj, M. Mattiuzzi, W. Mueller, L. L. Riedinger, T. Saitoh and P. O. Tjøm
Coexistence of Triaxial and Prolate Shapes in ^{171}Ir
Nucl.Phys. **A657**, 113 (1999)

90. K. Helariutta, J. F. C. Cocks, T. Enqvist, P. T. Greenlees, P. Jones, R. Julin, S. Juutinen, P. Jamsen, H. Kankaanpää, H. Kettunen, P. Kuusiniemi, M. Leino, M. Muikku, M. Piiparinen, **P. Rahkila**, A. Savelius, W. H. Trzaska, S. Törmänen, J. Uusitalo, R. G. Allatt, P. A. Butler, R. D. Page and M. Kapusta
Gamma-Ray Spectroscopy of $^{192-195}Po$
Eur.Phys.J. A **6**, 289 (1999)

91. M. Leino, H. Kankaanpää, R. D. Herzberg, A. J. Chewter, F. P. Heßberger, Y. Le Coz, F. Becker, P. A. Butler, J. F. C. Cocks, O. Dorvaux, K. Eskola, J. Gerl, P. T. Greenlees, K. Helariutta, M. Houry, G. D. Jones, P. Jones, R. Julin, S. Juutinen, H. Kettunen, T. L. Khoo, A. Kleinbohl, W. Korten, P. Kuusiniemi, R. Lucas, M. Muikku, P. Nieminen, R. D. Page, **P. Rahkila**, P. Reiter, A. Savelius, C. Schlegel, C. Theisen, W. H. Trzaska and H. J. Wollersheim
In-Beam Study of ^{254}*No*
Eur.Phys.J. A **6**, 63 (1999)

92. Y. Le Coz, F. Becker, H. Kankaanpää, W. Korten, E. Mergel, P. A. Butler, J. F. C. Cocks, O. Dorvaux, D. Hawcroft, K. Helariutta, R. D. Herzberg, M. Houry, H. Hubel, P. Jones, R. Julin, S. Juutinen, H. Kettunen, P. Kuusiniemi, M. Leino, R. Lucas, M. Muikku, P. Nieminen, **P. Rahkila**, D. Rossbach, A. Savelius and C. Theisen
Evidence of Multiple Shape-Coexistence in ^{188}*Pb*
EPJdirect **1**, A3, 1–6 (1999)

93. M. B. Smith, R. Chapman, J. F. C. Cocks, O. Dorvaux, K. Helariutta, P. M. Jones, R. Julin, S. Juutinen, H. Kankaanpää, H. Kettunen, P. Kuusiniemi, Y. Le Coz, M. Leino, D. J. Middleton, M. Muikku, P. Nieminen, **P. Rahkila**, A. Savelius and K. M. Spohr
First Observation of Excited States in ^{197}*At: The onset of deformation in neutron-deficient astatine nuclei*
Eur.Phys.J. A **5**, 43 (1999)

94. R. B. E. Taylor, S. J. Freeman, J. L. Durell, M. J. Leddy, S. D. Robinson, B. J. Varley, J. F. C. Cocks, K. Helariutta, P. Jones, R. Julin, S. Juutinen, H. Kankaanpää, A. Kanto, H. Kettunen, P. Kuusiniemi, M. Leino, M. Muikku, **P. Rahkila**, A. Savelius and P. T. Greenlees
γ *Decay of Excited States in* ^{198}*Rn Identified using Correlated Radioactive Decay*
Phys.Rev. C **59**, 673 (1999)

95. B. Cederwall, T. Bäck, R. Bark, S. Törmänen, S. Ødegård, S. L. King, J. Simpson, R. D. Page, N. Amzal, D. M. Cullen, P. T. Greenlees, A. Keenan, R. Lemmon, J. F. C. Cocks, K. Helariutta, P. M. Jones, R. Julin, S. Juutinen, H. Kettunen, H. Kankaanpää, P. Kuusiniemi, M. Leino, M. Muikku, **P. Rahkila**, A. Savelius, J. Uusitalo, P. Magierski and R. Wyss
Collective Rotational - Vibrational Transition in the Very Neutron-Deficient Nuclei ^{171,172}*Pt*
Phys.Lett. B **443**, 69 (1998)

96. M. Muikku, J. F. C. Cocks, K. Helariutta, P. Jones, R. Julin, S. Juutinen, H. Kankaanpää, H. Kettunen, P. Kuusiniemi, M. Leino, **P. Rahkila**, A. Savelius, W. H. Trzaska, J. Uusitalo, P. T. Greenlees and R. D. Page
Probing the Shape of ^{176}*Hg Along the Yrast Line*
Phys.Rev. C **58**, R3033 (1998)

97. G. N. White, N. J. Stone, J. Rikovska, S. Ohya, J. Copnell, T. J. Giles, Y. Koh, I. S. Towner, B. A. Brown, B. Fogelberg, L. Jacobsson, **P. Rahkila** and M. Hjorth-Jensen
Magnetic Dipole Moments Near ^{132}Sn: New measurement on ^{135}I by NMR / ON
Nucl.Phys. **A644**, 277 (1998)

Contents

Chapter 1

Introduction

One of the most commonly discussed properties of atomic nuclei is their shape or *deformation*. Already the fact that a nucleus, which in our current understanding to the zeroth order is a collection of A nucleons (where A ranges from 1 to a few hundred) moving independently in a mean field generated by themselves, can exhibit non-spherical shapes is rather intriguing. In any case, a vast body of both theoretical and experimental evidence exists which prove that a nucleus can not only be statically deformed but can dynamically assume different deformations based on the different intrinsic configurations it is driven to at different states of excitation. Areas of "static" deformation (in which the ground states are deformed and no dramatic changes occur if the nucleus is excited moderately) have been identified, the most famous being the rare-earth nuclei and the actinides. An extreme example of dynamical change is *superdeformation* in which the nucleus assumes a very elongated prolate shape at high excitation energy, while exhibiting a completely different shape in the ground state. More subtle examples are the areas of the nuclear chart in which several differently deformed configurations can be found in a very narrow range of excitation energy, and in the most spectacular cases, also at very low excitation energies. This latter phenomenon is often referred to as *shape-coexistence*.

Shape-coexistence has been rather well established in the region centered around the crossing of the magic Z=82 shell gap and the N=104 neutron mid-shell [1, 2, 3, 4]. Compelling experimental evidence has been gathered especially for the Pt and Hg isotopes below the the magic Pb (Z=82) shell gap as well as for the Pb isotopes themselves. For isotopes heavier than Pb, experimental data is more scarse. In this work the shape evolution, whether in the context of shape-

coexistence or a more "normal" onset of deformation, of very neutron deficient Pb, Po (Z=84), Rn (Z=86) and Ra (Z=88) nuclei is examined mostly through in-beam γ-ray measuments. Gamma-ray spectroscopy does not directly produce information on the deformation of the nuclei studied. One has to rely on models, which predict the behaviour of the excited states and thus the γ-ray transitions in order to extract information on the nuclear shapes. In the most simplistic approach the well known rotational behaviour of any quantal system can be used to ascertain that the body under scrutiny is well deformed. The method also gives information on the excited nuclei, something which, most methods directly probing the deformations can not do, being limited to measurements of the ground state properties. This is crucial to the study of shape coexistence in which by definition, excited structures are involved.

1.1 Theoretical predictions

Nuclear deformation can be calculated using many different models. Along with masses and radii, it is the most commonly used observable which is used to globally benchmarh the calculations. Here results of two *global* calculations of the ground state properties for which numerical results are publicly available are discussed.

In figure 1.1 the ground state quadrupole deformation parameters β_2[1], calculated with a classic microscopic-macroscopic model of Möller et al. [6] for nuclei in the area of interest are presented. As can be readily seen the magic shell gap at $Z = 82$ keeps not only all Pb isotopes but also all Bi (Z=83) isotopes practically spherical in this calculation. For the heavier elements a gradual change from a spherical shape at the closed $N = 126$ neutron shell towards strongly oblate, and still further away a sudden change to a strongly prolate shape is predicted. In elements heavier than Th (Z=92) the shift to a prolate ground state is not as drastic and happens at higher neutron numbers than for the lighter elements.

A more modern, Hartree-Fock type mean field calculation using the Gogny D1S interaction was used by Hilaire and Girod [7] to calculate the deformations of figure 1.2. The results shown are the deformations at the minima of mean field energies, no beyond mean-field configuration mixing techniques were used [2]. The overall pattern is very similar to the microscopic-macroscopic calculations with a few notable differences. These mean-field calculations find

[1] For definition see e.g Hill and Wheeler [5]

[2] Beyond mean field corrections can have profound effects on the calculated nuclear properties. A comprehensive review can be found for example in [8].

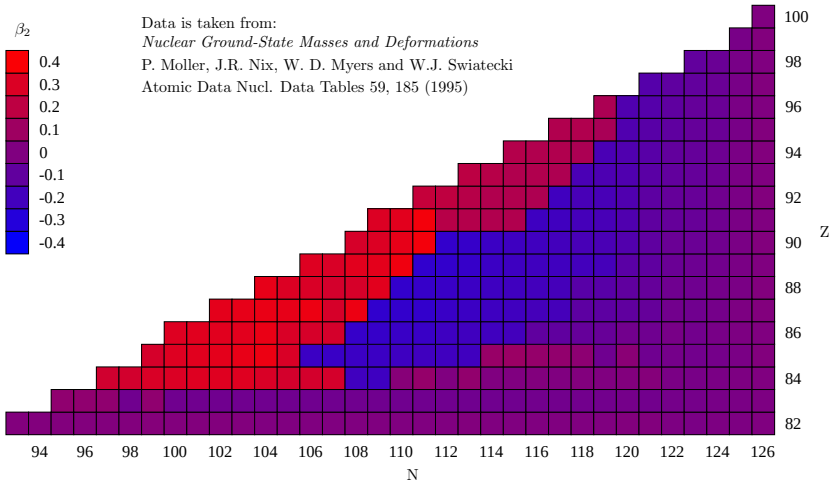

Figure 1.1: Ground state quadrupole deformation parameters β_2 for nuclei $Z \geq 82$, $N \leq 126$. Data are taken from [6] in which a macroscopic-microscopic model is used.

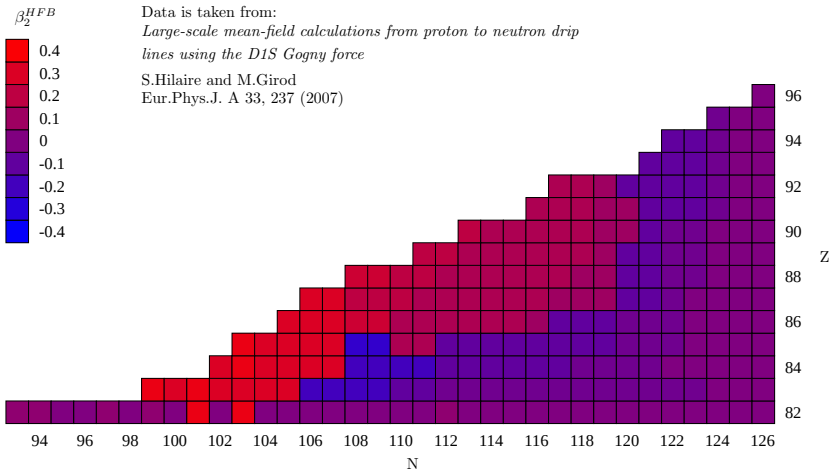

Figure 1.2: Quadrupole deformations β_2 for the ground states of $Z \geq 82$, $N \leq 126$ nuclei extracted from Hartee-Fock type mean field calculations using Gogny D1S interaction. Data are from [7]

that the Bi isotopes are deformed close to the $N = 104$ mid-shell, which is in better agreement with the experimental results [9, 10] than the microscopic-macroscopic calculations. On the other hand, lead isotopes ^{183,185}Pb are found to have strongly prolate deformed ground states, at variance with direct measurements of the charge radii of lead isotopes [11][3]. The large area of strong oblate deformation present in the microscopic-macroscopic calculations right of the $N - Z = 21$ line has shrunk to only a few isotopes of Po, Bi and At centered around ^{192}Po, and the area of modest prolate deformation present on elements heavier than Ac left of the $N - Z = 24$ line has taken over most of the area that was strongly oblate in the microscopic-macroscopic calculation.

A more detailed picture can be achieved by plotting the mean field energies as a function of deformation for each isotope. As an example, in figure 1.3 the data from Hilaire and Girod [7] has been used to produce such a plot for the even-even Po isotopes. The gradual change from sphericity in the closed and near-closed shell nuclei ^{210,208,206}Po through vibrational like minima to more oblate ground states in ^{194,192}Po can be considered as "normal" onset of deformation in which the slow growth of valence space provides the source of the collectivity required for deformation. The sudden change of the ground state from a strongly oblate shape to a strongly prolate shape between ^{192}Po and ^{190}Po is to be taken as a sign of shape-coexistence. Both prolate and oblate minima coexist at low, almost degenerate excitation energies in these nuclei and the dramatic change from a shape to another in the calculation is a manifestation of the prolate minimum reaching the ground state. The energy difference between the calculated minima in ^{190}Po is only 0.45 MeV and only 0.57 MeV for ^{192}Po, indicating that the exact neutron number at which the shape of the ground state changes is not necessarily well defined. From ^{188}Po onwards ground states are clearly more prolate deformed, but one should note that the oblate minimum does not suddenly completely disappear, but coexists with the prolate ground state.

While inspecting the same calculated data in a similar manner for the even-even Pb isotope chain the ground-state remains spherical from ^{208}Pb to the most neutron-deficient isotopes, as expected. The nuclei remain clearly spherical until an excited oblate minimum forms at ^{194}Pb. The oblate minimum remains the lowest excited minimum until at the N=104 neutron mid-shell (^{186}Pb) the prolate normally deformed minimum, first seen in ^{190}Pb, becomes practically degenerate in energy. Below the mid-shell the oblate minimum quickly vanishes, and at ^{182}Pb only the prolate minimum remains. The deformed minima disappear completely at ^{178}Pb. The scenario looks remarkably similar to the Po isotopes with the added complication of the strong spherical minimum,

[3] In ref.[11] beyond mean field correlations same as in [8] are discussed.

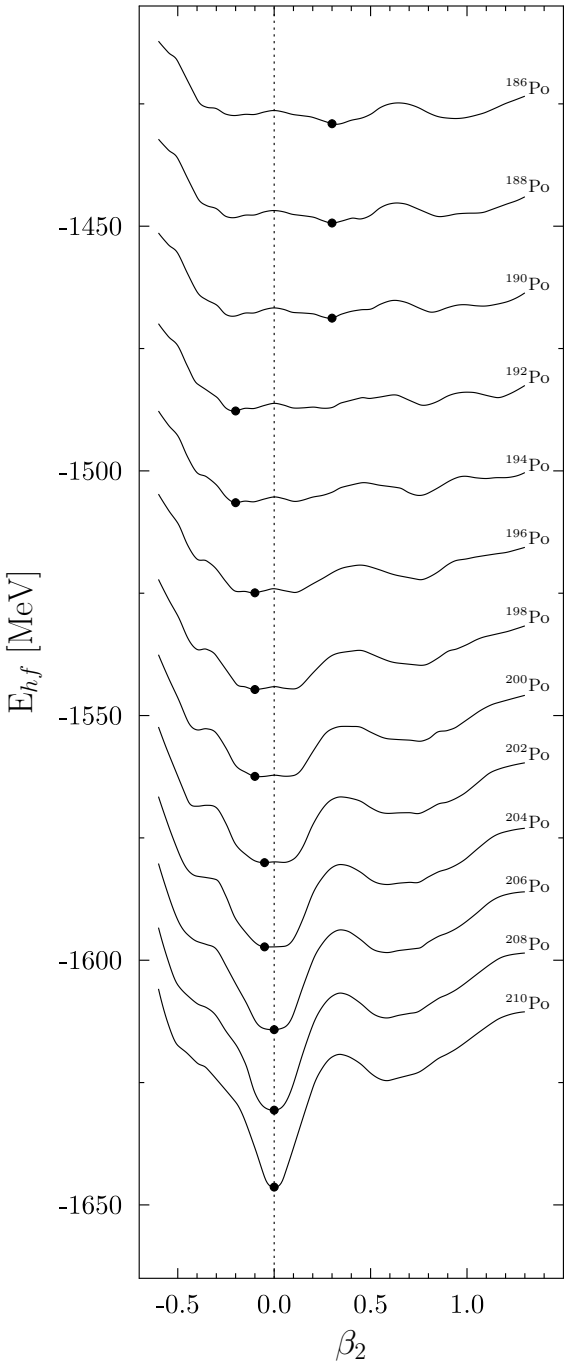

Figure 1.3: Mean field energies as a function of quadrupole deformation β_2 for $^{186-210}$Po extracted from Hartee-Fock type mean field calculations using the Gogny D1S interaction. Calculations have been performed on a 0.05 β_2 grid and the calculated curves smoothed while plotting. Energy minima corresponding to the deformations shown in figure 1.2 are indicated with black dots. Data are from [7]

generated by the Z=82 magic shell gap.

For the Rn and Ra isotopes the situation is more ambivalent in the light of these calculations. As can already be seen from figure 1.2, no strong deformed minima develope in these nuclei. Closer inspection of the data reveals that these isotopes are probably very γ-soft with mean deformations around $|\beta_2|$=0.15.

Several dedicated calculations have been published on Pb nuclei. Methods used range from early Strutinsky type calculations [3, 12, 13, 14] with the Woods-Saxon potential via relativistic mean field approaches [15, 16, 17, 18] to nonrelativistic mean field calculations using different parametrisations of the Skyrme force [18, 19, 20, 21, 22]. Most of the aforementioned calculations had some trouble in describing the observed phenomena. Only the most recent beyond mean field calculations [23, 24, 25, 26] manage to describe the low spin behaviour of the neutron deficient isotopes accurately. A completely different approach to the mean field models was used originally by Heyde et al. [27, 28]. In this shell-model based approach the different 0^+ states, corresponding to the different minima of shapes are created as $n$particle-$m$hole *intruder* excitations across the Z=82 shell gap. Since full shell model calculations are not possible for nuclei this heavy, different variants of the algebraic Interacting Boson Model (IBM) have been used to calculate the properties in Pb nuclei in a rather satisfactory manner [29, 30]. The $n$particle-$m$hole nomeclature has been widely adopted by the community studying shape coexistence in the region. Very often the prolate structures are referred to as 4p-4h intruder states and the oblate states as 2p-2h intruders, even without any direct connection to the shell model or IBM picture.

For Po isotopes especially detailed mean-field calculations of the low-spin structures are much more rare, though several investigations of the superdeformed regime exist [14, 22, 31]. Very early on, May et al. [12] predicted several low-lying states to be present in light Po nuclei. The paper by Smirnova et al. [32] might be the only systematic, modern beyond-mean-field calculation available. Results on ^{194,196}Po have been included in experimental papers of lifetime measurements [33, 34, 35]. Fortunately, several investigations using the IBM approach have been published [29, 36, 37, 38].

Systematical theoretical structure investigations on the N<126 Rn and Ra nuclei are practically non-existent. Several shell-model calculations have been performed in the vicinity of the neutron shell closure. The calculation by Zemel and Dobes [39] using the IBM approach coupled to two-quasiparticle excitations is the only one available in the literature which extends somewhat further away, namely to ^{202}Rn and to ^{204}Ra.

It should be noted that in most of the mean-field calculations prolate superdeformed minima lie very low in energy also in the very neutron deficient Z≥82 nuclei, in some cases becoming the ground states. In Pb isotopes superdeformed bands have this far been identified experimentally down to ^{190}Pb[40] and in Po isotopes only in ^{198}Po[41]. No superdeformed bands have been identified in neutron deficient Rn or Ra isotopes. Whether this is a consequence of the models predicting spurious minima or the failure of the experiments to populate and identify such highly deformed structures in these very fissile systems remains to be seen.

1.2 Experimental background

In figure 1.4 the variations in the root mean square (RMS) charge radii data for the ground states of the even-Z nuclei in the vicinity of the Z=82 shell gap is shown. Practically all of the data has been acquired through collinear laser spectroscopy. The figure presents all currently available *direct* data on the shapes of the isotopes in question. It is assumed that the deviations from the spherical finite range droplet model (FRDM) rms radius [42] are caused by deformation, if the compressibility of the nuclear matter can be considered to be constant. The sign of the deformation can not be extracted from the data.

Trying to explain the behaviour of the radii purely relying on the ground state properties would be very challenging. Fortunately studies of the excited structures can shed light on the mechanisms causing the apparently random variations in the ground state properties. Taking the Pt (Z=78) isotope chain as an example, the modified energy level systematics are plotted together with the radius data corrected for the bulk behaviour in figure 1.5. The sudden increase and saturation of the observed deformation in the radii data is explained in the $n$particle-$m$hole intuder picture as a more deformed intruder configuration reaching the ground state in isotopes near the N=104 mid-shell. In the figure the energy levels are normalised to the 0p-4h spherical or weakly deformed state having zero energy. In Hg (Z=80) isotopes the intruding structure does not reach the ground state in even-even isotopes, but in the odd-even isotopes the unpaired $i_{13/2}$ neutron is enough to polarise the nucleus to assume strongly deformed shape near the mid-shell when coupled to the intruder configuration. The Pb isotopes are "shape-stabilised" by the Z=82 magic number and remain (near) spherical throughout the chain of isotopes. The recent data on the Po isotopes from CERN, ISOLDE [45] reveals a strong onset of deformation in isotopes with N<114. The experimental data on Rn and Ra is rather old and does not extend far from the N=126 shell closure, thus remaining near spherical.

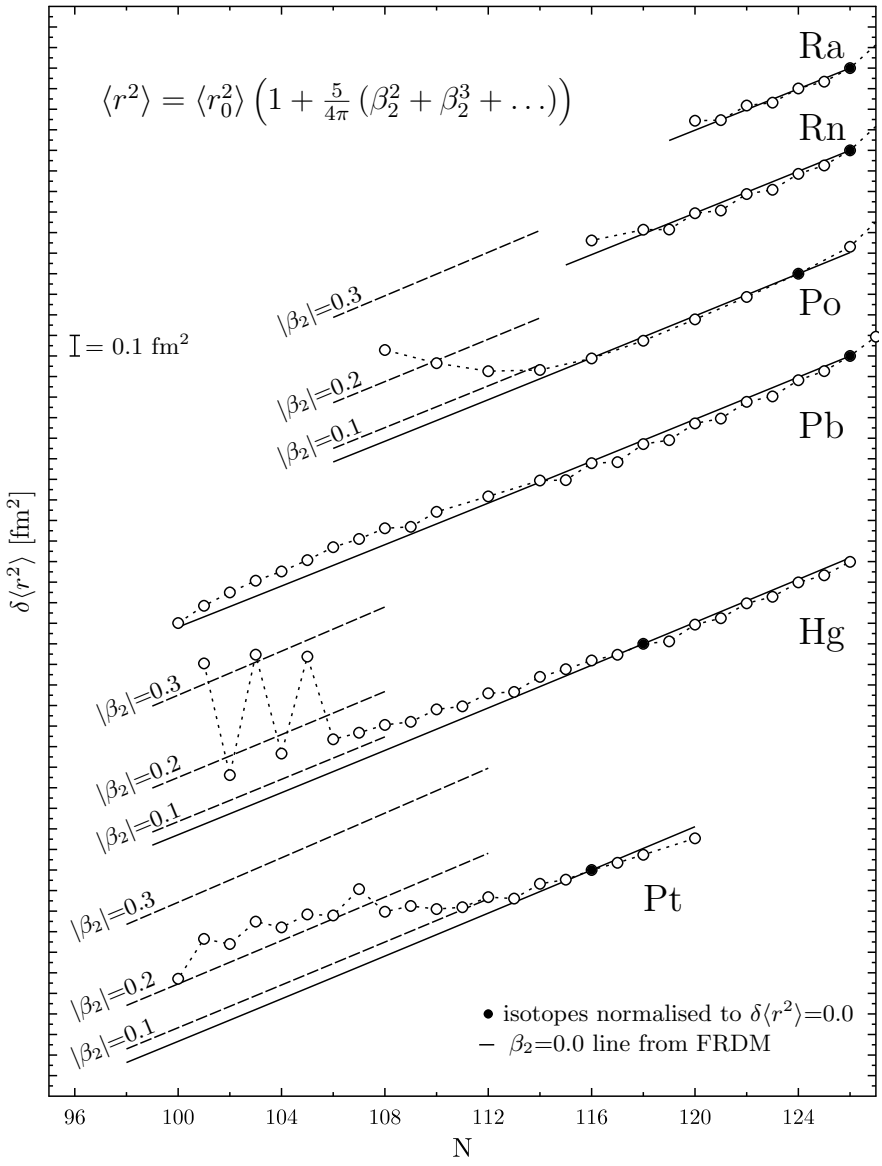

Figure 1.4: The root mean square charge radii data for the ground states of the even-Z nuclei in the vicinity of the Z=82 shell gap. Isodeformation lines for the isotopes exhibiting large deviations from the spherical FRDM are shown. The shift between the isotopes is arbitrary. Data are from: Pt [43], Hg [44], Pb [11], Po [45], Rn [46] and Ra [47].

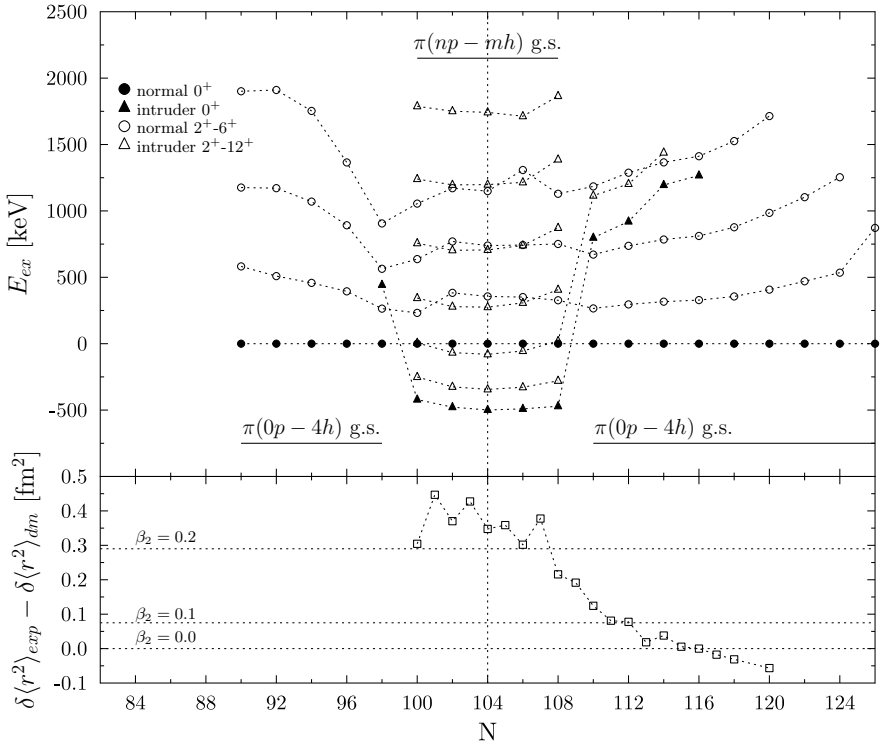

Figure 1.5: Radii and energy level systematics for the Pt nuclei. Energy level systematics have been normalised to the 0^+ state of the 0p-4h configuration. A droplet model reference for $\beta_2 = 0.0$ has been subtracted from the radius data. Data for the energy levels are from [48] and radii from [43].

As in the case of Pt nuclei, the information on the excited states has been crucial in understanding the behaviour of the radii also in Hg, Pb and Po nuclei [1]. These studies also provide information on the very neutron deficient nuclei, for which the direct data on the shapes has not yet been measured. The review of the in-beam γ-ray studies of neutron deficient Hg, Pb and Po isotopes by Julin et al. [2] covers most of the experimental data on the even-even isotopes in Pb and Po isotopes prior to this work. The identification of the γ-rays in ^{190}Po, discussed in the review, was later published in a separate paper [49]. Later on another investigation on ^{190}Po was published by Wiseman et al. [50]. An isomeric state in ^{192}Po, likely to have I^{π}=11^{-}, was reported in ref. [51] in 2003. In the wake of the large interest generated by the observation of three low lying

0^+ states in ^{186}Pb [4], a high statistics in-beam study was performed and it revealed an excited, likely oblate, band in the isotope [52, 53]. The lifetimes of nuclear levels provide an invaluable insight into the underlying physics. Lately, lifetimes of low lying yrast states have been measured in ^{186,188}Pb,^{194}Po[33, 34] and in ^{196}Po[35] providing direct evidence of collectivity in these nuclei. All the data available supports the picture, in which two intruder configurations play major role in Pb and Po nuclei. Above the mid-shell, the oblate 2p-2h intruder configuration is observed at low excitation energies, even becoming the ground state in ^{190,192}Po. At the mid-shell, the prolate 4p-4h configuration intrudes down to low energies, being practically degenerate with the oblate configuration in N=104 nuclei. Below the mid-shell the oblate intruder vanishes quickly, while the prolate configuration is observed in Pb isotopes down to N=100. In Po isotopes the yrast band in ^{190}Po resembles the known prolate bands in Hg and Pb nuclei, indicating the onset of prolate deformation also in the Po chain.

To date, ^{198}Rn, studied in one of the first RDT experiments at JYFL [54] is the lightest even-even Rn isotope, for which excited states are known. The odd-even isotopes have been recently explored down to a mass unit lighter [55] by the JYFL-KTH collaboration. Dobson et al. [56] have made extensive studies of Rn isotopes, in which the onset of deformation should take place, again at JYFL. The lightest Rn isotopes resemble the Po isotopes four mass units lighter. By analogy, it is therefore proposed that in ^{198,200,202}Rn the oblate intruder already plays a role in their structure.

For Ra isotopes, a brief report on excited states in ^{210,208,206}Ra by Cocks [57] was published in 1999. Since then, three further studies of the isomers identified in ref. [57] have been published. Two papers from the Yale SASSYER separator [58, 59] on the isomeric states in ^{208,210}Ra, respectively, have been published. Another study of the isomer in ^{210}Ra originating from GSI was published by Hessberger et al. [60]. In ref. [57] the behaviour of the yrast 8^+ state in ^{206}Ra is proposed to reflect the onset of deformation, slightly earlier than would be expected from a comparison with the Rn and Po isotopes.

In-beam γ-ray spectroscopy is not the only way to study shapes and their coexistence in exotic nuclei. More often α-decay studies are more efficient, especially in the very exotic cases. The special property of the α-decay process, preferential population of the daughter levels of similar structure and spin-parity, has been exploited in the shape coexistence scenario extensively. Since all even-even nuclei have 0^+ ground state spin and parity, the decays from the ground states to the *coexisting* 0^+ states have anomalously high branching ratios, if the ground state to ground state decay would result in a change in configuration and the ground state to excited state decay would not. Together with the observation of the decay of the excited 0^+ state, α-decay has probably

been the most succesfull tool of the trade in the Pb region. A review of the early decay work spearheaded by the Leuven group can be found in ref. [61]. Since then, most of the published results are from the SHIP separator at GSI and from RITU at JYFL [4, 62, 63, 64, 65, 66, 67, 68] to include only the ones dealing strictly with shape coexistence in even-even nuclei in the region.

Another way to investigate the low lying 0^+ states, which decay only by internal conversion, is to try to measure the prompt E0 decays of the states. Attempts to locate the excited band heads via in-beam conversion electron spectroscopy in several mid-shell Pb and Po nuclei have so far failed, apart from a study of ^{188}Pb by Le Coz et al. [69].

In this work, the knowledge of excited states in Pb nuclei has been advanced to the proton dripline, namely to ^{180}Pb. All the Ra isotopes studied by Cocks [57] have been revisited and excited bands,of a similar origin as observed in the mid-shell Pb nuclei, have been searched for in the Po nuclei. Further motivation for each case is provided in the corresponding chapters.

1.3 Experimental equipment and methods

The isotopes studied in this work are indeed very exotic. In the worst case they are only produced at the rate of approximately two, three atoms per hour. If the production would be background free, this would pose no problems. Unfortunately the nuclei of interest are embedded in a sea of byproducts which can be produced at rates tens of orders of magnitude higher. The transportation of the species of interest away from the production site to be measured in a more hospitable environment is also out of the question since the nuclear levels in question have lifetimes shorter than 10^{-9} s. Clerarly very specific equipment and methods are necessary to separate the signal from the vast background.

1.3.1 Detector and separator systems

In this work, two incarnations of the JUROGAM HPGe array have been used to detect the prompt γ-rays. JUROGAM I, used in the Po and Ra experiments, was built using 43 EUROGAM Phase I type [70] or GASP type [71] tapered, Compton suppressed HPGe detectors. The array used the infrastructure of the EUROGAM II array and the geometry of the original EUROGAM I array [72]. The absolute efficiency of the array was $\sim$4.5% at 1332 keV. More information on the array can be found from ref. [73]. In the Pb experiment the upgraded

JUROGAM II array was used. The rings of tapered detectors around θ=90° were replaced by EUROGAM II type clover detectors [74]. The EUROGAM II [72] geometry was used, allowing the use of 24 suppressed clover detectors and 15 tapered detectors. The efficency of the upgraded array is about 6% for 1.3 MeV γ-rays. Both arrays were operated at the target position of the RITU separator.

Prompt conversion electrons from ^{192}Po were measured with the SACRED device [75]. SACRED was a normal-conducting electron solenoid operated in collinear geometry at the target position of the RITU separator. The large δ-electron flux was suppressed by a high voltage barrier and the electrons were measured using a 25-element annular Si-detector. The detection efficiency was measured to be about 10% from 150 keV to 350 keV electrons. The resolution reached for 320 keV electrons from a ^{133}Ba source was 3-4 keV FWHM.

Recoil decay tagging (RDT) studies at JYFL are centered around the gas-filled separator RITU [76]. The device is a very efficient gas-filled recoil separator with transmission approaching 80% for symmetric reactions[77]. The downside of the high transmission is the complete lack of mass resolution. Identification of the recoiling products has to rely entirely on the decay properties. RITU was designed and initially used for α-decay studies in the Z>82, N<126 region thus it is especially suited for the studies undertaken in this thesis.

In all of the experiments the focal plane of the RITU separator has been equipped with the GREAT tagging spectrometer [78]. GREAT consists of:

- Two double sided silicon strip detectors (DSSD), into which the recoiling evaporation residues are implanted and are also used to detect their subsequent decays. Each detector has 60 vertical strips and 40 horizontal strips making a total of 2400 logical pixels.
- A multiwire proportional counter (MWPC), which is placed in front of the DSSDs. The signal from the MWPC can be used to identify the incoming recoils and in anti-coincidence to separate the decay events from the recoil like events.
- A box of 28 Si PIN-diodes. PIN diodes can be used to detect the charged particles which are produced in the different decay processes within the DSSD, but escape out.
- A planar Ge-detector placed directly behind the DSSDs within the vacuum chamber. The detector can be used to measure the low energy γ-rays and X-rays in a very efficient manner.

- A large volume clover detector positioned above the DSSDs, outside the vacuum chamber. The clover is used to measure high energy γ-rays, for which the effiency of the planar detector is low.

The standard GREAT system can be varied depending on the experimental requirements. The simplest of modifications is the addition of two more large volume Ge detectors outside the vacuum chamber, which was the approach taken in the Ra experiments.

1.3.2 Electronics and data acquisition

A new type of data acquisition, Total Data Readout (TDR) [79], was developed for the GREAT spectrometer. To reduce the adverse effects of dead-time induced by wide common gates required in some of the tagging experiments, the whole system was designed to be free running. All electronics channels run asynchronously, thus not inducing dead time on each other. The data items can be correlated to each other by using timestamps, acquired from the common 100 MHz clock distributed thoughout the system. The system is designed to maintain the time order of events at all stages, resulting in a single stream of time-ordered data containing the data from all the electronics channels.

The adverse side of this approach is that the natural grouping of data into events, inherent to the common gate systems, is lost. The data stream is not structured in any way and physically meaningful events must be constructed in software at a later stage. The event building and analysis of the TDR data is discussed in detail in the next chapter.

Initially all the electronics were analogue and the signal processing path from the pre-amplifiers to the TDR ADCs were built using commercially available NIM and CAMAC standard linear and timing filter amplifiers and constant fraction discriminators. The ADCs were purpose built VXI units. The ADCs were read out by VME processors which collated and merged the data from different ADC cards to be finally passed on to PCs for analysis and storage.

The latest developement has been the inclusion of digital electronics into the system. The count rates in the HPGe and Si detectors at the target position were limited by the bandwidth of the analogue processing. Two approaches have been used; one interim utilising TNT2 cards [80] and one, permanent solution, developed for the SAGE project (discussed in the final chapter) using commercial Lyrtech ADC modules. The processing path has been altered slightly to accomondate the higher data volumes generated by the digital elec-

tronics, moving the merge stage onto PC hardware.

1.3.3 Recoil decay tagging

The current method of choice for in-beam studies of heavy, exotic, short-lived neutron deficient nuclei is recoil decay tagging (RDT). The technique was first used in GSI at the late 1980's [81, 82]. Paul et al. [83] "re-invented" the technique at Daresbury in the mid-1990's. The method is a very straight forward addition of standard γ-ray or conversion electron in-beam spectroscopy on top of correlations based decay spectroscopy performed with a recoil separator. The main principle of the method is the delayed identification of the measured prompt radiation by transporting the source of the radiation into a relatively background-free location where it can be identified by it's characteristic decay.

In practice, with the current setup, the process is executed in reverse. When a decay matching the characteristics of the decay used as a "tag" is observed in a DSSD of the GREAT spectrometer the tagging process is triggered. The history of the pixel in which the decay took place, stored in the memory of the computer used to analyse the data, can be played back. If the recoil implantation corresponding to the decay is found within a reasonable search time at the same location, a search for the γ-ray or electron emission related to the recoil implantation can be done. In in-beam RDT the prompt radiation emitted within a time interval before the implantation, corresponding to the average flight time of the recoiling nuclei of interest through the recoil separator, is taken to be correlated with the recoil already identified by the decay characteristics. The method can be easily adapted for isomeric decays following the recoil implanatation and for cases in which a single decay does not provide a clean tag.

Chapter 2

Analysis of TDR data with Grain

The Grain software package was developed by the author, alone, to provide a way to analyse the data produced by the TDR data acquisition system (DAQ)[79]. TDR was developed as a part of the U.K. GREAT project [78] to instrument the new focal plane spectrometer. The triggerless nature of this novel DAQ meant that the existing data analysis systems could not be used with it without using an intermediate event builder software. Grain was developed to provide a single system capable of building the events from the TDR data stream and to provide a data analysis framework, which would cater especially for the more and more complicated correlation analyses required by the RDT and decay experiments. The software is distributed through the Grain website (`https://trac.cc.jyu.fi/projects/grain`). To this date, Grain has been used to analyse data resulting in 47 peer reviewed journal articles listed in the list of publications of the thesis.

2.1 Publication

The article on Grain published in Nuclear Instruments and Methods in Physics Research Section A: Accelerators, Spectrometers, Detectors and Associated Equipment in Volume 595, Issue 3 on the 11th of October 2008 is included on the following six pages.

Nuclear Instruments and Methods in Physics Research A 595 (2008) 637–642

Contents lists available at ScienceDirect

Nuclear Instruments and Methods in Physics Research A

journal homepage: www.elsevier.com/locate/nima

Grain—A Java data analysis system for Total Data Readout

P. Rahkila

Department of Physics, University of Jyväskylä, P.O. Box 35 (YFL), FI-40014 University of Jyväskylä, Finland

ARTICLE INFO

Article history:
Received 21 November 2007
Received in revised form
28 July 2008
Accepted 11 August 2008
Available online 20 August 2008

Keywords:
Data analysis
Total Data Readout
Recoil Decay Tagging
Java

ABSTRACT

Grain is a data analysis system developed to be used with the novel Total Data Readout data acquisition system. In Total Data Readout all the electronics channels are read out asynchronously in singles mode and each data item is timestamped. Event building and analysis has to be done entirely in the software post-processing the data stream. A flexible and efficient event parser and the accompanying software system have been written entirely in Java. The design and implementation of the software are discussed along with experiences gained in running real-life experiments.

1. Introduction

Nuclear physics experiments are usually instrumented using conventional common dead time data acquisition systems which are triggered by an event in a pre-defined detector. In decay spectroscopy and Recoil Decay Tagging (RDT) [1–3] experiments (in which decay spectroscopy is combined with in-beam spectroscopy) these systems inherently suffer from dead time losses since rather wide common gates have to be used in order to collect all the required information. These problems grow worse if either the focal plane count rate or the common gate width is increased. The former condition often arises from the fact that the reaction channel under study may form only a minor fraction of the total counting rate of the implantation detector. In the latter case one is usually either studying isomeric decays with half-lives of the order of tens of microseconds or using them as a "tag" in Recoil Isomer Tagging (RIT) experiments. To overcome these problems a novel Total Data Readout (TDR) method [4] was developed by the GREAT collaboration as part of a project to build a highly sensitive tagging spectrometer [5].

TDR is a triggerless data acquisition system in which all the electronics channels operate individually in free running singles mode. All the information is read out asynchronously by the front-end electronics consisting of gated analog-to-digital converters (ADCs) and bit-pattern registers. Data items are time-stamped with 10 ns precision using a 100 MHz clock signal, which is distributed throughout the whole system. The data are subsequently ordered within the TDR DAQ in a collate and merge software layer, after which the data form a single time-ordered stream ready to be processed by the analysis programs. Unlike the data emerging from a conventional data acquisition system, the data from the TDR collate and merge layer are not structured or filtered in any way, apart from the time ordering. Temporal and spatial correlations required to form events out of the raw data stream and the filtering to remove unwanted or irrelevant data have to be done entirely in the software which processes the data stream.

Grain was developed to provide a complete, self-contained, cross-platform data analysis system which could be used to analyse the raw TDR data stream. The core of the system lies in three functions: in the ability to form physically meaningful events from the data stream, in providing a relatively simple way for the experimentalist to run a physics based "sorting code" to extract the results for each experiment from these events and in allowing the user to visualise and analyse the data using histograms and n-tuples through a simple graphical user interface (GUI). A schematic of the Grain functionality is shown in Fig. 1. The main purpose of the software is to provide a tool for the online analysis at the RITU separator at the Accelerator Laboratory of the University of Jyväskylä (JYFL), where the TDR system along with the GREAT spectrometer are currently located, and to facilitate the subsequent offline analysis of the experimental data. The TDR DAQ currently consists of 480 independent spectroscopy channels each capable of running at 10 kHz. The analysis system should thus be able to process data up to the theoretical maximum counting rate of 4.8 MHz (corresponding to about 38 MB/s data rate as 64 bit data words are used) over the whole duration of an experiment, which can span up to a month of runtime. The GREAT TDR system also

E-mail address: panu.rahkila@phys.jyu.fi

0168-9002/$ - see front matter © 2008 Elsevier B.V. All rights reserved.
doi:10.1016/j.nima.2008.08.039

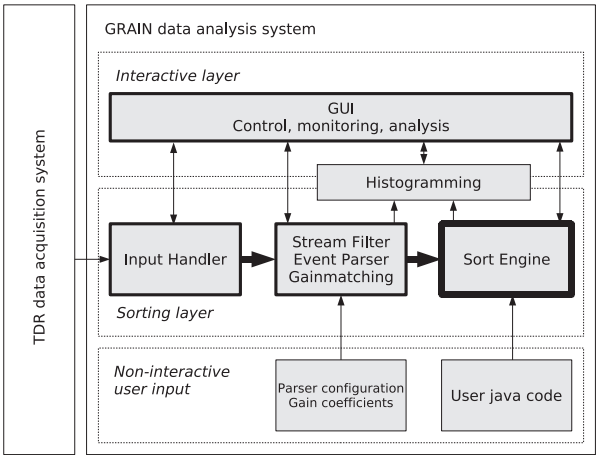

Fig. 1. Schematic of the data processing in Grain. Each data processing sub-task (thick boxes) runs on a separate thread which are interconnected by FIFOs (thick arrows) and supervised by the master thread running the GUI.

includes an event builder software, TDREB [6]. In normal online running conditions TDREB is used to filter data before it is passed on to Grain for online analysis and to the tape server for storage. Grain is used in offline analysis as a completely stand-alone system, regardless whether data under analysis have been filtered by the TDREB or not, and can be used online as stand-alone solution if required.

Grain has been implemented entirely in Java. The portability, object-oriented programming language and the incorporated, extensive user interface and networking libraries were the main motives behind the decision. Java has had a reputation of being too slow for calculation intensive tasks, such as data analysis, but in the recent years the arrival of just-in-time (JIT) compilers have lifted the performance to the same level as native, compiled languages (see e.g. Ref. [7]). Previous reports on the usage of Java in similar tasks [8,9] were also found to be mostly positive. The Grain executable is available for download at the development web page [10].

2. Stream filtering and event parsing

2.1. Stream filtering

Prior to building the events the TDR data stream must be filtered against unwanted data, which usually consists of vetoed and piled up signals. In traditional systems the vetoing and pile-up detection was incorporated into the front-end electronics and the data acquisition system would normally never see these data. In the TDR system the data analysis software is required to perform these tasks, though the TDR ADCs have a limited hardware-veto capability. For example, in the current JYFL TDR setup events from the Compton suppression shields of the target array are read out as bit-pattern data. Thus, the data from the target array germanium detectors and their BGO shields must be correlated pairwise in software in order to perform the suppression.

Pile-up rejection is based on the TDR ADCs capability to detect gates arriving at the ADC during the processing of the previous gate. These data are included in the stream as separate special data items and thus each channel needs to be self-correlated in time to find the piled-up data. Vetoed or pile-up data can be either discarded or marked and included in the events.

2.2. Event parsing

Two types of event parsers have been developed so far. Decay spectroscopy and tagging experiments require a parser which constructs events in which the trigger is any signal from the implantation detector. Stand-alone in-beam experiments require a trigger based on the multiplicity of hits in the detector array. In both cases time domain correlations were selected as the first stage of the event builder strategy. This was mainly done in order to maximise the input capacity of the system as the conditions used in the first stage of event parsing require only a single dynamic parameter, the time stamp, and a static definition of which data acquisition channels constitute the triggering detector group.

The decay/RDT event parser is almost entirely based on the time structure of the stream. A typical time structure of the stream, with respect to any signal in the implantation detector, taken from a tagging experiment at RITU is presented in Fig. 2. The individual components forming the structure can be roughly divided into three groups depending on the placement and role of the detector groups: (a) preceding, (b) prompt and (c) delayed events. Typical examples of these are presented in the upper panels of Fig. 2. In panel (a) the time spectra of the germanium array at the target position are shown. Flight time of the recoils through the separator is $\sim$1 μs. Panel (b) shows the timing of the transmission detector (a multiwire proportional counter) placed 240 mm upstream from the implantation detector. Panel (c) shows time structure of events in the planar germanium detector placed

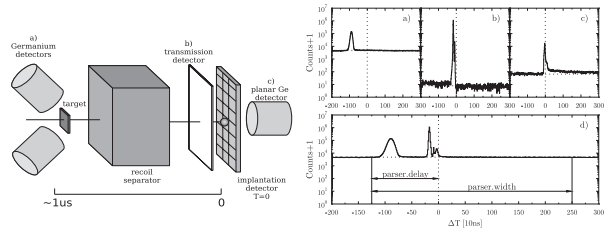

Fig. 2. Schematic illustration of a typical RDT setup and the time structure of a typical RDT experiment data stream with respect to any signal in the implantation detector. Panels (a)–(c) represent the typical response of some individual detector groups. Panel (d) shows the summed structure and the main event builder timing parameters.

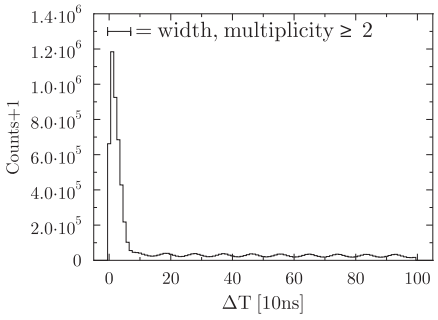

Fig. 3. Time structure of the TDR stream from a stand-alone γ-ray experiment. Data are histogrammed if more than one hit is registered in 1 μs window. In normal running conditions a 70 ns window would be used, as indicated in the figure. Oscillations in the background are caused by the structure of the beam produced by the JYFL K130 cyclotron.

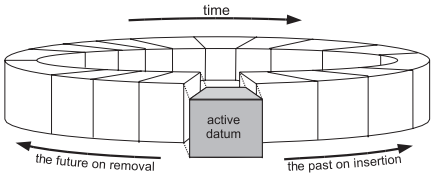

Fig. 4. Event search is performed in a ring-buffer, which provides efficient access to data preceding and following any data item.

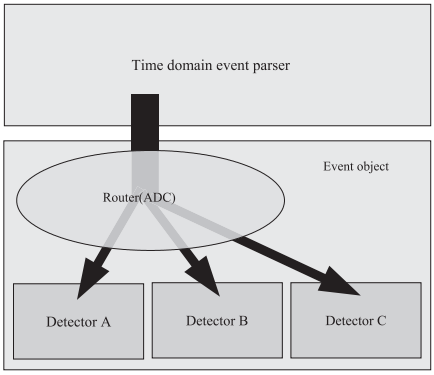

Fig. 5. Data are routed to the detector objects within the event object based on the origin of the data.

next to the implantation detector exhibiting prompt and delayed components.

In decay or RDT experiments events can be simply defined at the first stage as a time slice of the stream, which is triggered by any datum from a predefined group of ADC channels. As the data are buffered in time order, it is possible to easily extend the slice to cover also data in the past and in the future with respect to the triggering data. The parameters needed to construct the slice are the address of the triggering channel, offset of the slice (delay) and the extent of the slice (width). By varying these parameters the parser can be configured for different types of requirements of RDT, RIT or decay spectroscopy experiments.

Pure in-beam experiments usually use a hit-multiplicity trigger where a certain number of coincident hits is required in a defined time window. In the case of TDR the event parsing is rather straightforward. As the data are already time ordered and filtered, and can be easily buffered in memory, one can simply count the number of hits over a given period after each individual hit. The input parameters required are the width of the coincidence window, the set of channels over which the multiplicity is calculated and the minimum required multiplicity. Fig. 3 shows a typical time structure of the TDR data stream in a stand-alone γ-ray experiment.

Both event parsers have been implemented around a ring-buffer, which holds the data objects. Access to the data preceding and following a certain data item can be done by iterations in the buffer. On insertion and removal the data item is checked whether it is a triggering item, a vetoing item or a piling-up item. In any of these cases corresponding data are searched in the buffer and flagged if found. All the data are checked on removal whether it is flagged as triggered and if so, dispatched to the next level of event parser. Data are also gainmatched at this stage using user provided gainmatching coefficients (Fig. 4).

Once the group of data forming an event has been identified, the internal event structure needs to be assigned. At the second

stage of event building the data forming the event slice are fed into an event object. The data items are routed into sub-objects describing different detectors according to the source of the data i.e. the ADC or bit-pattern unit channel number. The routing table is defined in the sub-detector objects at the implementation time. A schematic drawing of the routing is shown in Fig. 5. Several different event types have been predefined and users select the type which is appropriate for their analysis from the user interface.

3. System implementation

The general design of the analysis system is shown in Fig. 1. In order to benefit from modern computer hardware with multiple processor cores available on most machines, the data processing system was designed to be multithreaded. Each individual main subsystem thread is indicated in the figure with a thick border. Users interact with the GUI running the master thread and providing interactive analysis functions as well as serving as the control thread for data sorting jobs. The sort layer consists of an input handler thread reading raw TDR data from a disk, tape or network source, an event builder thread which filters and gainmatches the data and constructs the events and a sort engine thread which uses the user code to extract the relevant data from the events. The data are relayed in the sorting layer from thread to thread using first-in, first-out buffers (FIFOs) which are indicated in the figure by thick arrows. The GUI thread starts the worker threads at the beginning of each data sorting job.

3.1. Sort engine

The sort engine uses the Java dynamical class loading capability. Grain provides abstract (skeleton) sorter classes which the user needs to implement and which provide access to the event data. Users can thus write their own data reduction routines in Java using all the features of the language as long as this inheritance relationship is fulfilled. Compiled classes can be loaded into the Java Virtual Machine (JVM) dynamically at runtime. Histogramming and other basic analysis services are provided via JAIDA [11], the Java implementation of the AIDA (Abstract Interfaces for Data Analysis) definition [12]. A new binner had to be added to the JAIDA histogrammer since rather large multidimensional histograms are required in nuclear physics analysis. The histograms and n-tuples created in the sort engine are available through the GUI at runtime.

3.2. Correlation framework

During the last decade the RDT technique [1–3] has been widely used in the studies of the structure of neutron deficient nuclei and super-heavy nuclei (see e.g. review articles [13,14]). In RDT the identification is based on spatial and temporal correlations of the recoiling reaction product and the subsequent, often discrete, decay events. Similar correlation tasks are used also in pure decay spectroscopy.

A large amount of information per event needs to be stored in a concerted manner often for several hours and over several event generations in order to perform these correlations. The Grain correlation framework is based on the discrete position sensitivity provided by the double-sided silicon strip detectors used in GREAT and the fact that all the event information is already encapsulated in the event object. The framework consists of a container object which provides a time ordered, time constrained stack of event objects per implantation detector pixel and routines to insert an event into the container and to retrieve the history of any given pixel based on the current event. The framework is presented to the user as a class library which is available to be used in the sort code. This framework simplifies correlation analysis greatly as the user does not need to implement event accounting and memory management and they are handled in a consistent manner for all the users.

3.3. User interface and analysis functions

The Grain GUI has been implemented using the standard Java Swing toolkit and Java2D graphics (see Fig. 6). A standard GUI design, with menus and toolbars, was selected as it is already familiar to most users. Histograms can be browsed with a tree widget and displayed on the main panel, several at a time if required. Information about the progress of the analysis jobs and the results for the interactive analysis are displayed in the logger window. Standard zooming and scrolling functions are provided for both one- and two-dimensional histograms. Peak-area integration and fitting of Gaussian peak-shapes and exponential decay-curves are provided for one-dimensional histograms. Two-dimensional histograms (matrices) can be sliced either on the standard GUI or on a separate widget geared towards coincidence analysis. N-tuples can also be used in the interactive analysis through AIDA evaluators and filters. Histograms can be exported to ASCII and Radware [15] formats. The ASCII format can also be imported along with ROOT histograms through the hep.io.root package [16]. The spectrum view can be printed using the printing system provided by the operating system or exported to a variety of formats. The AIDA XML data format used by Grain through JAIDA libraries to store histograms and n-tuples is an open standard. Several other AIDA-compliant tools [9,17–19] can be used to read, view and analyse the files instead of Grain if so required.

4. Performance and usage

4.1. Performance

The data sorting performance of the whole analysis system has been analysed in two ways. First, only simple through-put tests were run on a modern computer with a dual-core AMD processor running 64-bit Linux operating system and 64-bit Java version 1.6 from Sun Microsystems. Later, the performance of different parts of the data sorting chain has been analysed using the Netbeans Java Profiler [20].

To demonstrate the performance of the sorting a typical RDT experiment was selected as a test case. Actual data from an experiment using a heavy ion fusion evaporation reaction $^{36}Ar + {}^{144}Sm \rightarrow {}^{180}Hg^{*}$ to produce light Hg isotopes were used. In optimum operating conditions the total counting rate of the detectors was about 400 kHz, mainly originating from the target array germanium detectors, corresponding to a data rate of about 3.2 MB/s from the TDR. Data were written to disk without any TDREB prefiltering, and later analysed offline. The throughput was derived from the time it took to analyse a 10 GB portion of the data using different triggering schemes. The results are shown in Table 1. It should be noted that the RDT triggering would be used to extract data from reaction channels produced with very low cross-sections whereas the gamma-multiplicity triggering would be used for different reaction channels with higher cross-sections, making comparison between the trigger types somewhat meaningless. In early experiments the histogramming of raw data was noticed to have a serious impact on the sorting performance

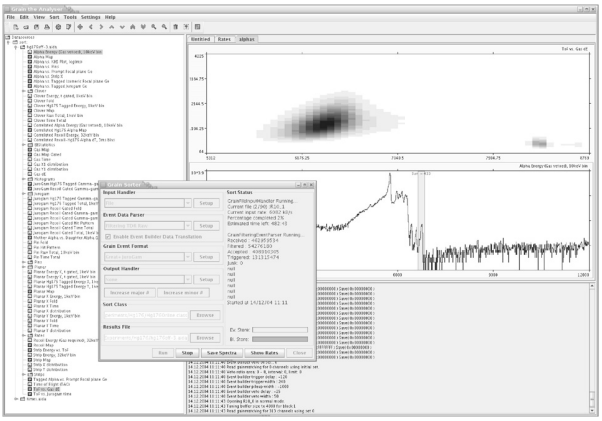

Fig. 6. Screenshot of the Grain GUI. Main window displaying two- and one-dimensional histograms, histogram tree and logger window along with the sort control window are shown.

Table 1
Maximum throughput of the Grain sorter in different configurations

Trigger	With raw histogramming (MB/s)	W.o. raw histogramming (MB/s)
RDT	19	44
γγ	13	22
γγγ	17	28

See text for details.

on-line. This is clearly reflected in the current results and is likely to be caused by the high memory bandwidth required to constantly update the histograms. A buffering histogramming subsystem is used to alleviate the problem somewhat. Online histogramming of the raw data is also performed in the TDR DAQ, so it can be safely turned off if the performance degradation is too high.

The current implementation of the system can effectively use two processor cores per sort, while in uniprocessor systems the threading model causes higher overheads and the performance is degraded. An upgrade to allow the use of several parallel sorting pipelines to utilise new multicore chips is in planning. Apart from the threading issues the performance scales rather linearly with the integer operation performance of the processor core in question. As especially the correlation analysis can be quite memory-intensive, high bandwidth memory architecture and large CPU cache can result in substantial increases in the performance.

As can be seen, the throughput without raw histogramming is over an order of magnitude higher than a typical RDT experiment currently requires and close to that for stand-alone experiments. In decay experiments data rates are always much lower as the target area detectors are not used. In the case the input rate would exceed the rate Grain can process data real-time, a safety feature which starts skipping input data buffers is implemented in the input handler receiving data over the network in the online configuration. The complete data stream can thus still be written to storage by the TDR acquisition system at the expense of loss of statistics in the online analysis.

The event parser has been found to be the bottleneck in the sorting performance by using the Java profiler. About 65% of the execution time is spent in the event parser thread, out of which about a half is spent in the actual event search in the ring-buffer. This bottleneck is partly alleviated by the multithreading as the parser utilises a single processor core and the other parts of the system run in the other available cores.

4.2. Usage

Grain has been used as an on-line analysis tool in over 50 experiments since 2002, catering for very different experiments ranging from decay spectroscopy of very heavy elements [21] to RDT studies in the $A\sim100$ region [22] and the development of the novel β-tagging technique [23]. In vast majority of cases Grain has also been the main tool in offline analysis. In total 23 peer-reviewed papers using Grain were published 2004–2007.

5. Conclusions

Analysis of the triggerless, TDR generated data have been implemented in a flexible, efficient manner. The use of Java language and platform has been a major contributor to the success of the system. Platform independence has granted simple installation and operation on the three current major personal computer operation systems, making it easy for users to deploy the software where required. Java language and the use of object oriented techniques have not only simplified development of the system itself, but has simplified the users task of sort code writing, especially when complicated correlation schemes have to be used. The amount and variety of users and experiments utilising the system as well as the amount of publications for which the data analysis has been mostly conducted using Grain also demonstrates the success of the system.

Acknowledgements

I would like to thank all the people who have used the software and contributed through bug reports and suggestions. This work has

been supported by the EU 5th Framework Programme "Improving Human Potential—Access to Research Infrastructure". Contract no. HPRI-CT-1999-00044 and the EU 6th Framework programme "Integrating Infrastructure Initiative—Transnational Access", Contract no.: 506065 (EURONS) and by the Academy of Finland under the Finnish Centre of Excellence Programmes 2000–2005 (Nuclear and Condensed Matter Physics Programme at JYFL) and 2006–2011 (Nuclear and Accelerator Based Physics Programme at JYFL).

References

[1] K.-H. Schmidt, et al., Phys. Lett. 168B (1986) 39.
[2] R.S. Simon, et al., Z. Phys. A 325 (1986) 197.
[3] E.S. Paul, et al., Phys. Rev. C 51 (1995) 78.
[4] I. Lazarus, et al., IEEE Trans. Nucl. Sci. NS-48 (2001) 567.
[5] R.D. Page, et al., Nucl. Instr. and Meth. B 204 (2003) 634.
[6] Great TDR software ⟨http://ns.ph.liv.ac.uk/tdr_software.html⟩.
[7] J.M. Bull, L.A. Smith, L. Pottage, R. Freeman, Benchmarking java against C and Fortran for scientific applications, in: JGI '01: Proceedings of the 2001 Joint ACM-ISCOPE Conference on Java Grande, ACM, New York, NY, USA, 2001, pp. 97–105.
[8] K.B. Swartz, D.W. Visser, J.M. Baris, Nucl. Instr. and Meth. A 463 (2001) 354.
[9] Jas3 software ⟨http://jas.freehep.org/jas3⟩.
[10] Grain software ⟨http://trac.cc.jyu.fi/projects/grain⟩.
[11] Jaida project ⟨http://java.freehep.org/jaida⟩.
[12] Aida project ⟨http://aida.freehep.org⟩.
[13] R. Julin, K. Helariutta, M. Muikku, J. Phys. (London) G 27 (2001) R109.
[14] R.D. Herzberg, J. Phys. (London) G 30 (2004) R123.
[15] Radware software ⟨http://radware.phy.ornl.gov⟩.
[16] Rootio package ⟨http://java.freehep.org/freehep-rootio⟩.
[17] Openscientist software ⟨http://openscientist.lal.in2p3.fr/⟩.
[18] Physicist interface (pi) project ⟨http://lcg-pi.web.cern.ch/lcg-pi/⟩.
[19] Paida software ⟨http://paida.sourceforge.net/⟩.
[20] Netbeans profiler ⟨http://www.netbeans.org/products/profiler/⟩.
[21] R.D. Herzberg, et al., Nature (London) 442 (2006) 896.
[22] M. Sandzelius, et al., Phys. Rev. Lett. 99 (2007) 022501.
[23] A.N. Steer, et al., Nucl. Instr. and Meth. A 565 (2006) 630.

2.2 Future developments

The Grain package is rather system specific and due to the lack of available man hours, there is no current plan to extend the functionality to deal with data from other sources than the TDR system at JYFL. In the local scope, four main improvements are currently under development:

- User defined mapping of the DAQ channels to the data objects is required. Different configurations of read-out system are required for different experiments and the existing hard-coded mapping would mean increased complexity in the event generation.
- More robust triggering scheme for the multiplicity selection. The current multiplicity trigger does not allow grouping of the DAQ channels into logical groups, thus reducing the usability for example in those cases where the clover detectors should be used as a trigger. The SAGE spectrometer also needs this functionality.
- Data-parallelisation. The system is currently task-parallel. A scheme has been developed which allows also data-parallel operation during off-line analysis, also in the cases where tagging or correlations are used. This would allow more efficient uses of the modern, multi-core processors.
- Developement of a object database driven event storage. In the current implementation it is possible to use "n-tuples" for dynamic analysis. The implementation is rather restrictive and to allow sophisticated analysis without the need to resort the data time and time again, databases with advanced query engines are currently evaluated.

The biggest problem faced in the development is currently the stagnation of the JAIDA project [84]. A decade ago when the Grain developement was started a decision to use AIDA [85] compliant tools was made. At that time the CERN computing division strongly advocated the use of AIDA in the LHC data analysis and with such a large projected user base the choise was considered safe. History has shown that the ROOT [86] based systems have been taken into use and the AIDA developement has practically stopped. In the future it might necessary to re-evaluate the situation and switch from JAIDA to another library offering similar functionality.

Chapter 3

Study of ^{180}Pb: Shape coexistence at the proton drip-line

In-beam γ-ray studies of ^{184}Pb[87] and ^{182}Pb[88] at JYFL in the late 1990's confirmed that the prolate 4p-4h intruder configuration minimises its energy at the N=104 neutron mid-shell, as expected. The rise of the prolate minimum is rather rapid beyond the mid-shell and studies of more neutron deficient lead nuclei should reveal how far the collective excited regime, driven by the intruder configutarions extends. Another interesting question arises from the proximity of the proton drip-line. Already in ^{180}Pb we are at the edge of the proton drip-line since one proton ($S(p)$) and two proton ($S(2p)$) separation energies are listed as 930(50) keV and 200(25) keV, respectively, in the most recent AME mass evaluation [89]. What are the possible effects on the excited spectra of the fact that, based on extrapolation from the Pb level systematics, *all* of the excited states are proton unbound? Furthermore, in a simple shell model picture a neutron sub-shell gap between the $2f^{-}_{7/2}$ and $1i^{+}_{13/2}$ levels is found at N=100. If the neutrons from the shell-model intruder orbital ($1i^{+}_{13/2}$) play crucial role in the collective phenomena, a change in structure could be observed going from $^{182}\mathrm{Pb}_{100}$ to $^{180}\mathrm{Pb}_{98}$.

Before the current experiments performed at JYFL in the spring 2009, very little was known about ^{180}Pb. Toth et al. [90] identified the isotope for the first time 1996 at the Lawrence Berkeley National Laboratory using a rotating

recoil catcher wheel system. From the few α-decays detected they assigned ^{180}Pb to have E_α = 7.23(4) MeV and $T_{1/2} = 4^{+4}_{-2}$ ms. This identification was based purely on expected yields and α-decay systematics. Later, Toth et al. [91] used the Fragment Mass Analyser at Argonne National Laboratory to confirm the identification through mass separation and genetic correlations with daughter nuclei. They cited improved α-decay data; E_α = 7250(15) keV and $T_{1/2} = 4.5(11)$ ms. The number of identified atoms of ^{180}Pb is not explicitly given, but from the mother-daughter correlated spectra one can estimate that approximately ten correlated events were detected.

It is interesting to note that the lightest lead isotope for which detailed theoretical calculations on the excited structures are published is ^{182}Pb [24, 25, 26]. This is because the theorists involved did not expect experimental results to emerge for lighter isotopes in the near future [92, 93].

3.1 Production and Experimental details

In the earlier studies of light lead isotopes at JYFL, rather asymmetric reactions, such as Ca+Sm, were used. For the study of ^{180}Pb a different approach was taken. The first ever RDT experiment[81, 82] employed the reaction ^{90}Zr+^{90}Zr in the radiative capture channel to study ^{180}Hg. These types of cold-fusion reactions are very favourable for RDT, since the number of open evaporation channels is minimised and the competition from fission is also suppressed due to the low excitation energy of the compound nucleus. Exactly the same approach has been used extensively in the in-beam studies of very heavy elements where targets in the vicinity of the the doubly-magic ^{208}Pb are used with beams of doubly-magic ^{48}Ca. For the light lead region no doubly-magic combination of beam and target, which provides the most favourable reaction Q-values, exist. The closest possible alternative is to use the aforementioned symmetric reactions of N=50 targets and beams to reach Pb in a reaction as cold as possible. In this case a combination ^{90}Zr and ^{92}Mo was required. Both Mo-induced [91] and Zr-induced [94] reactions have been used to produce lead nuclei in the past. Unfortunately, neither of the beams was available at JYFL at the time, which lead to the succesfull development of a Zr-beam using a sputtering method by the ion source group.

The newly developed ^{90}Zr beam was accelerated to 400 MeV by the JYFL K130 cyclotron and was incident on a self-supporting, metallic 1 mg/cm^2 target of ^{92}Mo isotopically enriched to 96%. Prompt γ-rays were detected by the JUROGAMII Ge-array. Evaporation residues (ER) were separated from the beam particles and other unwanted products by the RITU separator and were

implanted into the DSSDs of GREAT spectrometer. All detectors were instrumented using the TDR data acquisition and electronics apart from the clover detectors of JUROGAMII for which the TNT2-D digital front-end electonics[80] was used. The experimental equipment is described in detail in section 1.3. Events were constructed from the raw data by the Grain software, which was also used to analyse the data as described in chapter 2.

3.2 Data-analysis and results

The decay event spectra were internally gain-matched and calibrated using the known α-particle energies of ^{177,179,180}Hg and ^{176}Pt taken from [48]. The resolution (FWHM) for the 6 MeV α-particles was measured to be ~25 keV.

The recoil decay tagging analysis was complicated by an α-decaying isomer in ^{179}Tl. The isomer has been recently studied by Andreyev et al. [95] who report α-particle energy of E_α = 7207(5) keV and half-life of $T_{1/2}$=1.46(4) ms. As

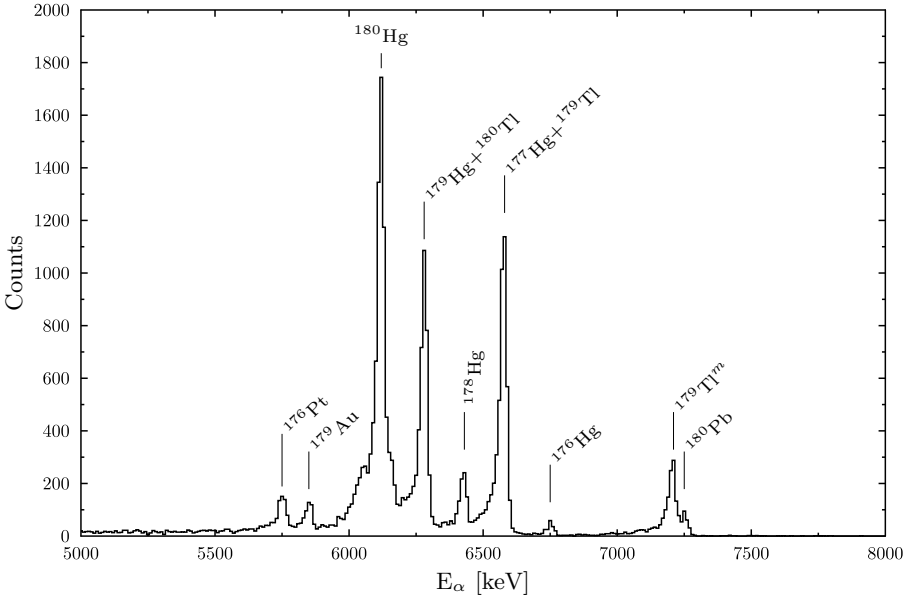

Figure 3.1: A decay event spectrum observed within 16 ms of evaporation residue implantation. The main products that were identified have been labelled.

can be seen from figure 3.1, in which α-decays occuring within 16 ms of recoil implantation are shown, it is populated much more strongly than ^{180}Pb and since the half-life is shorter, it cannot be separated based on the correlation times. Even if the decay energies are separated by over 40 keV, the finite resolution of the detector leads to a situation where ^{179}Tl^{m} and ^{180}Pb can not be completely separated using the standard single recoil-α correlation alone.

In this case genetic correlations within the ^{180}Pb decay chain can be used as a tag in RDT since both the α-decay daughter of ^{180}Pb, ^{176}Hg, and the grand-daughter, ^{172}Pt, have relatively short half-lifes, 20 ms and 96 ms, respectively [48]. The clean separation achieved is demonstrated in figure 3.2, in which the α-decay energies of the mother nuclei are plotted against the α-decay energies of the daughter nuclei for ER-α-α types of chains in which the ER-mother search time was limited to 12 ms and the mother-daugter search time to 60 ms. Now ^{179}Tl^{m} can be easily separated from ^{180}Pb since the α-decay energies of the daughter nuclei differ by more than 300 keV.

Even though the tag generated by requiring full energy α-decays (α_f) of both ^{180}Pb and ^{176}Hg following the implantation of an ER is very clean, the method suffers from a severe loss of efficiency since approximately 40% of the α-particles escape from the detector without depositing their full energy (α_e). It is immediately seen that only $\sim$ 36% of ER-α_f-α_f-chains can be recovered. Fortunately, since the half-life of the ^{180}Pb α-decay grand-daughter is also rather short, some of the events which are lost can be recovered by using decay chains in which α-particles from either the ^{180}Pb (ER-α_e-α_f-α_f) or from the ^{176}Hg (ER-α_f-α_e-α_f) decay escape, but are followed by a full energy ^{172}Pt α-decay.

The α-decay energy E_α = 7254(7) keV and half-life $t_{1/2}$ = 4.1(3) ms for ^{180}Pb were extracted from the ER-α_f(^{180}Pb)-α_f(^{176}Hg) decay chains. The data are shown in figure 3.3. The half-life was extracted from a fit to the logarithmically binned lifetime data as described in [96, 97]. The values are in good agreement with recently reported results (E_α = 7254(10), $t_{1/2}$ = 4.2(5)) from dedicated decay measuments at the SHIP velocity filter by Andreyev et al. [66], although our values have slightly better precision due to higher statistics. During the 160 h of irradiation with an average beam current of 7 pnA, 271 ER-α_f(^{180}Pb)-α_f(^{176}Hg) decay chains were observed. The production cross section for ^{180}Pb is estimated to be $\sim$10 nb, by taking into account the measured 60% probability for observing the full energy of the α-particles and assuming 80% coverage of the focal plane distribution and 60% RITU transmission[77]. This is one of the lowest, if not the lowest, cross-section ever utilised in a successful RDT experiment.

In figure 3.4 the singles γ-spectra tagged by the decays chains of ^{180}Pb are

shown. The spectrum on the top panel a) is tagged by the ER-α_f-α_f decay chains and is used to unambigusouly identify the γ-rays in ^{180}Pb. Four γ-lines can be clearly identified, a high energy one at 1168 keV and three closely spaced at 278, 312 and 380 keV. The bottom panel b) exhibits a spectrum for which also the ER-α_e-α_f-α_f or ER-α_f-α_e-α_f chains were accepted as a tag.

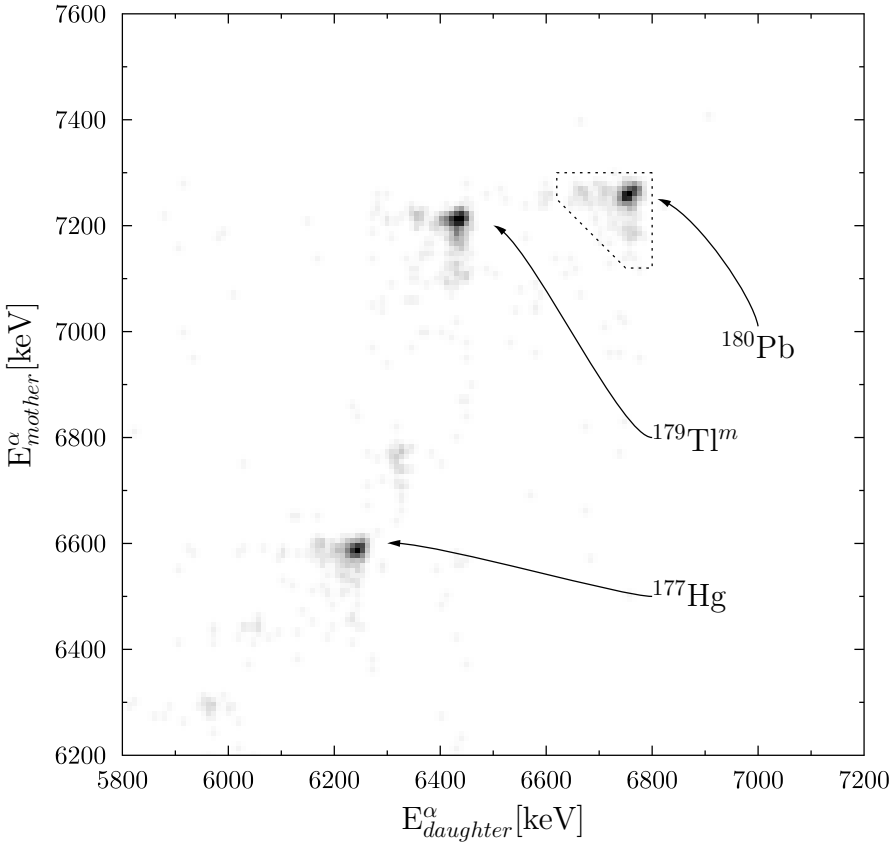

Figure 3.2: A plot showing the correlated daughter α-particle energy vs. mother α-particle energy. A correlation time of 12 ms was used for the recoil-mother pair and 60 ms for the mother-daughter pair. The correlated mother-daughter decays are labelled with respect to the mother isotope. The dashed area was used as a tag to identify ^{180}Pb in the ER-α_f-α_f chains. See text for details.

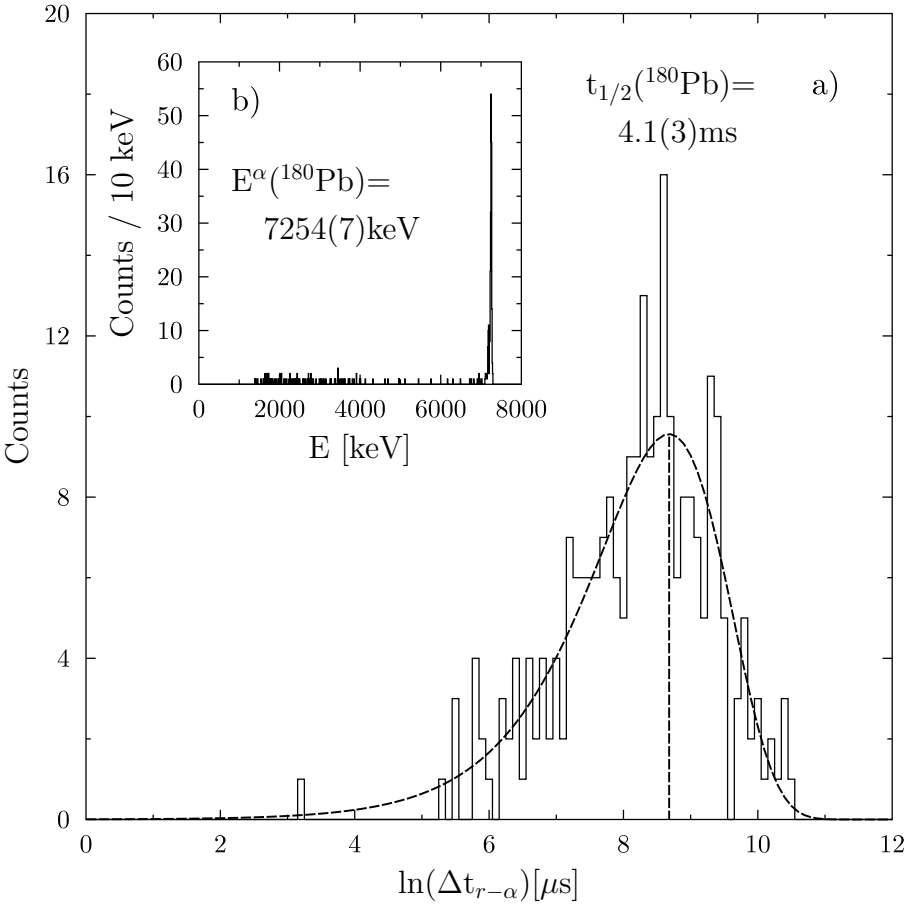

Figure 3.3: In panel a) the logarithmically binned lifetime data for ^{180}Pb, extracted from ER-α_f(^{180}Pb)-α_f(^{176}Hg) decay chains, is shown. In the insert panel b) the α-decay energies for the events preceded by an evaporation residue within 12 ms and followed by a full energy ^{176}Hg α-decay within 60 ms are shown.

The spectrum in panel b) was used to extract the intensities of the transitions, since at this low level of statistics the statistical errors are significant. The details are presented in table 3.1.

Obviously the statistics available rule out any γ-γ coincidence analysis, angular distribution or correlation analysis. Therefore the observed γ-rays are ordered based on the intensity data and systematical trends extrapolated from the

heavier lead isotopes. The high-energy 1168 keV γ-ray is assigned to correspond to the 2^+ to 0^+ transition, analogous to the heavier isotopes, while the three lower energy γ-rays are proposed to form a rotational band above the 2^+ state. The M1 multipolarity of the low energy γ-rays can be excluded since the K X-ray yield should be $\sim$5 detected counts in this case. As could be expected based on the systematical trends, all observed excited states are indeed unbound in the sense that they lie above the one or two proton separation energies.

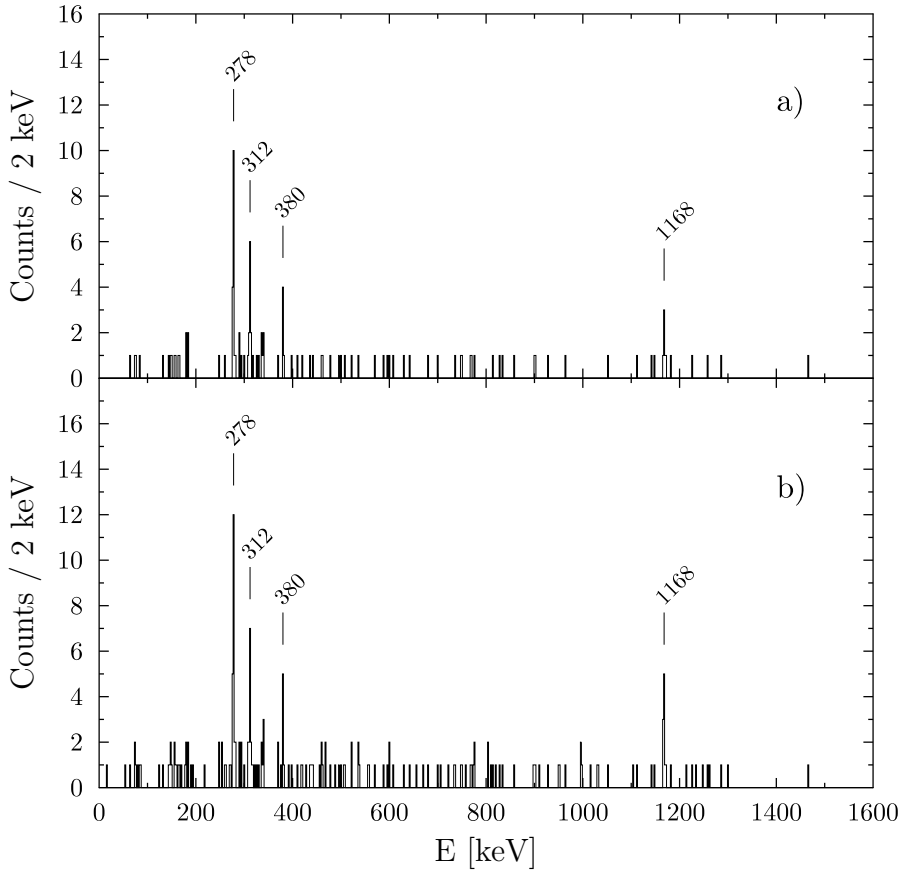

Figure 3.4: Singles γ-ray energy spectra tagged by the ^{180}Pb decay chains. Panel a) shows a spectrum generated by demanding a ER-α_f-α_f chain as a tag, whereas for panel b) ER-α_f/α_e-α_e/α_f-α_f chains were also accepted.

Table 3.1: Gamma-ray transitions assigned to ^{180}Pb in the present work. The energies (E_γ) in keV, raw intensities (counts), relative intensities without (I_{rel}) and with the correction for internal conversion ($I_{rel,icc}$) assuming pure E2 character, as well as the tentative level assignments are given.

E_γ (keV)	counts	I_{rel} (%)	$I_{rel,icc}$ (%)	$I_i^\pi \rightarrow I_f^\pi$
278(1)	19(5)	93(21)	107(25)	$(4^+) \rightarrow (2^+)$
312(1)	11(4)	56(17)	62(19)	$(6^+) \rightarrow (4^+)$
380(1)	6(3)	33(14)	36(15)	$(8^+) \rightarrow (6^+)$
1168(1)	9(3)	100(33)	100(33)	$(2^+) \rightarrow 0^+$

3.3 Discussion

The level scheme based on the above arguments is shown on the left hand side of figure 3.5. The proposed level scheme follows the systematical trends extrapolated from the heavier isotopes, as seen in figure 3.6. The near-parabolic behaviour of the prolate intruder states, with the minima close to the N=104

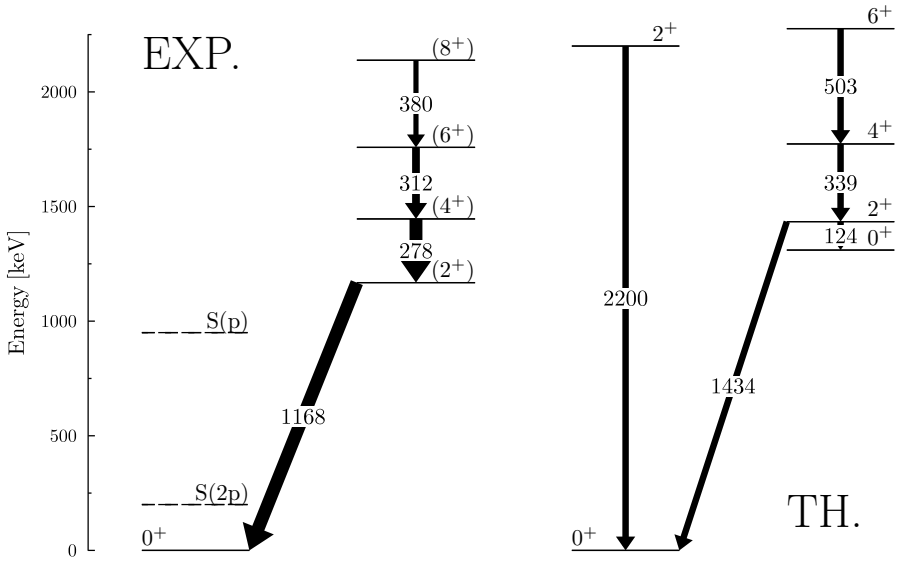

Figure 3.5: Level schemes of ^{180}Pb. The experimental level scheme is shown on the left, while on the right hand side the level scheme from beyond mean field calculation is shown. See text for details.

mid-shell, continues smoothly down to N=98.

Results of a beyond mean-field calculation for ^{180}Pb were provided by M. Bender (CENBG, CNRS/IN2P3, France) and P.-H. Heenen (Université Libre de Bruxelles, Belgium). The method is based on configuration mixing of angular momentum and particle-number projected self-consistent mean-field states. The Skyrme interaction SLy6 and density-dependent zero-range pairing have been used. Exactly the same method was used by Bender et al. [24] to calculate the properties of $^{194-182}$Pb and the reference should be consulted for details of the calculations.

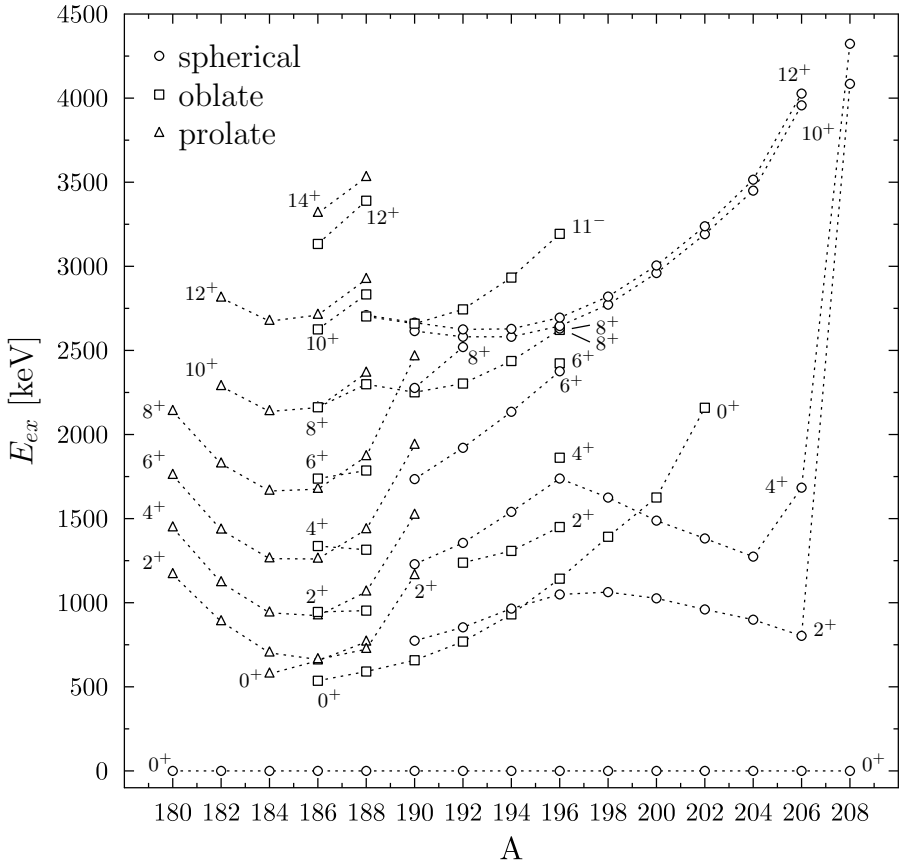

Figure 3.6: Level systematics for even-even lead isotopes. Data are from present study (^{180}Pb), [98] (^{184}Pb) and [48] (^{182}Pb, ^{186}Pb-^{208}Pb).

The level energies and the transition probabilities related to the axially symmetric quadrupole collective mode can be extracted from the calculations. Figure 3.5 shows the low-lying level scheme from the calculations on the right hand side. The ground-state is found to nearly-spherical, as expected for a Pb nucleus. The excited 0^+ state is rather strongly prolate, with a rotational band build on the top of it. The β_2 value of 0.30-0.32 can be extracted from the calculated transition quadrupole moments, which within the band are approximately $Q_T = 900$ fm^2. The calculated Q_T from the prolate 2^+ to the ground state is only about one tenth of this. In spite of this only the high-energy transition to the ground state is seen, since the transition rate is proportional to E^5 and "only" to Q_T^2. The calculations reveal a second excited 2^+ at 2.2 MeV which is intepreted to be of a vibrational character. No oblate deformed structures are found, at least at low excitation energies. All in all these calculations are in reasonable agreement with the experimental data, especially after taking into the account the fact that the excitation energies of the levels are typically overestimated by the model (see eg. [24]).

In figure 3.7 the aligned angular momenta, i_x, for the prolate bands in $^{180-188}$Pb are shown. Interesting deviations from the expected rotational behaviour above the 2^+ states are noted, specially the low-spin behaviour of ^{180}Pb and ^{188}Pb are very similar. Slight deviations from the rotational behaviour are also seen for the other isotopes. In ^{188}Pb the distortion is attributed to strong mixing of prolate, oblate and spherical states [33, 34, 99, 100]. Since in ^{180}Pb the oblate minimum has already disappeared, if the depression is related to mixing, it is most likely due to mixing of prolate and spherical states.

Other interesting possibilities which might influence the structures are the effects of the levels being proton-unbound. In light nuclei this leads to Thomas-Ehrmann shifts [101, 102], in which unbound excited levels are pushed down due to the lowering of the Coulomb energy. The shifts are especially strong for $s_{1/2}$ levels since they do not feel the centrifugal barrier. In lead nuclei, the $3s_{1/2}$ lies just below the Fermi level and is involved in the ground states as a particle-state and in the intruder states as a hole-state, if the classic np-nh picture is used. Unfortunately the theoretical calculations show that the Coulomb barrier is so high in these heavy nuclei that the $\pi s_{1/2}$ does not see the continuum. Furthermore the $\pi s_{1/2}$ is crossed by other downsloping orbitals already at modest deformations, thus lowering the relative importance in deformed systems [103].

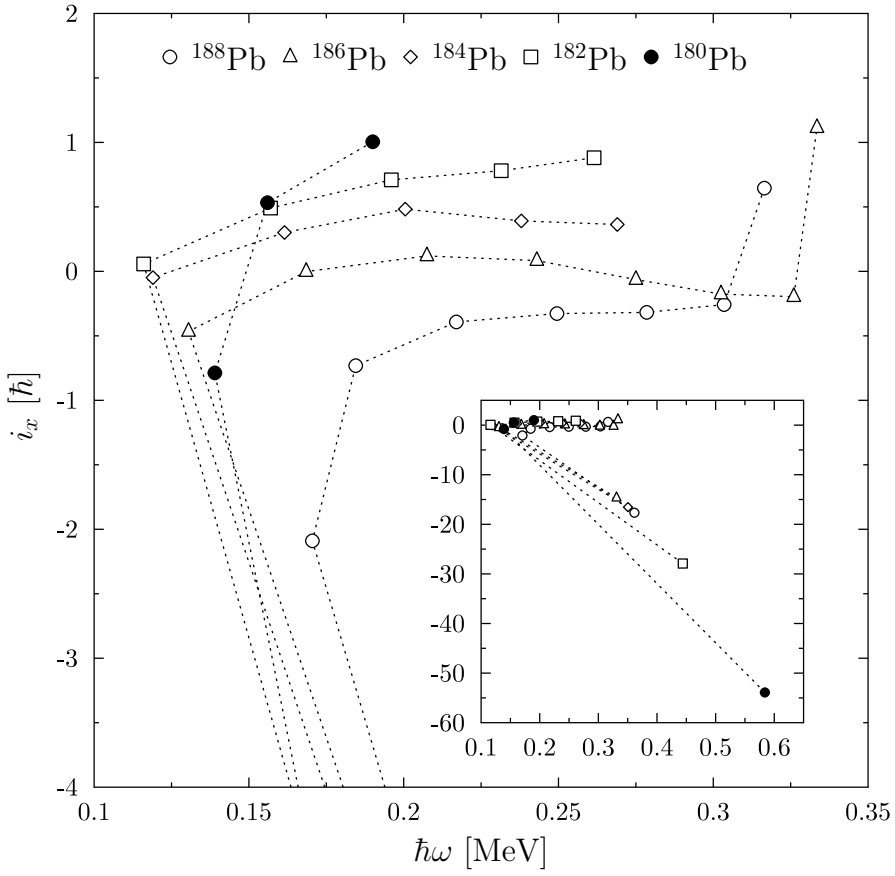

Figure 3.7: Aligned angular momentum i_x of the prolate bands in light Pb isotopes. An appropriate Harris reference $\mathcal{J}_0 = 27\hbar^2/MeV$, $\mathcal{J}_1 = 199\hbar^4/MeV^3$ has been subtracted. The insert shows the full scale plot with the $2^+ \rightarrow 0^+$ transitions included.

Chapter 4

An excited prolate band in ^{192}Po

One experimental signature of shape coexistence is the observation of (two or more) rotational bands which can be assigned to configurations having different deformations in the same nucleus. In Pt and Hg nuclei such bands are well known. At Z=82, bands assigned to both prolate and oblate deformed configurations have been observed in ^{186,188}Pb [52, 53]. In the polonium isotopes, oblate bands have been identified for N<106 [104, 105, 106]. The ground state of ^{190}Po is assumed to be mostly oblate but the rotational band observed remarkably resembles the prolate bands in the lighter isotones above spin 4 [49, 50]. As noted already in section 1.1 the prolate minimum should already lie low in ^{192}Po. The last time ^{192}Po was probed via in-beam γ-spectroscopy was in the late 1990's using the DORIS array [105]. The developments in the detector systems have since increased the γ-γ detection efficiency by a factor of $\sim$50. It was therefore proposed to perform a new RDT study of ^{192}Po to search for non-yrast deformed structures. Conversion electron data from an earlier measurement which failed to locate any excited 0^+ states was also available.

4.1 Experimental details

In the γ-ray measurement the JUROGAM array was used to detect prompt radiation. The recoiling nuclei were separated from the beam and fissioned products by the RITU separator. The GREAT spectrometer was used to identify the products via the RDT method. The triggerless TDR data acquisition system was used to read out all the channels. The equipment is described in more detail in section 1.3. The data were analysed with the Grain software described in chapter 2. Data were collected in two parts. In the first experiment the reaction ^{147}Sm(^{48}Ti,3n)^{192}Po was used. The targets were self-supporting and 750 μg/cm^2 thick. The beam was accelerated to 218 MeV and was incident on the target for approximately 120 h with an avegare intensity of 10 pnA. In the second part a metallic, self-supporting 500μg/cm^2 target of ^{160}Dy was bombarded with a 178 MeV ^{36}Ar beam for 41 hours. The average beam current was 15 pnA. In both experiments the beam current was limited by the counting rates in the JUROGAM array.

The SACRED electron spectrometer [75] was used in the conversion electron measurement to detect prompt electrons and was operated in conjuction with the RITU separator. The focal plane was instrumented using the MkII RITU detection system [107]. The detector systems were instrumented using standard analogue electronics and data were collected with the TARDIS data acquisition system[108]. Data analysis was performed using Grain precursor C++ codes [109]. The reaction used was the same as in the second part of the γ-ray run, ^{36}Ar+^{160}Dy, using the same beam energy and targets. The electron counting rate in SACRED limited the beam current to 2 pnA. Data were collected for a total of 8 days.

4.2 Results

4.2.1 Singles γ-ray data

A recoil decay tagged γ-ray spectrum for ^{192}Po was constructed using the known α-decay energy (E$_\alpha$=7167(7) keV) and half-life (T$_{1/2}$=0.0332(14) s) [48]. A total of 8×10^4 recoil correlated α-decays of ^{192}Po were observed when data from both γ-ray experiments were combined. The resulting γ-ray spectrum is shown in figure 4.1. The known yrast band up spin I$^\pi$=10$^+$ is observed along with several previously observed but unplaced γ-rays. Six previously unknown transitions at 381, 411, 492, 523, 532 and 721 keV are assigned to ^{192}Po. The

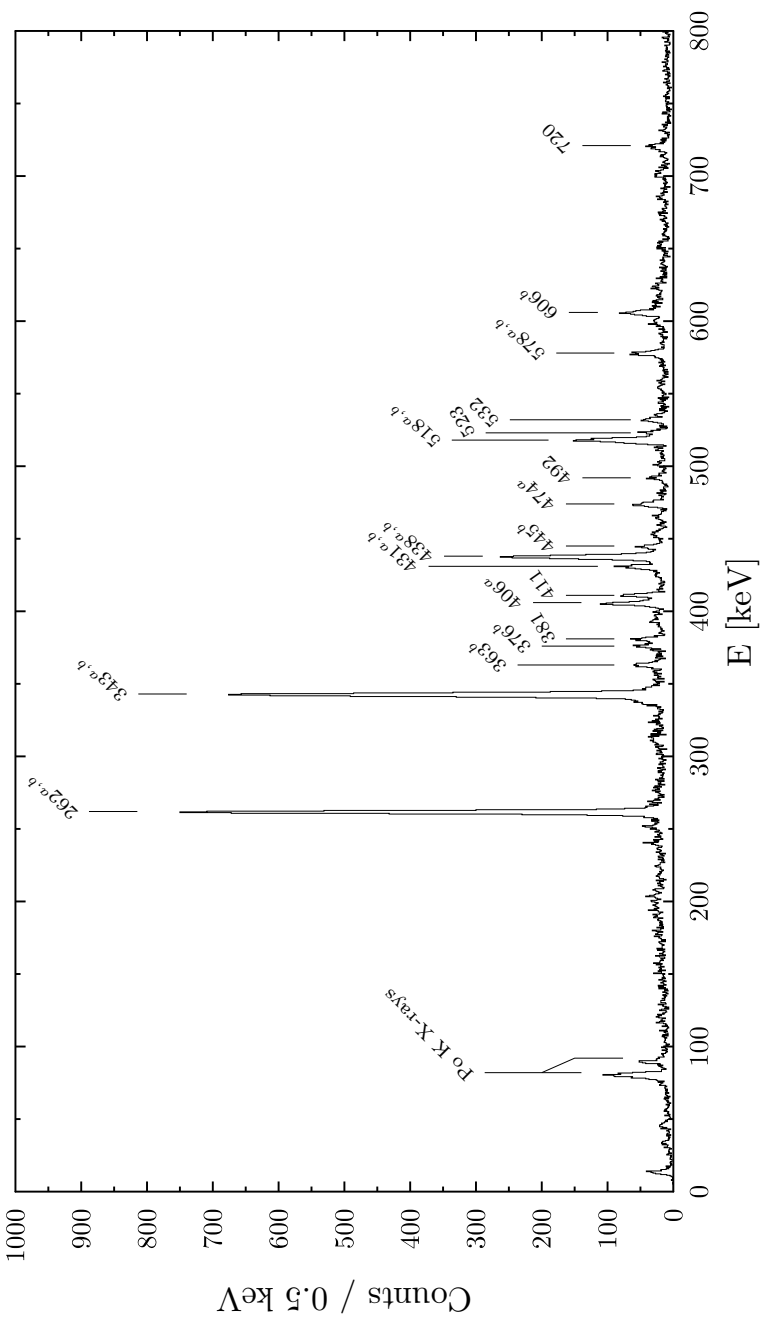

Figure 4.1: Recoil decay tagged singles γ-rays in ^{192}Po. Peaks are labeled with their energy rounded to the closest keV. Peaks labeled with *a* have been identified in previous in-beam measurements [106]. Peaks that are labelled with *b* have been seen in the decay of a 580 ns isomer in ^{192}Po [51].

Table 4.1: Energies and relative intensities of the γ-rays attributed to ^{192}Po. For the previously known yrast band transitions the spin assignments are given along with the relative γ-ray intensities corrected for pure E2 conversion and the relative intensities expected for the K and L_{tot} internal conversion electrons. These have been normalised to the K conversion of the $(2^+) - \ 0^+$ 262 keV transition. Conversion coefficients are taken from [110]. Previous observations are indicated.

E_γ (keV)	I_{rel} (%)	I_{icc} (%)	$I_i^\pi - I_f^\pi$	$I_{e^-}^K$ (%)	$I_{e^-}^L$ (%)	P.o.[1]
261.8(0.3)	86(2)	94(2)	$(2^+) \rightarrow \ 0^+$	100	82	a,b
342.7(0.3)	100(2)	100(2)	$(4^+) \rightarrow (2^+)$	63	34	a,b
363.2(0.4)	6(1)					b
376.4(0.4)	5(1)					b[2]
380.8(0.4)	5(1)					
405.6(0.4)	14(1)					a
411.2(0.4)	9(1)					
430.9(0.4)	10(1)					a,b
437.7(0.3)	43(1)	42(2)	$(6^+) \rightarrow (4^+)$	16	6	a,b
444.5(0.4)	5(1)					b
474.1(0.4)	8(1)					a
492.3(0.4)	4(1)					
518.2(0.3)	30(1)	28(2)	$(8^+) \rightarrow (6^+)$	8	3	b
523.4(0.4)	7(1)					
532.3(0.4)	6(1)					
577.9(0.4)	11(1)	11(1)	$(10^+) \rightarrow (8^+)$	2	1	b
605.9(0.4)	10(1)					b
720.6(0.4)	7(1)					

[1] Previously observed in: a) in-beam γ-ray spectroscopy [106], b) decay of the $T_{1/2} = 580(100)$ns, $I^\pi=(11^-)$ isomer [51].
[2] Not labeled in Fig. 2 of ref.[51], but clearly present in the spectrum.

details are presented in table 4.1.

4.2.2 Coincidence data from the γ-ray measurements

A γ-γ matrix for ^{192}Po was constructed from the recoil decay tagged data. In total 15×10^3 unfolded tagged γ-γ events were detected. The matrix was further analysed using the Radware software suite [111]. Both recoil gated and recoil decay tagged γ-γ-γ cubes were also constructed, but the statistics available were too low to facilitate meaningful analysis.

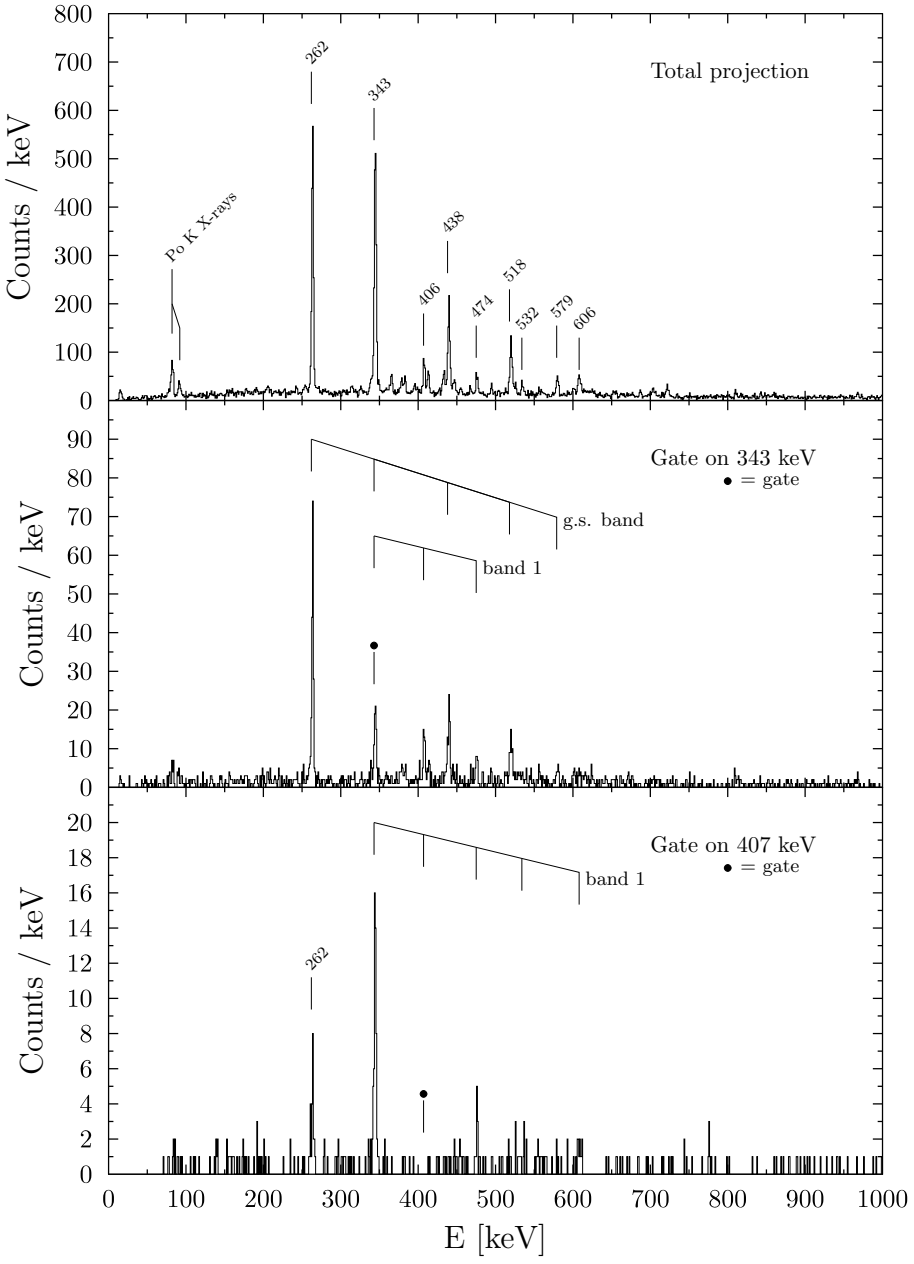

Figure 4.2: Gamma-gamma coincidence data for ^{192}Po. On the top panel the total projection from the γ-γmatrix is shown. Two gated spectra are shown on the lower panels. Gating conditions are indicated in the figure.

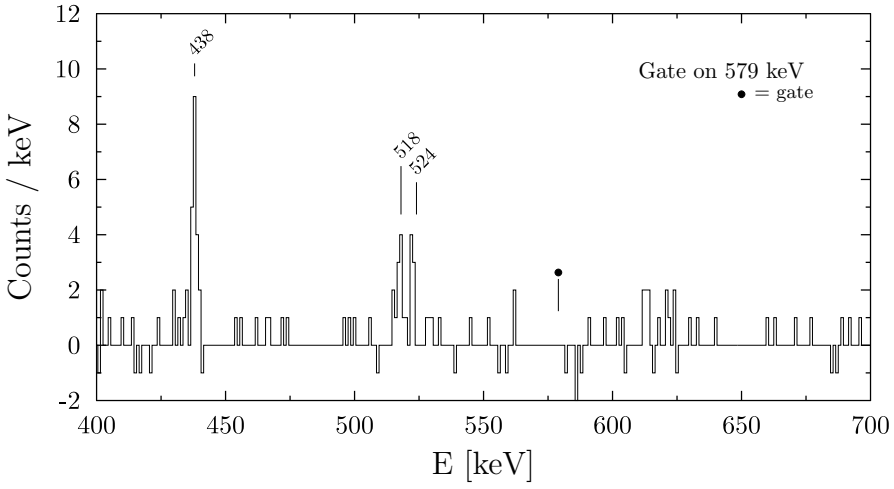

Figure 4.3: Gate from the prompt γ-γ matrix showing the transitions in coincidence with the previously known 578 keV 10^+-8^+ transition.

The total projection of the recoil decay tagged γ-γ matrix is shown in the top panel of figure 4.2. The known yrast, oblate band of 262, 343, 438, 518 and 578 keV γ-rays is clearly observed. Several other prominent peaks are also evident. On the middle panel of figure 4.2 γ-ray spectrum gated by the known 4^+-2^+, 343 keV transition is shown. The gating transition is clearly at least a doublet. The other members of the yrast band are observed in addition to two other coincident γ-rays at the energy of 406 and 475 keV. The result of placing a gate on the 406 keV transition is shown on the bottom panel of figure 4.2. The yrast 262 keV 2^+-0^+ transition is clearly seen along with a very strong 343 keV peak. Weaker peaks at 475 and 608 keV are also visible.

In figure 4.3 a 578 keV gate on the prompt γ-γ matrix is shown. The spectrum clearly shows the known, yrast 438 keV 6^+-4^+ and 518 keV 8^+-6^+ transitions, expected to be in coincidence with the gating, yrast 578 keV 10^+-8^+ line. In addition a γ-ray at 524 keV is observed with an intensity comparable to the 10^+-8^+ transition. No clear sign of a γ-ray around 630 keV, where the 12^+-10^+ is expected to be based on extrapolation from lower spin members of the band, is seen. Therefore the 524 keV transition is assigned to be the 12^+-10^+ transition.

4.2.3 Conversion electron data

The singles electron spectrum generated for ^{192}Po by using the RDT method is shown in figure 4.4. Two strong concentrations of counts can be identified. The peak at 179 keV is identified as the K-shell conversion of the 262 keV, 2^+-0^+ transition. The counts centered at 250 keV have two sources. L-shell conversion of the 262 keV transition results in a distribution of electrons having mean energy of 246keV and the K conversion of the 343 keV transition to a monoenergetic peak at 250 keV. Unfortunately due to the finite resolution of the detector, which was measured to be 5.0 keV for 320 keV electrons, the peaks can not be fully resolved. Even the M-shell conversion of the 262 keV transition can distort the peak shape since the mean energy of the electrons is 258 keV.

Based on the γ-ray data, it is possible to estimatethe number of electrons expected for each peak. The K and L electron yields calculated for the yrast transitions in ^{192}Po are shown in table 4.1. Pure E2 character was assumed for

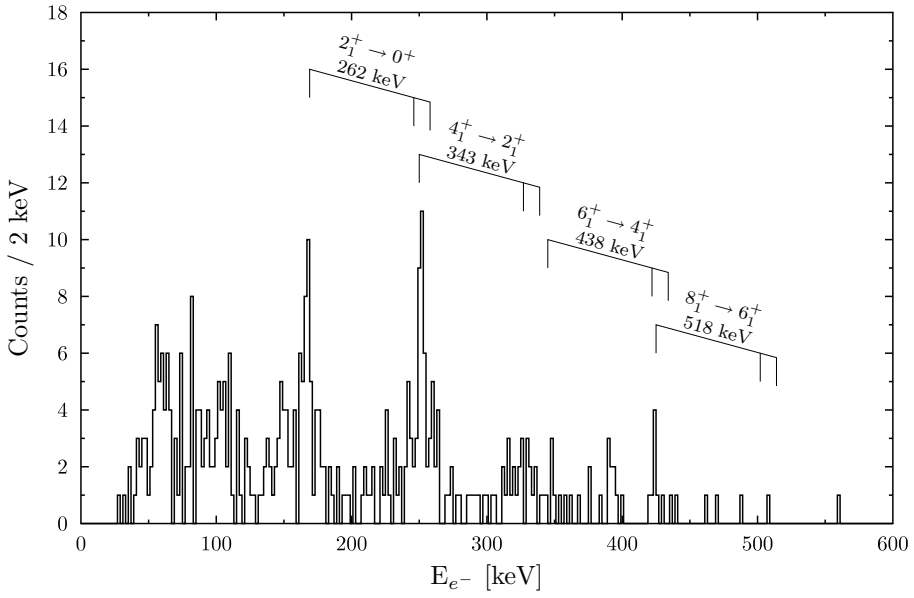

Figure 4.4: Recoil decay tagged singles electrons from ^{192}Po. Locations of electrons from the K, L and M conversion of the known yrast transitions are indicated. Low energy background originates from the unsuppressed δ-electrons.

all the transitions in the calculation. Taking into account the relative efficiency of the SACRED spectrometer, which is measured to be essentially flat within the errors from 150 keV to 300 keV [75], contributions to the counts at 250 keV from the two transitions can, in principle, be estimated. In this case, no firm conclusion can be reached. From the 34(6) counts observed in the 179 keV peak corresponding to the K-shell conversion of the 2^+-0^+ transition, approximately 28 counts is expected for the L-shell conversion peak at 246 keV and 21 counts for the 250 keV K-shell conversion peak of the 343 keV transition. Only a single peak is observed at 250 keV, having 31(6) counts. It is assumed to have components from both of the electron lines expected in the approximate energy range. The L-shell conversion of the 343 keV transition should result in a peak of ∼10 counts centered at 327 keV. A broad distribution of 10 counts centered at the right energy is observed.

An electron line of 10 counts at 392 keV is observed in the spectrum. It is assumed to originate from K-shell conversion since no counts are observed at 315 keV. The transition energy would thus be 485 keV. Inspection of the γ-ray spectra reveal no peaks at the exact energy, the closest match being a weak, unplaced 492 keV transition. The 406 keV transition would have L-conversion electrons centered at 393 keV, but the calculated yield based on the γ-ray intensities, along with the missing intensity at 315 keV do not support this scenario.

4.3 Discussion

The newly observed band in ^{192}Po, labelled band 1 in figure 4.2, can be assumed to feed into the ground state band at $I^\pi = 4^+$ at 605 keV based on the coincidence data. The relative γ-ray intensities of the transitions in the known yrast band support this intepretation since a large increase in intensity is seen when going from the 6^+-4^+ to the 4^+-2^+ transition, indicating strong side feeding.

The 343 keV transition is proposed to be at least a doublet of consecutive transitions, again based on the coincidence data and supported by the intensity figures. Assuming that the 406 keV transition is the lowest transition of band 1, which can be used as a clean gate, whether the 343 keV transition is a doublet or a triplet can be judged based on the intensity ratio of the 343 keV to the 2^+-0^+ transition in the spectrum gated by the 406 keV transition. The ratio is found to be 3:1, suggesting a triplet nature. On the other hand, the intensity of the 343 keV line in the spectrum gated by itself shows no deviation from the intensity pattern extrapolated from the higher members of the non-yrast band.

From the data alone it is impossible to say whether the 343 keV transition is only a doublet, leading to 406 keV transition being the lowest observed transition within the new band or whether the 343 keV line is a triplet of consecutive transitions and the 343 keV line is also a member of the band.

The 406 and 475 keV transitions can be assigned as band members from the 343 keV gated coincidence spectrum. Based on the 406 keV gate, the 605 keV transition is also in coincidence with the 406 and 475 keV lines. From weaker coincidences with the 475 keV and 605 keV, sum-of-gates data and the interpolation of the transition energies, a 532 keV γ-ray is also assigned to the band. Angular correlation and distribution analysis was not possible for the new band due to the low statistics. For the 406 keV transition M1 multipolarity can be tested using the electron data. The K-shell conversion peak at 315 keV should have $\sim$10 counts, if the transition multipolarity was M1. Only few counts above the background are detected, thus the 406 keV transition is most

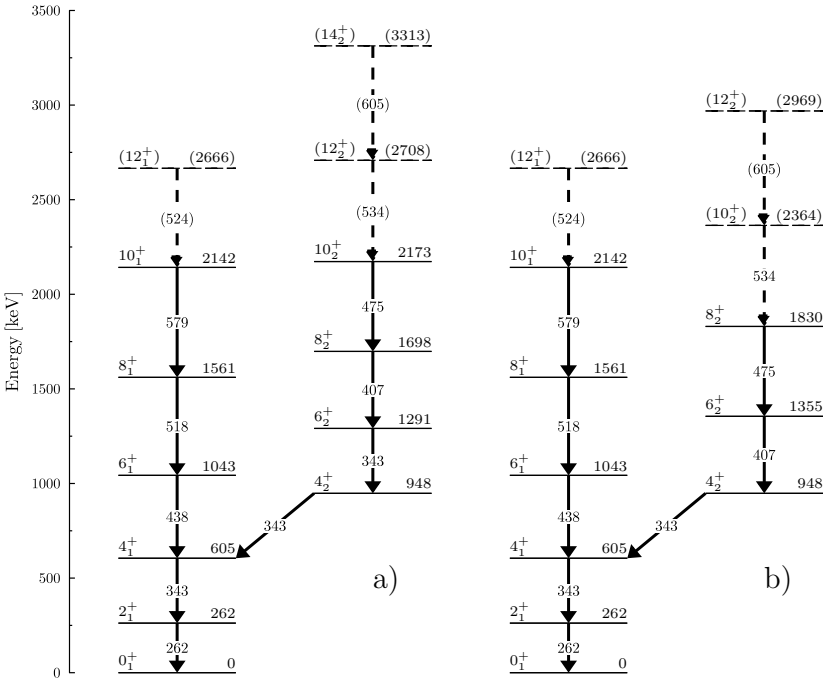

Figure 4.5: Two possible level schemes for ^{192}Po. The validity of neither one can be confirmed from the data alone.

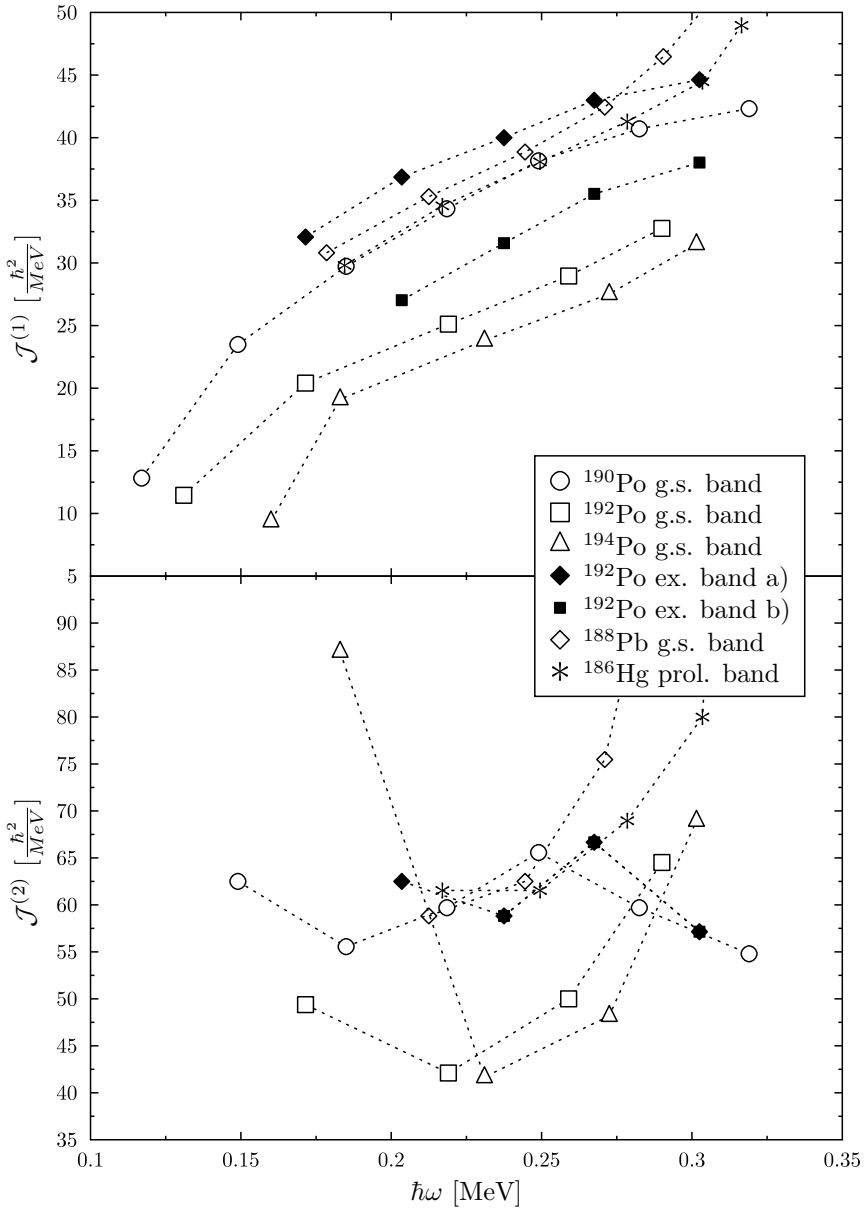

Figure 4.6: Kinematic (top) and dynamic (bottom) moments of inertia for the oblate g.s. bands of ^{192,194}Po up to spin I=10, for the g.s. band of ^{190}Po, the prolate bands in ^{188}Pb and ^{186}Hg above spin I=2 and for the two possible assignments of the excited band in ^{192}Po.

likely of E2 character. The other transitions in the band are assumed to be of the same multipolarity.

The spins of band 1 can be at least limited by feeding arguments. The transition to the $I^{\pi} = 4_1^+$ state has to originate from a state with I = 4 or lower. If the 948 keV state is assigned higher spin, band 1 would be yrast at spins I≥6 and should be populated more than the oblate band in a heavy ion evaporation reactions.

The possible level schemes are shown in figure 4.5. For these, the lowest observed level in band 1 was assigned the maximum possible spin, I = 4.

Kinematic and dynamic moments of inertia for the oblate bands in ^{192,194}Po and prolate bands in ^{190}Po, ^{188}Pb and ^{186}Hg are in figure 4.6. Here ^{188}Pb and ^{186}Hg are used instead of the isotones of ^{192}Po since in nuclei with Z>82 a better agreement in level systematics is reached if nuclei differing with an α-particle are used.

From the kinematic moment of inertia plot it is seen that level scheme option a) corresponds to a more prolate rotor, similar to the reference prolate bands, whereas option b) has more intermediate values, somewhere half-way between the known prolate and oblate bands. The scenario a) exhibits a very similar

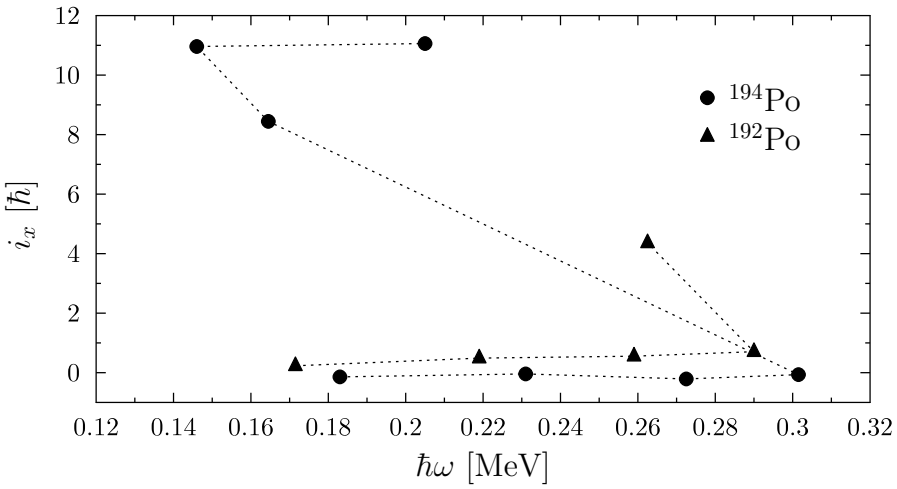

Figure 4.7: Aligned angular momentum i_x for the yrast bands in ^{192,194}Po. Harris reference $\mathcal{J}_0 = 13\hbar^2/MeV$, $\mathcal{J}_1 = 206\hbar^4/MeV^3$ has been subtracted.

"downbend" as has been already observed in ^{190}Po by Wiseman et al. [50]. This is in contrast to the well known upbends observed in the prolate bands in Pb and Hg isotopes. The dynamic moments for the two bands obviously overlap and lie very close to the known prolate bands at medium spin before the upbend starts to affect the Pb and Hg isotopes and the downbend the in Po isotopes. Based on this circumstancial evidence, along with the mean-field predictions of almost degenerate oblate and prolate minima, the yrare band in ^{192}Po should be tentatively assigned a prolate shape and the level scheme containing the triplet of 343 keV transitions should be assumed to be correct.

In ^{194}Po a sharp backbend, likely to have its origin in the alignment of two $i_{13/2}$ neutrons, was reported by Helariutta et al. [106]. The tentatively assigned 524 keV (12^+) to (10^+) transition in ^{192}Po would indicate that similar backbend is also taking place in ^{192}Po above $\hbar\omega = 0.3$ MeV, see figure 4.7.

No sign of the 580(100) ns isomer observed at the SHIP separator [51] was observed. The isomeric ratio is not known and if it is very small, combined with the half-life comparable with the flight time through the separator, the non-observation is plausible. It should be noted that the γ-rays observed in the decay of the isomer are not seen in connection with the excited band structure apart from the 606 keV transition, which based on the high intensity in the singles spectrum could be a doublet.

The character of the 392 keV electron line is of special interest. Based on the available statistics, it can be ruled out that L-shell conversion of the 406 keV transition is responsible, K/L ratio being ∼2:1. More likely and interesting scenarion is the possible E0 nature of the transition. The lack of L-shell conversion electrons at 469 keV is an indication of E0 nature since the transition should be 85% K-shell converted. In the beyond mean field calculations for ^{194,196}Po [33, 34, 35], the first excited 0^+ state is oblate and is located slightly above the 2_1^+ state, matching the known 0^+ energy in ^{196}Po well. The excitation energy is thus plausible, even if in ^{192}Po the prolate minimum can cause a deviation from the pattern. A VMI-fit to the proposed prolate band results in an excitation energy of 646 keV for the unperturbed 0^+ state.

The newly observed, excited band in ^{192}Po can not firmly be assigned spin-parities or even excitation energies. Evidence based on comparisons to the known prolate and oblate bands in the neighbouring nuclei reveal that the band is most likely based on a prolate shape. This is supprted by modern mean-field calculations, which predict nearly degenerate oblate and prolate minima in ^{192}Po. The puzzle could be solved by a measurement, in which high statistics triples γ-γ-γ data for ^{192}Po would be gathered.

Chapter 5

^{206,208,210}Ra: onset of deformation in Ra isotopes?

In polonium and radon nuclei very similar patterns in the onset of deformation have been observed [56]. This suggests that the mechanism responsible should be similar. All current evidence points to particle-hole intruder states playing a major role in the onset of significant deformation in the isotopes with A$\leq$200. There is no reason to expect similar phenomema not to occur in the elements with higher Z and it is therefore of considerable interest to try to locate deformed structures also in the Ra-isotopes.

When the studies at JYFL were initiated more than 10 years ago, ^{212}Ra was the lightest isotope for which excited states were known. Results of the early experiments on ^{206,208,210}Ra were published in a brief report by Cocks [57]. Since then, data on ^{210}Ra from Yale [59] and GSI [60] has been published. In another publication from the Yale group [58], the decay of an isomeric state in ^{208}Ra was discussed.

In this work excited states in ^{206,208,210}Ra have been studied in three experiments. Isomers in ^{208}Ra and ^{210}Ra were studied at the focal plane of the RITU separator using the GREAT spectrometer. Two clover detectors from the JUROGAMII array were used in addition to the GREAT clover detector at the focal plane to boost the γ-ray detection efficiency by a factor of 1.5. In-beam spectroscopy was not attempted for these nuclei since the high beam currents required for the isomer studies prevented the use of the germanium detectors at the target position. For ^{206}Ra in-beam RDT data was collected using the

JUROGAM HPGe array. A beam of ^{40}Ar accelerated to 183 MeV was used in all experiments. Targets used for ^{206}Ra,^{208}Ra and ^{210}Ra were 1mg/cm^2 thick metallic foils of ^{170}Yb, ^{172}Yb and ^{174}Yb, respectively. All Ra isotopes of interest were thus produced in the 4n evaporation channel. The average beam current in the in-beam ^{206}Ra experiment was 15 pnA during the 5 day run. In the isomer experiments the beam current was 100 pnA and the beam was on target for 30 h in the ^{210}Ra run and 48 h in the ^{208}Ra run. All datasets, collected using the TDR DAQ, were analysed using Grain software.

5.1 Results

5.1.1 ^{210}Ra

A 2.2μs isomeric state was observed in previous works and was assigned to ^{210}Ra. In ref. [57] no direct explanation on how the assignment was achieved is given. Ressler et al. [59] base their assignment solely on ref. [57]. Hessberger et al. [60] used excitation functions and comparisons to HIVAP statistical code calculations to assign the isomer to ^{210}Ra.

In the current work, γ-rays from the 2.2μs isomer are assigned to ^{210}Ra by using the RDT method. The correlations of delayed γ-rays emitted within 20 μs of the recoil implantation with the α-decays of the recoils within 10 s of the implantation are shown in figure 5.1. Clean RDT assignments were impaired by the fact that ^{209}Ra and ^{210}Ra have very similar α-decay energies, 7003(10) keV and 7016(4) keV, and half-lives, 4.7(2) s and 3.7(2) s. From the six clusters of counts with α-decay energies close to 7.0 MeV, two have centroids at an α-particle energy 12 keV lower than the other four. From the two low energy clusters the one at a γ-ray energy of 644keV is assigned to the $9/2^-$ to the $5/2^-$ ground state transition in the decay of an $I^\pi = 13/2^+$ isomer in ^{209}Ra by Hauschild et al. [112]. The result was obtained using RDT method at VASSILISSA separator. Ressler et al. [59] associate both 644 and 765 keV γ-rays with ^{209}Ra. The γ-rays are indeed coincident and are thus firmly assigned to ^{209}Ra. The four clusters at γ-ray energies of 577, 603, 750 and 774 keV are then claimed to originate from ^{210}Ra. Data from the experiment aimed to study ^{208}Ra was used in the RDT analysis since the count rates in the DSSD allowed longer correlations and ^{209,210}Ra were produced in large enough quantities from the contaminants in the target. Gamma-rays assigned to ^{210}Ra are shown in table 5.1. The intensities were extracted from the RDT data while transition energies and the relative contributions of the 602/604 keV doublet are from γ-γcoincidence analysis.

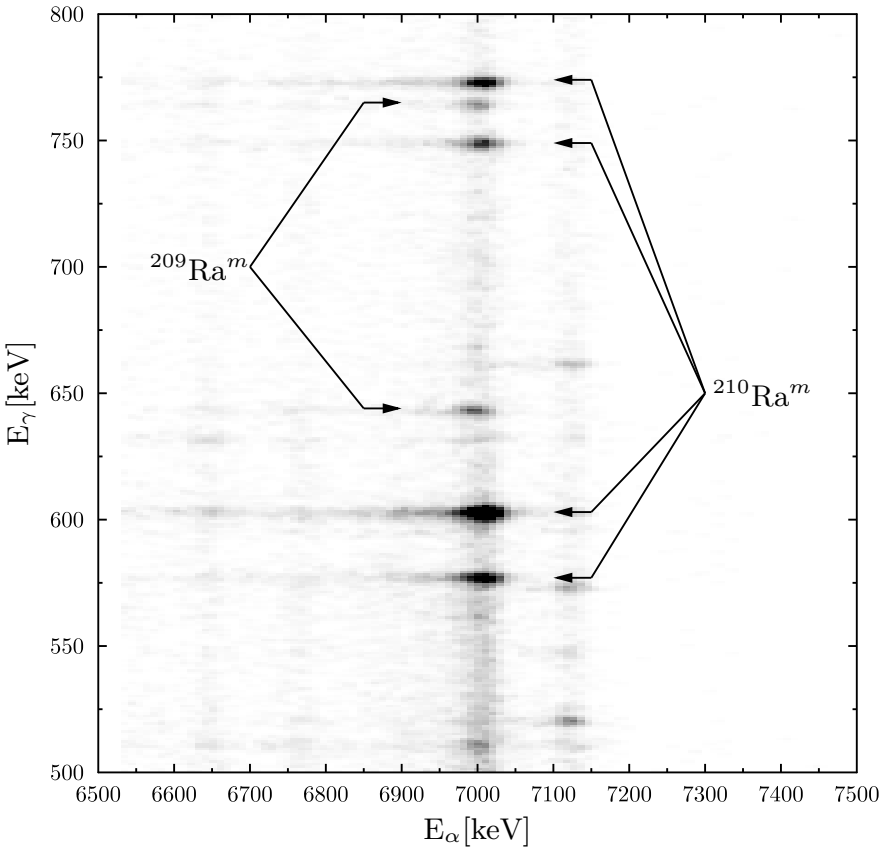

Figure 5.1: Correlations of the delayed γ-rays emitted by implanted recoils and the subsequent α-decays of the recoils. The γ-rays were emitted within 20 μs of a recoil implantation and a search time of 10 s was used in the recoil to α-decay correlations. The transitions depopulating isomers in ^{209}Ra and ^{210}Ra are labelled.

Gamma-rays within 7 μs of a recoil implantation were selected for subsequent analysis. Two matrices, one with coincidences in any pair of the clover detectors and the other with coincidences between any of the clover detectors and the planar detector were constructed. Figure 5.3 shows the spectra obtained by placing different gates on the matrices. The data confirms the basic structure of the level schemes from Ressler et al. [59] and Hessberger et al. [60]. The γ-ray energies given in ref. [60] are found to be slightly higher than the ones measured in the current work and in ref. [59]. The level scheme constructed is

Table 5.1: Gamma-ray transitions assigned to ^{210}Ra. The energies (E_γ) in keV, relative intensities without (I_γ) and with the correction for internal conversion (I_{rel}), assuming the given multipole character, as well as the tentative level assignments are given.

E_γ (keV)	I_γ (%)	I_{rel} (%)	$Mult.$	$I_i^\pi - I_f^\pi$
95.7(1)	14(1)	182(13)	$E2$	$(8^+) - (6^+)$
577.1(1)	100(4)	100(4)	$(E2)$	$(4_1^+) - (2^+)$
601.5(1)	62(6)	61(6)	$(E2)$	$(6^+) - (4_2^+)$
603.7(1)	156(9)	156(9)	$(E2)$	$(2^+) - 0^+$
749.6(1)	71(4)	70(4)	$(E2)$	$(4_2^+) - (2^+)$
773.9(1)	107(4)	105(4)	$(E2)$	$(6^+) - (4_1^+)$

shown in figure 5.9. The logarithmic binning method suggested in [96, 97] was used to extract the lifetime of the isomeric state. The half-life is found to be 2.24(2) μs, see figure 5.2.

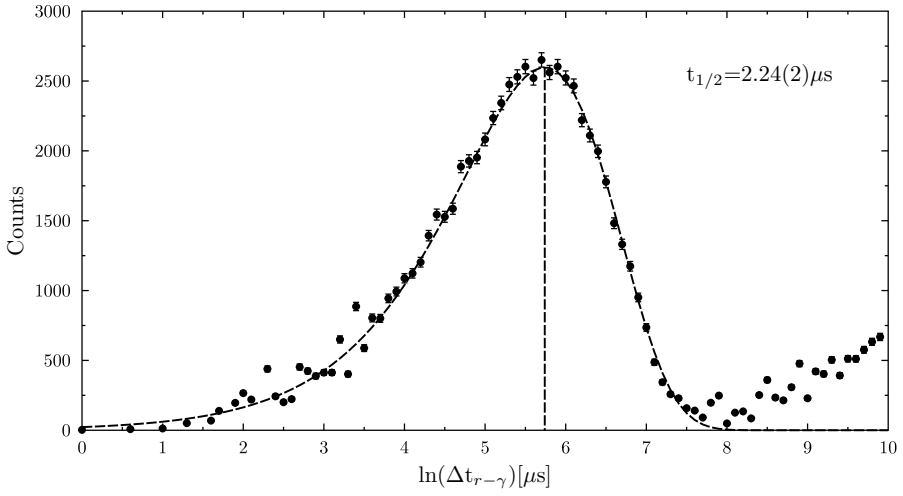

Figure 5.2: The recoil-γ-ray time difference distribution for the 774 keV transition in ^{210}Ra. The final value for the half-life was calculated from the weighted average of the half-lives obtained for each γ-ray depopulating the isomer. Only the fit component corresponding to the signal from the isomeric decay is shown.

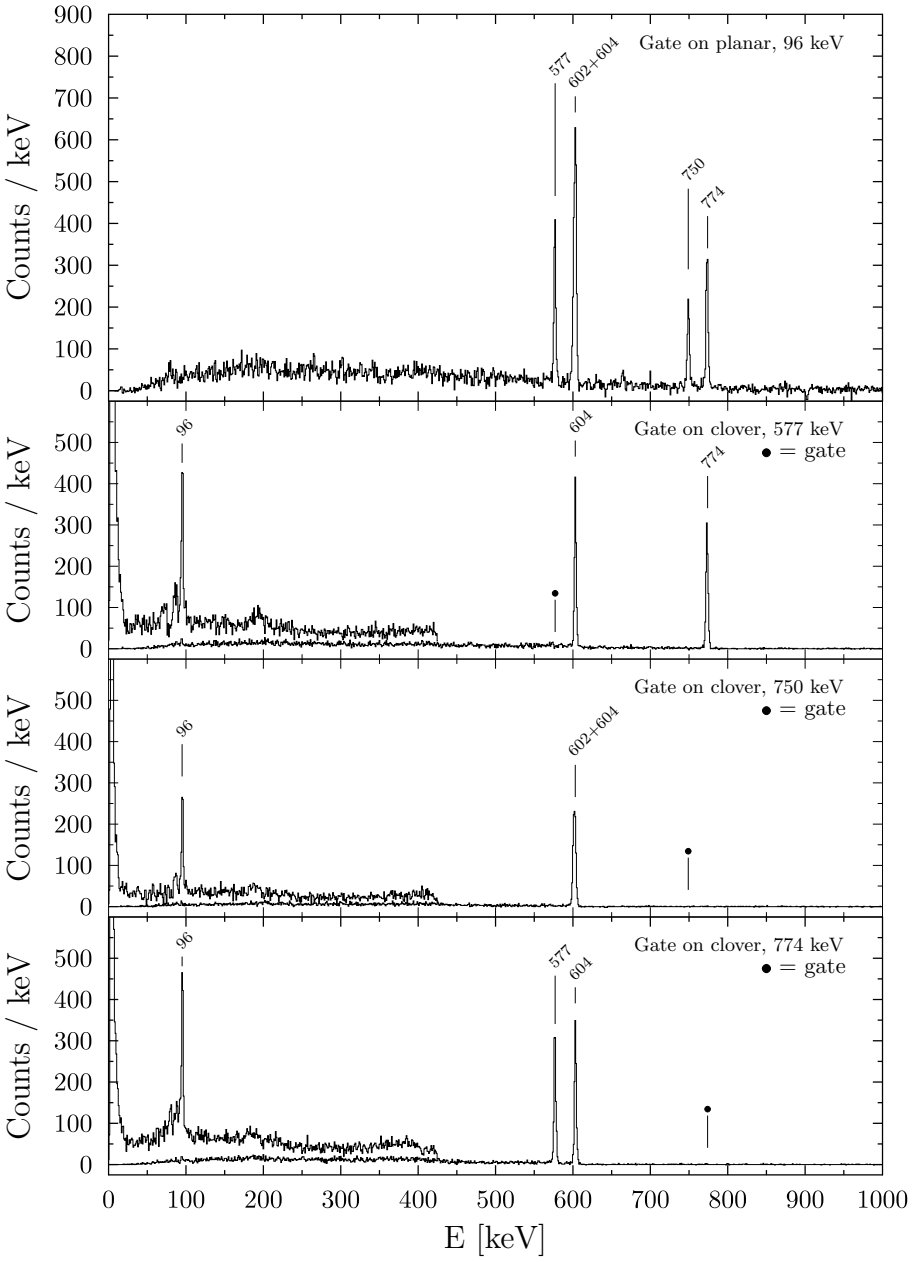

Figure 5.3: Gated spectra from the clover-clover matrix (full energy spectrum) and planar-clover matrix (low energy spectrum). Gates are indicated.

5.1.2 ^{208}Ra

In the study of ^{208}Ra the RDT method was also employed. Figure 5.4 shows the α-decay spectrum from the ^{40}Ar+^{172}Yb reaction, for which the α-decays were required to have taken place within 4 s of the recoil implantations. As in the case of ^{210}Ra, it is seen that the ^{208}Ra α-decay does not provide a clean tag since the α-decay energy and half-life of ^{207}Ra^{g} are exactly the same, 7.13 MeV and 1.3 s. The relative contribution of ^{207}Ra in the gating peak can be estimated to be a few percent based on the measured yield of the ^{207}Ra^{m} in the spectrum and the known isomeric ratio [113].

The delayed γ-rays emitted within 1 μs of a recoil implantation and tagged with the ^{207,208}Ra α-decay, are shown in figure 5.5. The γ-rays observed constitute the decay sequence of a 250(10) ns isomer and have been previously reported by Ressler et al. [58], who quote 250(30) ns for the half-life. Cocks [57] states the half-life to be 270 ns without an error estimate and does not give explicit details of the decay path, although energy level systematics are shown. In ref.

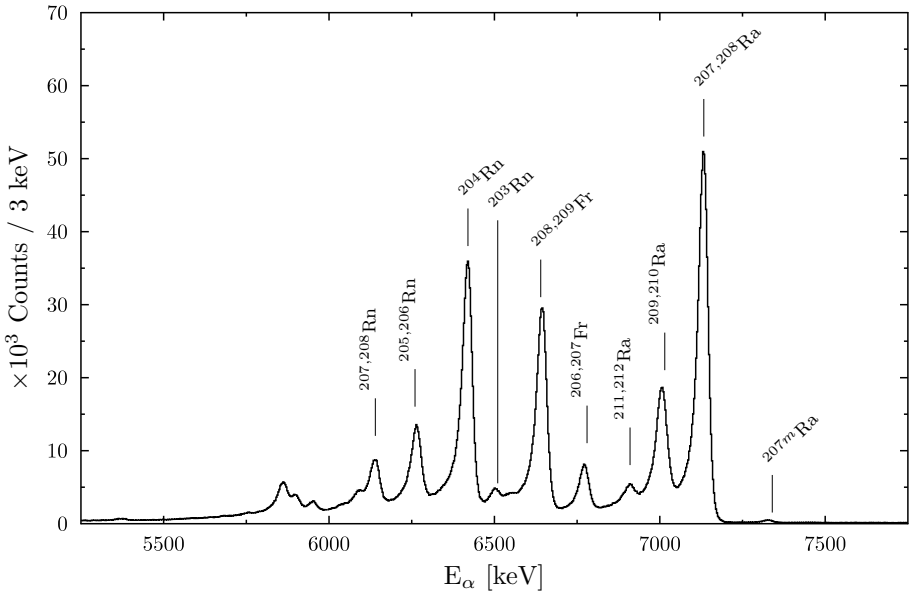

Figure 5.4: Decay event energy spectrum correlated with a recoil implantation at maximum 4 s before the decay. The most prominent peaks have been labelled. Data are from the ^{40}Ar+^{172}Yb reaction.

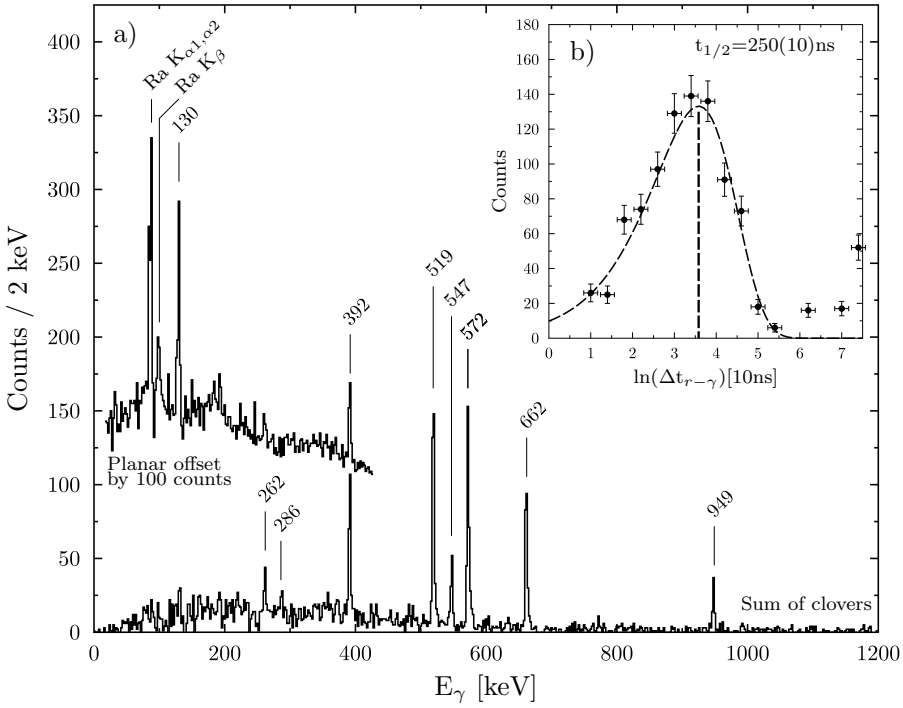

Figure 5.5: Panel a): Delayed singles γ-rays detected in the clover detectors and in the planar detector within 1 μs of a recoil implantation which could be correlated with an α-decay of ^{208}Ra. Panel b): Time spectrum used to extract the half-life of the isomer in ^{208}Ra. Summed data from all transitions were used. Only the fit component corresponding to the isomeric decay is shown.

[58] the assignment of the isomer to ^{208}Ra is based on ref. [57], in which the RDT method was used. The details of the observed γ-rays are tabulated in table 5.2. All γ-rays are observed to follow the same time distribution and are thus assumed to be fed by the decay of a single isomeric state. A fit to the summed data reveals the half-life of 250(10) ns, shown in panel b) of figure 5.5.

A level scheme, shown in figure 5.9, was constructed based on the rather limited γ-γ coincicence data from the decay of the isomeric state. The decay path via the 6_1^+ and 4_1^+ states involving the 519, 572, 662 and 392 keV γ-rays could be extracted from the coindicence data. Other transitions have been placed in the level scheme based on energy sum and intensity balance arguments. Typical coincidence spectrum, produced as a sum of two gates, is shown in figure 5.6. The $I^\pi=8^+$ assignment of the isomeric state is based on the energy and half-life

Table 5.2: Gamma-ray transitions assigned to ^{208}Ra. The energies (E_γ) in keV, relative intensities without (I_γ) and with the correction for internal conversion (I_{rel}), assuming the given multipole character, as well as the tentative level assignments are given. Relative intensities are normalised to the 519 keV transition.

E_γ (keV)	I_γ (%)	I_{rel} (%)	$Mult.$	$I_i^\pi - I_f^\pi$
130(1)	14(2)	54(7)	$E2$	$(8^+) - (6_2^+)$
262(1)	11(3)	22(7)	$M1$	$(6_2^+) - (6_1^+)$
286(1)	6(3)	6(3)	$E2$	$(6_1^+) - (4_2^+)$
392(1)	44(7)	46(7)	$E2$	$(8^+) - (6_1^+)$
519(1)	100(11)	100(11)	$E2$	$(2^+) - 0^+$
547(1)	27(6)	27(6)	$E2$	$(6_2^+) - (4_2^+)$
572(1)	95(11)	95(11)	$E2$	$(4_1^+) - (2^+)$
662(1)	71(10)	71(10)	$E2$	$(6_1^+) - (4_1^+)$
949(1)	22(6)	22(6)	$E2$	$(4_2^+) - (2^+)$

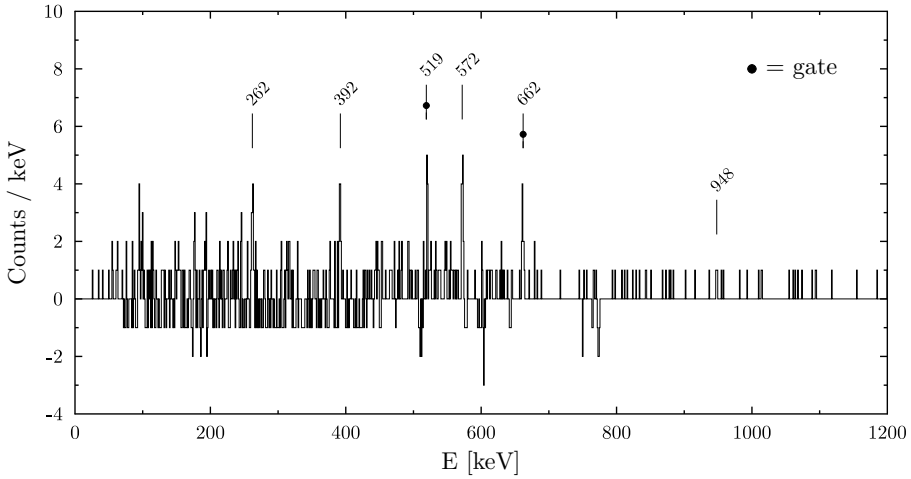

Figure 5.6: Sum of 519 keV and 662 keV gated background subtracted spectra from the ^{208}Ra α-tagged clover-clover matrix.

extrapolation from the heavier Ra isotopes. The tentative assignment of the weak 286 keV transition as the 6_1^+ to 4_2^+ transition confirms the ordering of the 546 and 949 keV transitions, and fixes the level energy of the 4_2^+ state.

5.1.3 ^{206}Ra

^{206}Ra was studied in-beam using the ^{40}Ar+^{170}Yb reaction and the RDT method. In figure 5.7 a plot of the α-decay energies vs. the logarithm of the time difference between a recoil implantation and an α-decay are shown. The ^{206}Ra decays are well separated from the decays of the other products and no other decays are known having the same energy and half-life.

The singles γ-ray spectrum resulting from recoil gating and tagging with the ^{206}Ra α-decays are presented in figure 5.8. Four γ-rays reported by Cocks [57] are clearly observed in the tagged spectrum. In addition, several weaker, low energy transitions are seen, along with the newly observed 520 and 674 keV transitions. The results for the tagged γ-rays are summarised in table 5.3. Based on the measured intensities and systematics, the assignment of the 474, 578, and 710 keV transitions as the cascade of E2 transitions from the 6^+ state to the ground state is confirmed. On the other hand, assuming an E2

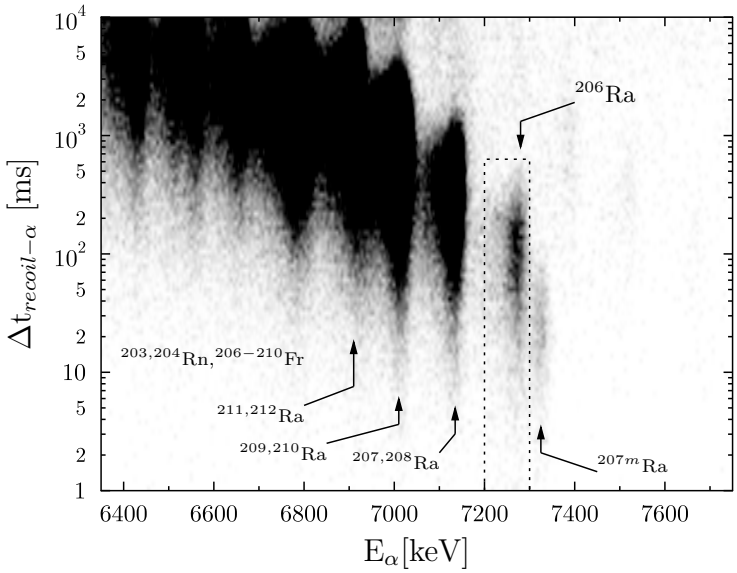

Figure 5.7: Decay time vs. the α-particle energy from the ^{40}Ar+^{170}Yb reaction. The conditions used to select ^{206}Ra are shown as dashed lines.

Table 5.3: Gamma-rays in ^{206}Ra. The energies (E_γ) in keV, relative intensities without (I_γ) and with the correction for internal conversion (I_{rel}), along with yield of K-shell conversion electrons, assuming the given multipole character, as well as the tentative level assignments are given. Relative intensities are normalised to the 2^+-0^+ transition and the K-electron yields to the γ-ray intensity of the 2^+-0^+ transition to allow the comparison to the X-ray yield. The X-ray yields per K-shell vacancy are 0.73 for the K_α and 0.20 for the K_β lines.

E_γ (keV)	I_γ (%)	I_{rel} (%)	$Mult.$	I_K (%)	$I_i^\pi - I_f^\pi$
Ra K_α	76(6)				
Ra K_β	25(3)				
180(1)	14(2)	25(3)	$E2$	2.8	
		53(7)	$M1$	33.5	
222(1)	9(1)	11(2)	$E2$	1.1	
		21(3)	$M1$	11.1	
246(1)	36(3)	44(3)	$E2$	3.8	
		76(6)	$M1$	35.2	
276(1)	6(1)	7(1)	$E2$	0.5	
		12(2)	$M1$	4.6	
308(1)	4(1)	5(1)	$E2$	0.3	
		7(2)	$M1$	2.4	
474(1)	100(5)	100(5)	$E2$	3.8	$(2^+) - 0^+$
520(1)	11(2)	11(2)	$E2$	0.3	
578(1)	85(5)	100(5)	$E2$	1.6	$(4^+) - (2^+)$
674(1)	15(2)	15(2)	$E2$	0.2	
710(1)	42(4)	41(4)	$E2$	0.5	$(6^+) - (4^+)$

multipolarity, the observed intensity of the 246 keV transition is higher than that of the 710 keV 6^+-4^+ transition, albeit within the errors. The imbalance suggests that the nature of the 246 keV transition is not likely to be 8^+-6^+, as suggested by Cocks [57]. Further evidence is provided by the relatively high $K_{\alpha,\beta}$ X-ray yield, which can be reasonably well explained by assuming that the low energy γ-rays all have a pure M1 multipolarity. The other possible explanation of the X-ray intensity requires the existence of several, almost completely converted transitions. Since the total conversion coefficients are $\alpha_{tot} > 5$ for E<150 keV M1 transitions, this scenario can not be completely ruled out by the current statistics. More exotic multipolarities could also affect the situation.

No delayed γ-rays were associated with ^{206}Ra. This indicates that if isomeric states exist in this nucleus they have lifetimes in the range of 1 to 100 ns and

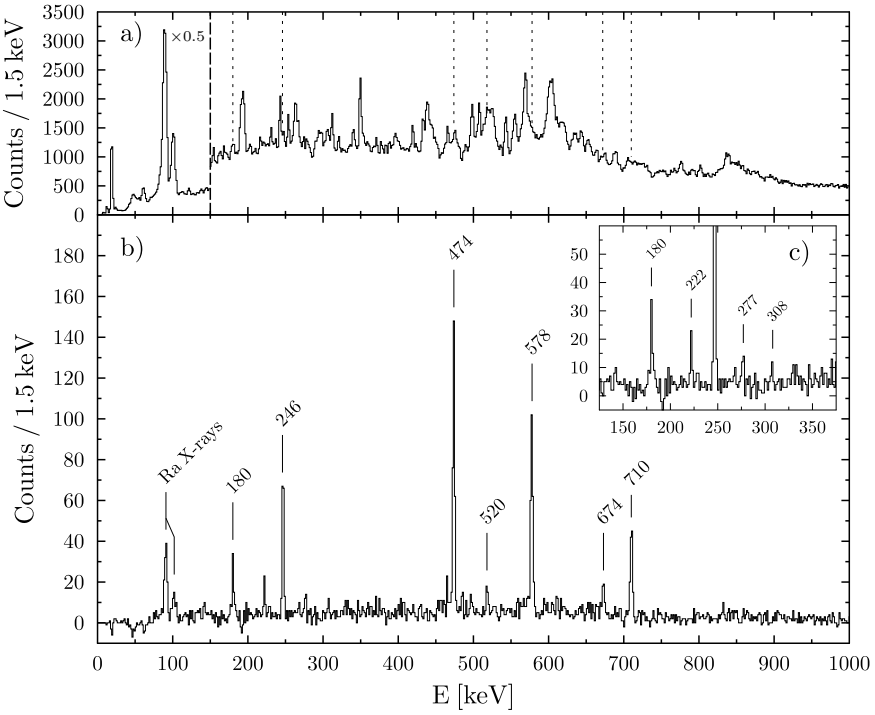

Figure 5.8: Total singles recoil gated γ-ray spectrum from the experiment aimed to study ^{206}Ra is shown on the top panel a). On the bottom panel, γ-rays tagged with the α-decay of ^{206}Ra are shown. In the insert c) the region around the weak, low energy γ-rays is enlarged. The tagged spectra have been background subtracted. The positions of the γ-rays labelled in panel b) have been indicated with dashed lines in panel a). Time-random background has been subtracted from the spectra in panels b) and c).

decay in-flight wihtin the separator. The level of prompt γ-γ statistics available is very low and cannot reliably be used to establish coincidence relationships of the γ-rays.

5.2 Discussion

The experimental information gathered in the previous section has been collected into the level schemes shown in figure 5.9.

Low-spin states up to $I^\pi = 8^+$ in even-even Po and Rn isotopes with 116 $< N <$126 are well described by the IBA + two-quasiparticle model of Zemel and Dobes [39]. At that time experimental data on level energies in the Ra isotopes was limited to ^{214}Ra. Still in the same paper predicted level energies down to ^{204}Ra are shown. In figure 5.10 this prediction is shown together with the currently available data. The agreement is rather amazing. In the figure all known states up to $I^\pi = 8^+_1$ in ^{206,208,210}Ra (data taken from present work and [57, 58, 59, 60]), ^{212}Ra [114] and the closed neutron-shell nucleus ^{214}Ra [115], where these states form the $\pi(h^6_{9/2})$ multiplet, are shown.

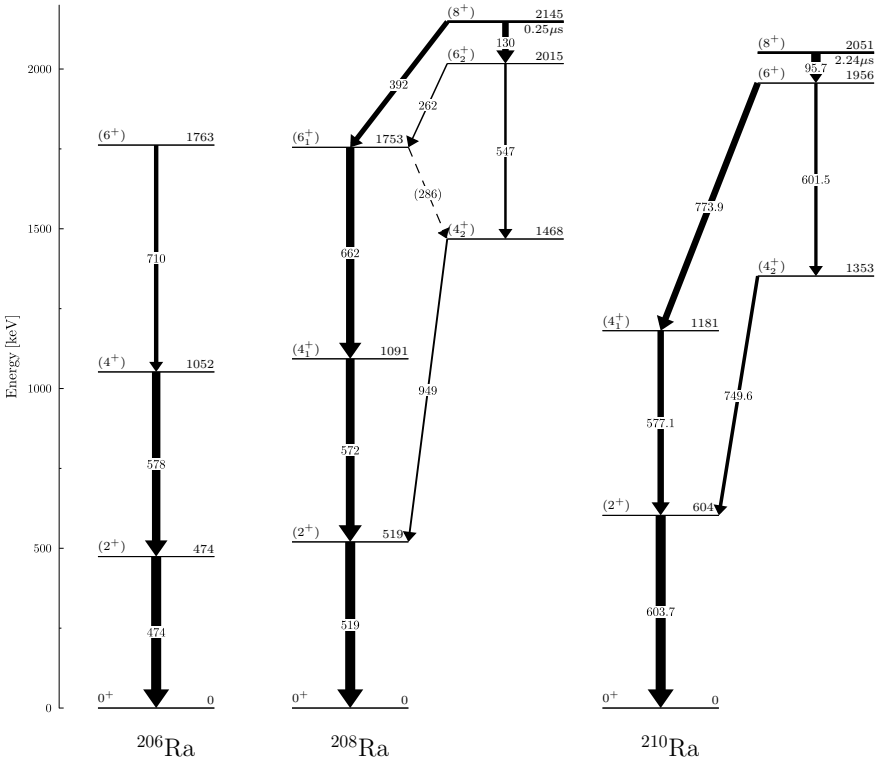

Figure 5.9: Level schemes of ^{206,208,210}Ra from this work.

Experimentally, a gradual increase of excitation energy is observed for the 8^+_1 states. These states in Ra isotopes are presumed to have a dominant $\pi(h^n_{9/2})$ character. The energy increase with decreasing neutron number is presumably due to the fact that the interactions between the neutron hole states and $h_{9/2}$ proton states become increasingly repulsive as the neutron shell is depleted [116]. The excitation energy of the 6^+_1 state increases in a similar manner when going from ^{214}Ra to ^{210}Ra, but then drops, being on a similar level in ^{208}Ra and ^{206}Ra. The gradual increase in the 6^+ energy expected for the $\pi(h^n_{9/2})$ configuration, and seen in the Po isotopes, is represented by a 6^+_2 level observed in ^{208}Ra. A dramatic decrease in the energy of the 4^+_1 state is observed between ^{214}Ra and ^{210}Ra, after which the falling trend flattens slightly. Similarly to the Rn isotones a second 4^+ state is observed in ^{210}Ra and ^{208}Ra. The gradual smooth decrease of the 2^+_1 energy between ^{212}Ra and ^{206}Ra is indicative of a gradual increase in collectivity, attributed to an increasing number of 2^+ components of neutron hole origin.

In the IBA-QP calculations [39] the 8^+_1 states are found to be rather pure quasiproton $\pi(h^n_{9/2})$ states. The irregular behaviour of the yrast 4^+ and 6^+ energies is explained as a change from the $\pi(h^n_{9/2})$ configuration to a more

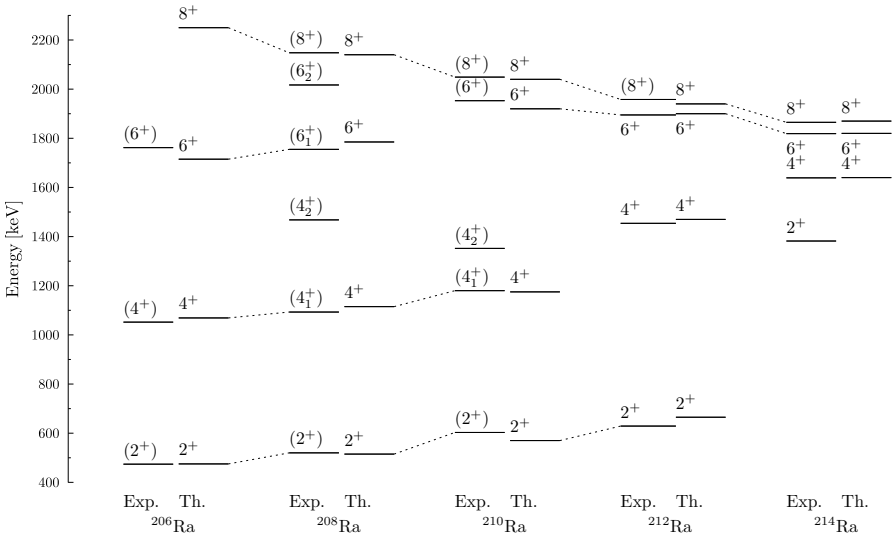

Figure 5.10: Experimental and theoretical systematics of levels below the 8^+_1 state in $^{206-214}$Ra. Experimental data are from current work and [48]. Theoretical predictions are from [39].

mixed configuration with dominant collective components in the wave-functions of these states in the lightest isotopes. The 2^+ states are found to be largely collective.

On closer inspection of the level schemes constructed in this work and shown in figure 5.9, a few details in favour of the above description arise.

Both 4^+ states in ^{210}Ra are populated via decay from the $\pi(h^6_{9/2})6^+$ state, and both decay to the 2^+_1 state. A transition strength ratio $B(E2;6^+ \rightarrow 4^+_2)/B(E2;6^+ \rightarrow 4^+_1)$ of 2.2 was deduced using information given in table 5.1. This value indicates that the 4^+_2 state is predominantly of $\pi(h^6_{9/2})4^+$ character, while 4^+_1 state is more of a mixed nature.

In ^{208}Ra, the decay from the $\pi(h^6_{9/2})8^+$ state to the 6^+_1 state is hindered with respect to decay to the 6^+_2 state by a factor of $\sim$300 (see data in table 5.2). This supports the association of the 6^+_2 state with the $\pi(h^6_{9/2})6^+$ configuration. It also indicates a more mixed nature for the wavefunction of the 6^+_1 state. The 4^+_2 state in this nucleus is fed mainly by the decay from the 6^+_2 state and is therefore presumably also dominated by the quasiproton configuration. No 923 keV γ-ray corresponding the E2($\pi(h^6_{9/2})6^+_2 \rightarrow 4^+_1$) was observed, revealing that the 4^+_1 state is probably dominated by a more collective or neutron configuration.

Differing from the earlier interpretation of ref. [57], the improved in-beam study of ^{206}Ra reveals that there is, very likely, still no sign of an abrupt decrease in level energies due to intruding deformed structures. Actually, a closer examination of level energy systematics of even-even Po and Rn nuclei indicates that such changes may not be expected until ^{204}Ra. If a linear increase in the energy of the yrast 8^+ levels is assumed when going from ^{214}Ra to ^{206}Ra, the 8^+ level in ^{206}Ra should lie approximately 500 keV above the yrast 6^+ level. This is supported by the IBM+QP calculations [39], for which the maximum error in comparison to the experimental energies is 50 keV for the states included in the calculation. If the hindrance of the corresponding E2 transition would be similar to that for the 392 keV E2($8^+ \rightarrow 6^+$) transition in ^{208}Ra, the half-life of the 8^+ level in ^{206}Ra could well be of the order of 100ns. Such a decay would take place inside RITU unseen by the detectors at the target as well as the focal plane. All the observed states in ^{206}Ra can be associated with the corresponding yrast states in ^{208}Ra and thus to dominantly collective or quasineutron states.

The low energy γ-rays observed in-beam in the study of ^{206}Ra are most likely of M1 character and form a rotational-like structure. Such a dipole band could be a relatively strongly populated shears band similar to those observed in

^{205}Rn, ^{204}At and ^{206}Fr [117, 118]. The relative internal conversion-corrected intensity for the strongest 246 keV M1 transition would then be 76(6), which indicates that a large fraction of the decay out of this band drains via unobserved transitions or an isomeric state. It is difficult to determine any order for the candidate M1 transitions without γ-γ coincidences as the possible shears band may well be irregular and the decay out from the band may well take place from several states. It should be also noted that shears bands are associated with (near-)spherical nuclei.

It would be of considerable interest to study excited states in even-A Ra isotopes closer to the proton drip-line and verify a possible onset of intruder structures. The maximum production cross-section measured for the next isotope, ^{204}Ra, is 50 nb [119]. Attempts to observe its excited states have so far failed. Recent results, for example in chapter 3, show that this now is well within the current scope of state-of-the-art in-beam spectroscopy.

Chapter 6

Experimental limits and future directions

6.1 Currie limits

The most used definition of "detection limits" in nuclear science was introduced by Currie [120] in 1968. Three limits are introduced; decision limit (L_C), detection limit (L_D) and determination limit (L_Q). The first two are further described in the following section.

The decision limit is a *a posteriori* limit, something, which can be applied after the measurement to decide whether a measured signal is large enough to warrant a claim of detection. In the specific case of radioactivity, the limit is:

$$L_c = k_\alpha \sqrt{\mu_s + \sigma_B^2} \tag{6.1}$$

in which, μ_s is the mean background signal, σ_B is the standard deviation of the background and k_α is the symmetric fractile of the gaussian distribution, describing the risk level which is acceptable for the measurement. The α-value is the probablility for the error of the first kind, i.e. for claiming detection when the signal is not present. The original treatise by Currie is limited to single channel analyser (SCA) data. An extension of the method to γ-ray spectra can be found in the work of De Greer [121], in which also the low statistics

cases requiring the use of Poisson distribution is covered. In the paper a table giving maximum background levels for given net signals and risks are given in the case of low statistics.

Once the decision limit is defined for a given measurement process, the detection limit can be calculated. Therefore it is a *a priori* limit, which can be applied before the actual measurement. The detection limit is intimately related to the decision limit and the error of the second kind, in which one fails to detect the signal even if it is present. Very often the risks of the errors of the first (α) and second (β) kind are set to be equal ($k_\alpha = k_\beta = k$). In this case the detection limit for radioactivity simplifies to the often seen:

$$L_D = k^2 + 2L_C \tag{6.2}$$

In the case of nuclear structure studies, the above approximation is often not valid. The standard accepted signal level for detection is at least 3σ. On the other hand the errors of the second kind are more tolerated since "no result" is (socially) more acceptable than "wrong result". Thus, the detection limit should probably, in this case, be calculated explicitely. In ref. [120] the general case is given as:

$$L_D = L_C + \frac{k_\beta^2}{2} + \left(1 + \sqrt{1 + \frac{4L_C}{k_\beta^2} + \frac{4L_C^2}{K_\alpha^2 k_\beta^2}}\right) \tag{6.3}$$

The limits for detection can therefore be defined from the measured background and signal levels and the error probabilities accepted for the errors of both kinds. In the following, risks of α=0.05% (k_α=3.291, close to 3σ limit) are accepted for the error of the first kind and risks of β=5% (k_β=1.645) for the errors of the second kind.

6.2 Current limits of feasibility for in-beam RDT studies.

As seen in chapter 3, in-beam γ-ray spectroscopy can be currently used to study nuclei with production cross-sections as low as 10 nb, when the RDT method is utilised. Even so, the use of α-α correlations and the high γ-ray energy from the 2^+ state, makes ^{180}Pb a less than perfect case for a low statistics

experiment. In the case of RDT studies, the feasibility of an experiment can be simply estimated by two factors. First, the yield of decays, which can be used as a tag is required and secondly, the amount of γ-rays detectable per tag needs to be estimated.

Inspecting the γ-ray data, presented in table 6.1, for some of the very neutron deficient cases studied, ^{180,182}Pb, ^{192,190}Po, ^{198}Rn and ^{206}Ra, reveals a consistent picture of the γ-ray statistics available in RDT studies. The amount of γ-rays from the 2^+-0^+ transition per tagged recoil is practically a constant, on average 6 γ-rays per 100 decays. The yields have been normalised to 300keV γ-rays detected using the Jurogam II array, since this is the array to be used in the future experiments and the approximate energy at which the low-spin transitions are expected in the key experiments to come. In the cases of ^{206}Ra and ^{192}Po, the expected and known isomeric states, respectively, are assumed to lower the prompt γ-ray yield. The low energy 4^+-2^+ transitions in Pb nuclei have been used instead of the 2^+-0^+ γ-rays to minimise the error in relative effiencies between the different arrays used. This might have an effect on the slightly low yield in the case of ^{182}Pb.

The amount of γ-rays expected per tag can be easily calculated. Since the α-decays are correlated with the respective, detected recoils, the number of prompt γ-rays detected for a given α-decay should be

$$N_\gamma = N_\alpha \times \epsilon_\gamma \times \frac{1}{1+\alpha_{tot}} \times F \tag{6.4}$$

in which ϵ_γ is the γ-ray detection efficiency, α_{tot} the total conversion coefficient and F the fraction of the intensity flux passing through the transition in question. It should be noted that the values obtained are a factor of $\sim$2 too low if the ground state is expected to be 100% fed by the prompt yrast cascade. The reason for this is currently not known. Taking into the account the internal conversion, probabilities of finding the wrong recoil in the RDT process and not accepting all the correct γ-rays into the final spectra, due to timing conditions etc. does not fully account for the missing intensity. The experiments have been performed using different detector systems, electronics and data acquisition systems and have been analysed by several people using different analysis codes, thus the systematic errors stemming from the measurement system and analysis methods should not be very large or likely.

From the ^{206}Ra, ^{190,192}Po and ^{180}Pb data, the average background at 300 keV was extracted. The background was calculated as the average number of counts in the energy range of 200-400 keV for the Ra and Po isotopes and 0-600 keV for ^{180}Pb, excluding the known transitions. The extracted values in units of counts/keV are 5-6$\times 10^{-4}$ per tagged recoil in all the cases. Since the

Table 6.1: Yields of γ-rays per 100 α-decays, $N^{abs}_{\gamma/\alpha}$, for several neutron deficient Pb,Po,Rn and Ra isotpes. Isotopes, detector arrays used, the γ-ray energies in question, α-decay and γ-ray yields, relative efficiencies normalised to 300 keV and absolute efficiencies at 1.3 MeV are given. The results are normalised to 300 keV γ-ray detected by Jurogam II. Transitions in question are the 2^+-0^+ transitions, except in the Pb cases where the 4^+-2^+ transitions are used.

	Array	E_γ [keV]	N_α	N_γ	ϵ^{300keV}_{rel}	$\epsilon^{1.3MeV}_{abs}$	$N^{abs}_{\gamma/\alpha}$[%]
^{206}Ra	Jurogam I	474	8600	260	0.79	4.5	5.1
^{198}Rn	Jurosphere	339	2400	35	0.95	1.5	6.2
^{192}Po	Jurogam I	262	80000	3700	1.04	4.5	5.9
^{190}Po	Jurogam I	233	1800	98	1.07	4.5	6.8
^{182}Pb	Jurosphere	231	3500	55	1.07	1.5	5.9
^{180}Pb	Jurogam II	278	270	19	1.04	6.0	6.8

backgrounds were extracted from a wide energy range, the standard deviation is assumed to be small. In this case the equation 6.1 reduces to $L_C = k\sqrt{\mu_S}$, for which the values of $\bar{L}_C = \mu_S + k\sqrt{\mu_S}$, the total amount of counts in the SCA, in the low statistics Poisson limit can be read from Table 2 of ref. [121].

The average resolution in the measurements was about 3 keV FWHM at 300 keV. In [121] a SCA window width of 1.25 times the FWHM is recommended to maximise the signal-to-noise ratio. A window width of 4 keV is used in the following.

The lowest γ-ray yield detectable can now be deduced. The expected background in the 4 keV SCA window can be calculated for different amounts counts in a 300keV peak, using the results deduced above. For a given amount of counts in a peak, the required amount of α-decays is calculated using the ratio 0.06 γ-rays per α-decay. From the amount of required α-decays the average background is calculated using the value 6×10^{-4} counts per keV per tagged recoil, leading to the value 0.0024 counts per 4 keV SCA window per α-decay. The calculated background level can now be compared to the background limits for a given $\bar{L}_C$ value, given in Table 2 of ref. [121]. It is noted that all values of counts down to 2 counts in a peak are detectable with the calculated background level. The corresponding amount of required α-decays is 33. The detection limit can be now calculated using the L_C value of 33, k_α=3.291 and k_β=1.645. The value is L_D=54.

Knowing the amount of α-decays which is needed in order to detect at least the assumed 300 keV 2^+-0^+ transition, the feasibility of experiments on light Pb, Po, Rn and Ra can be considered. In the following, 14 day experiments are

considered. The beam intensity is assumed to be 30pnA and target thickness 500μg/cm^2. The focal plane coverage is assumed to be 80% and the fraction of α-decays for which full energies are detected is taken to be 55%.

In the current work, the production cross section for ^{180}Pb is deduced to be 10 nb. The cross section for ^{178}Pb has not been given in any of the reports in which the identification is claimed [122]. The cross section drops by a factor of 30 when going from ^{182}Pb to ^{180}Pb and based on this a upper limit of 300 pb is estimated for the ^{178}Pb cross section. Using the ^{78}Kr+^{104}Pb reaction, same as in ref [122], and assuming a 40% RITU transmission for the reaction, 34 full energy α-particles from the decay of ^{178}Pb is expected. This is below the detection limit. Further, the 2^+-0^+ transition is ^{178}Pb is not likely to be in the low-energy region used in the calculation above. In this light, ^{180}Pb is the lightest Pb isotope for which in-beam spectroscopy is feasible.

Production cross sections for ^{188}Po using several reactions are given in ref [123]. Using the measured value of 8 nb for the ^{50}Cr+^{142}Nd reaction, over 400 α-decays should be detected in 14 days. The experiment is therefore deemed feasible. Alternative reactions exist. A cross section of 30 nb is calculated for the ^{144}Sm(^{47}Ti,3n)^{188}Po reaction by Andreyev et al. [123]. A possible cold-fusion reaction would be ^{90}Zr+^{100}Ru. For ^{144}Sm(^{46}Ti,4n)^{186}Po, Andreyev et al. [123] cite 200 pb cross-section. This would give 10 α-decays in a two week experiment, far below the detection threshold. In both cases the RITU transmission was estimated to be 25%.

Two cross-section values for ^{196}Rn exist in the literature. Kettunen et al. [67] give a value of 2 nb for the ^{142}Nd(^{56}Fe,2n)^{196}Rn and Pu et al. [124] give 4 nb for the ^{166}Er(^{36}Ar,6n)^{196}Rn. Using the first value and reaction would give $\sim$126 full energy α-decays, comfortably above the detection limit. The transmission of RITU separator is expected to be 30%. Possible alternative reactions are ^{52}Cr+^{147}Sm, for which 2 nb cross section has been measured [125] and ^{80}Kr+^{119}Sn. In ref. [65] a 120 pb production cross-section is given for ^{194}Rn using ^{52}Cr+^{144}Sm. Since only 8 α-decays is expected to be seen, the isotope is not suitable for in-beam studies.

Leino et al. [126] give a cross-section value of 40 nb for the production of ^{204}Ra in the ^{35}Cl+^{175}Lu reaction. If the transmission is assumed to be 20% for such an asymmetric reaction, over 1300 α-decays should be observed in two weeks. For the isotope ^{202}Ra, a production cross-section of 25 pb is given for the ^{170}Yb(^{36}Ar,4n)^{202}Ra reaction in ref. [127]. At this level, a single α-decay is expected to be seen in a two week experiment.

Based on the above analysis, three possible cases of in-beam experiments on

even more neutron deficient even-even nuclei in the region exist: ^{204}Ra, ^{196}Rn and ^{188}Po. The physics cases are very interesting in each of the cases and all have already in fact been proposed to the JYFL program advisory committee, which has approved all of them. Production trials have been run, but full experiments have not been performed yet. The analysis shows that production cross-sections down to a one nanobarn level are feasible in the region of intrest if only knowledge of the 2^+ level energies is required. If required, the calculations performed above for the estimated 2^+-0^+ transitions can be extended relatively easily for the other transitions of the yrast cascade.

6.3 Future directions

Finding excited states for the first time in nuclei is not the only way of studying nuclear properties. Several new directions have been explored lately, which provide extremely valuable information on nuclear structure in the neutron deficient trans-lead nuclei.

Measurements of transition probablities in nuclei provides direct evidence on the collective phenomena. Recent differential plunger measurements of Pb and Po nuclei [33, 34, 35] close to the N=104 mid-shell have revealed changes in collectivity of the rotational bands at low spins, supporting the scenario in which the low spin states in these nuclei are admixtures of several low-lying configurations. The first experiments utilising the Coulomb excitation of post accelerated radioactive beams of Rn and Po isotopes [128, 129] at the REX-ISOLDE facility in CERN have been recently performed. Coulomb excitation is a unique tool in a sense, since it can reveal the sign of the quadrupole moment of the nucleus through the determination of the diagonal matrix elements, as well as the transition probabilities. The first Coulomb excitation experiment using neutron deficient Pb beams [130] is planned for the Autumn 2010.

The SAGE spectrometer [131], recently commissioned at JYFL, will provide unique data on shape-coexistence in the region through the simultaneous measurement of γ-rays and conversion electrons in RDT experiments. This allows direct searches for E0 transitions and E0 components in other transitions, both being fingerprints of shape-coexistence. Plans of constructing a recoil-shadow electron spectrometer for RDT studies have also been made. The device would allow the determination of lifetimes of excited 0^+ states in the ps-ns range.

Neighbouring nuclei with odd numbers of protons or neutrons provide a more challenging experimental field than the even-even nuclei on which this thesis has focused in. The rewards can be high, though. The coupling of the odd

nucleon to the even-even core can provide valuable information on the structural properties. Good examples of this approach have been the studies of Bi isotopes in the vicinity of the neutron mid-shell [9] and the first odd-neutron Pb isotope beyond the mid-shell [132].

As can be seen, the shape-evolution and shape coexistence in the Pb region is currently receiving a lot of experimental attention. Even if the new even-even cases for which in-beam RDT measurements are possible are starting to run out, other novel approaches through which the underlying physics can be probed even better are becoming available.

Bibliography

[1] J. L. Wood, K. Heyde, W. Nazarewicz, M. Huyse, and P. Van Duppen, "*Coexistence in even-mass nuclei.*", *Phys. Rep.* **215** (1992) 101.

[2] R. Julin, K. Helariutta, and M. Muikku, "*Intruder States in Very Neutron-Deficient Hg, Pb and Po Nuclei.*", *J.Phys.(London)* **G27** (2001) R109.

[3] W. Nazarewicz, "*Variety of Shapes in the Mercury and Lead Isotopes.*", *Phys.Lett.* **305B** (1993) 195.

[4] A. N. Andreyev, M. Huyse, P. Van Duppen, L. Weissman, D. Ackermann, J. Gerl, F. P. Hessberger, S. Hofmann, A. Kleinbohl, G. Munzenberg, S. Reshitko, C. Schlegel, H. Schaffner, P. Cagarda, M. Matos, S. Saro, A. Keenan, C. Moore, C. D. O'Leary, R. D. Page, M. Taylor, H. Kettunen, M. Leino, A. Lavrentiev, R. Wyss, and K. Heyde, "*A Triplet of Differently Shaped Spin-Zero States in the Atomic Nucleus* ^{186}*Pb.*", *Nature(London)* **405** (2000) 430.

[5] D. L. Hill and J. A. Wheeler, "*Nuclear Constitution and the Interpretation of Fission Phenomena.*", *Phys. Rev.* **89** (1953) 1102.

[6] P. Moller, J. R. Nix, W. D. Myers, and W. J. Swiatecki, "*Nuclear Ground-State Masses and Deformations.*", *At.Data Nucl.Data Tables* **59** (1995) 185.

[7] S. Hilaire and M. Girod, "*Large-scale mean-field calculations from proton to neutron drip linesusing the D1S Gogny force.*", *Eur.Phys.J. A* **33** (2007) 237.

[8] M. Bender, G. F. Bertsch, and P.-H. Heenen, "*Global study of quadrupole correlation effects.*", *Phys. Rev. C* **73** (2006) 034322.

[9] A. Hurstel, Y. Le Coz, E. Bouchez, A. Chatillon, A. Gorgen, P. T. Greenlees, K. Hauschild, S. Juutinen, H. Kettunen, W. Korten,

P. Nieminen, M. Rejmund, C. Theisen, J. Wilson, A. N. Andreyev, F. Becker, T. Enqvist, P. M. Jones, R. Julin, H. Kankaanpaa, A. Keenan, P. Kuusiniemi, M. Leino, A. P. Leppanen, M. Muikku, J. Pakarinen, P. Rahkila, and J. Uusitalo, "*Prolate deformation in the ^{187,189}Bi isotopes.*", *Eur.Phys.J. A* **21** (2004) 365.

[10] P. Nieminen, S. Juutinen, A. N. Andreyev, J. F. C. Cocks, O. Dorvaux, K. Eskola, P. T. Greenlees, K. Hauschild, K. Helariutta, M. Huyse, P. M. Jones, R. Julin, H. Kankaanpää, H. Kettunen, P. Kuusiniemi, Y. L. Coz, M. Leino, T. Lönnroth, M. Muikku, P. Rahkila, A. Savelius, J. Uusitalo, N. Amzal, N. J. Hammond, C. Scholey, and R. Wyss, "*γ -ray spectroscopy of ^{191,193}Bi.*", *Phys. Rev. C* **69** (2004) 064326.

[11] H. De Witte, A. N. Andreyev, N. Barré, M. Bender, T. E. Cocolios, S. Dean, D. Fedorov, V. N. Fedoseyev, L. M. Fraile, S. Franchoo, V. Hellemans, P. H. Heenen, K. Heyde, G. Huber, M. Huyse, H. Jeppessen, U. Köster, P. Kunz, S. R. Lesher, B. A. Marsh, I. Mukha, B. Roussière, J. Sauvage, M. Seliverstov, I. Stefanescu, E. Tengborn, and K. Van de Vel, "*Nuclear Charge Radii of Neutron-Deficient Lead Isotopes Beyond $N = 104$ Midshell Investigated by In-Source Laser Spectroscopy.*", *Phys. Rev. Lett.* **98** (2007) 112502.

[12] F. R. May, V. V. Pashkevich, and S. Frauendorf, "*A Prediction on the Shape Transitions in Very Neutron-Deficient Even-Mass Isotopes in the Lead Region.*", *Phys.Lett.* **68B** (1977) 113.

[13] R. Bengtsson and W. Nazarewicz, "*Shape Coexistence in the Neutron Deficient Pb Isotopes and the Configuration-Constrained Shell Correction Approach.*", *Z.Phys.* **A334** (1989) 269.

[14] W. Satula, S. Cwiok, W. Nazarewicz, R. Wyss, and A. Johnson, "*Structure of superdeformed states in Au—Ra nuclei.*", *Nucl.Phys.* **A529** (1991) 289.

[15] S. Yoshida and N. Takigawa, "*Shape dependence of pairing gap energies and the structure of Hg and Pb isotopes.*", *Phys.Rev.C* **55** (1997) 1255.

[16] S. Yoshida, S. K. Patra, N. Takigawa, and C. R. Praharaj, "*Structure of neutron-deficient Pt, Hg, and Pb isotopes.*", *Phys.Rev.C* **50** (1994) 1398.

[17] T. Nikšić, D. Vretenar, P. Ring, and G. A. Lalazissis, "*Shape coexistence in the relativistic Hartree-Bogoliubov approach.*", *Phys. Rev. C* **65** (2002) 054320.

[18] M. Bender, T. Cornelius, G. A. Lalazissis, J. A. Maruhn, W. Nazarewicz, and P. G. Reinhard, "*The $Z = 82$ Shell Closure in Neutron-Deficient Pb Isotopes.*", *Eur.Phys.J.A* **14** (2002) 23.

[19] N. Tajima, H. Flocard, P. Bonche, J. Dobaczewski, and P. H. Heenen, "*Diabatic effects in Pb-186: A Generator coordinate analysis.*", *Nucl. Phys.* **A551** (1993) 409.

[20] J. Meyer, P. Bonche, M. S. Weiss, J. Dobaczewski, H. Flocard, and P. H. Heenen, "*Quadrupole and octupole correlations in normal, superdeformed and hyperdeformed states of 194Pb.*", *Nucl.Phys.* **A588** (1995) 597.

[21] R. R. Chasman, J. L. Egido, and L. M. Robledo, "*Persistence of deformed shapes in the neutron-deficient Pb region.*", *Physics Letters B* **513** (2001) 325.

[22] J. Libert, M. Girod, and J.-P. Delaroche, "*Microscopic descriptions of superdeformed bands with the Gogny force: Configuration mixing calculations in the $A \sim 190$ mass region.*", *Phys.Rev.C* **60** (1999) 054301.

[23] T. Duguet, M. Bender, P. Bonche, and P. H. Heenen, "*Shape coexistence in 186Pb: beyond-mean-field description by configuration mixing of symmetry restored wave functions.*", *Phys.Lett.B* **559** (2003) 201.

[24] M. Bender, P. Bonche, T. Duguet, and P.-H. Heenen, "*Configuration mixing of angular momentum projected self-consistent mean-field states for neutron-deficient Pb isotopes.*", *Phys. Rev. C* **69** (2004) 064303.

[25] R. R. Rodríguez-Guzmán, J. L. Egido, and L. M. Robledo, "*Beyond mean field description of shape coexistence in neutron-deficient Pb isotopes.*", *Phys. Rev. C* **69** (2004) 054319.

[26] J. L. Egido, L. M. Robledo, and R. R. Rodríguez-Guzmán, "*Unveiling the Origin of Shape Coexistence in Lead Isotopes.*", *Phys. Rev. Lett.* **93** (2004) 082502.

[27] K. Heyde, J. Jolie, J. Moreau, J. Ryckebusch, M. Waroquier, P. V. Duppen, M. Huyse, and J. L. Wood, "*A shell-model description of 0+ intruder states in even-even nuclei.*", *Nucl.Phys.* **A466** (1987) 189.

[28] K. Heyde, J. Schietse, and C. De Coster, "*Proton 4p-4h intruder excitations in heavy even-even nuclei.*", *Phys.Rev.C* **44** (1991) 2216.

[29] C. D. Coster, B. Decroix, and K. Heyde, "*Evidence for proton four-particle–four-hole intruder excitations in neutron deficient nuclei in the Pb region.*", *Phys. Rev. C* **61** (2000) 067306.

[30] R. Fossion, K. Heyde, G. Thiamova, and P. Van Isacker, "*Intruder bands and configuration mixing in lead isotopes.*", *Phys. Rev. C* **67** (2003) 024306.

[31] S. J. Krieger, P. Bonche, M. S. Weiss, J. Meyer, H. Flocard, and P. H. Heenen, "*Super-deformation and shape isomerism: Mapping the isthmus.*", *Nuclear Physics A* **542** (1992) 43.

[32] N. A. Smirnova, P. H. Heenen, and G. Neyens, "*Self-consistent approach to deformation of intruder states in neutron-deficient Pb and Po.*", *Physics Letters B* **569** (2003) 151.

[33] T. Grahn, A. Dewald, O. Moller, R. Julin, C. W. Beausang, S. Christen, I. G. Darby, S. Eeckhaudt, P. T. Greenlees, A. Gorgen, K. Helariutta, J. Jolie, P. Jones, S. Juutinen, H. Kettunen, T. Kroll, R. Krucken, Y. Le Coz, M. Leino, A. P. Leppanen, P. Maierbeck, D. A. Meyer, B. Melon, P. Nieminen, M. Nyman, R. D. Page, J. Pakarinen, P. Petkov, P. Rahkila, B. Saha, M. Sandzelius, J. Saren, C. Scholey, J. Uusitalo, M. Bender, and P. H. Heenen, "*Lifetimes of intruder states in* ^{186}Pb, ^{188}Pb *and* ^{194}Po.", *Nucl.Phys.* **A801** (2008) 83.

[34] T. Grahn, A. Dewald, O. Moller, R. Julin, C. W. Beausang, S. Christen, I. G. Darby, S. Eeckhaudt, P. T. Greenlees, A. Gorgen, K. Helariutta, J. Jolie, P. Jones, S. Juutinen, H. Kettunen, T. Kroll, R. Krucken, Y. Le Coz, M. Leino, A. P. Leppanen, P. Maierbeck, D. A. Meyer, B. Melon, P. Nieminen, M. Nyman, R. D. Page, J. Pakarinen, P. Petkov, P. Rahkila, B. Saha, M. Sandzelius, J. Saren, C. Scholey, and J. Uusitalo, "*Collectivity and Configuration Mixing in* $^{186,188}Pb$ *and* ^{194}Po.", *Phys.Rev.Lett.* **97** (2006) 062501.

[35] T. Grahn, A. Dewald, P. T. Greenlees, U. Jakobsson, J. Jolie, P. Jones, R. Julin, S. Juutinen, S. Ketelhut, T. Kröll, R. Krücken, M. Leino, P. Maierbeck, B. Melon, M. Nyman, R. D. Page, P. Peura, T. Pissulla, P. Rahkila, J. Sarén, C. Scholey, J. Sorri, J. Uusitalo, M. Bender, and P. H. Heenen, "*Collectivity of* ^{196}Po *at low spin.*", *Phys. Rev. C* **80** (2009) 014323.

[36] C. D. Coster, B. Decroix, J. D. Beule, and K. Heyde, "*An algebraic approach to shape coexistence: new symmetries and applications.*", *Phys.Scr.* **T88** (2000) 33.

[37] C. D. Coster, B. Decroix, K. Heyde, J. Jolie, H. Lehmann, and J. L. Wood, "*Particle-hole excitations in the interacting boson model (IV). The U(5)-SU(3) coupling.*", *Nucl.Phys.* **A651** (1999) 31.

[38] A. M. Oros, K. Heyde, C. De Coster, B. Decroix, R. Wyss, B. R. Barrett, and P. Navratil, "*Shape Coexistence in the Light Po Isotopes.*", *Nucl.Phys.* **A645** (1999) 107.

[39] A. Zemel and J. Dobes, "*Low-spin states in even Po and Rn isotopes and the interplay between collective and quasiparticle configurations.*", *Phys. Rev. C* **27** (1983) 2311–2316.

[40] A. N. Wilson, G. D. Dracoulis, A. P. Byrne, P. M. Davidson, G. J. Lane, R. M. Clark, P. Fallon, A. Gorgen, A. O. Macchiavelli, and D. Ward, "*Observation of a superdeformed band in* ^{190}*Pb.*", *Eur.Phys.J. A* **24** (2005) 179.

[41] B. Singh, R. Zywina, and R. B. Firestone, "*Table of Superdeformed Nuclear Bands and Fission Isomers: Third Edition (October 2002).*", *Nuclear Data Sheets* **97** (2002) 241.

[42] W. D. Myers and K. H. Schmidt, "*An Update on Droplet-Model Charge Distributions.*", *Nucl.Phys.* **A410** (1983) 61.

[43] F. Le Blanc, D. Lunney, J. Obert, J. Oms, J. C. Putaux, B. Roussière, J. Sauvage, S. Zemlyanoi, J. Pinard, L. Cabaret, H. T. Duong, G. Huber, M. Krieg, V. Sebastian, J. E. Crawford, J. K. P. Lee, M. Girod, S. Péru, J. Genevey, and J. Lettry, "*Large odd-even radius staggering in the very light platinum isotopes from laser spectroscopy.*", *Phys. Rev. C* **60** (1999) 054310.

[44] G. Ulm, S. K. Bhattacherjee, P. Dabkiewicz, G. Huber, H. J. Kluge, T. Kuhl, H. Lochmann, E. W. Otten, K. Wendt, S. A. Ahmad, W. Klempt, R. Neugart, and the ISOLDE Collaboration, "*Isotope Shift of* ^{182}*Hg and an Update of Nuclear Moments and ChargeRadii in the Isotope Range* ^{181}*Hg -* ^{206}*Hg.*", *Z.Phys.* **A325** (1986) 247.

[45] T. Cocolios. PhD thesis, Katholieke Universiteit Leuven, 2010.

[46] W. Borchers, R. Neugart, E. W. Otten, H. T. Duong, G. Ulm, K. Wendt, and the ISOLDE Collaboration, "*Hyperfine Structure and Isotope Shift Investigations in* $^{202-222}$*Rn for the Study of Nuclear Structure beyond* $Z = 82$.", *Hyperfine Interactions* **34** (1987) 25.

[47] S. A. Ahmad, W. Klempt, R. Neugart, E. W. Otten, P. G. Reinhard, G. Ulm, K. Wendt, and the ISOLDE Collaboration, "*Mean Square Charge Radii of Radium Isotopes and Octupole Deformation in the* $^{220-228}$*Ra Region.*", *Nucl.Phys.* **A483** (1988) 244.

[48] "Evaluated nuclear structure data files (ensdf) and experimental unevaluated nuclear data list (xundl)." Http://www.nndc.bnl.gov/ensdf/.

[49] K. Van de Vel, A. N. Andreyev, R. D. Page, H. Kettunen, P. T. Greenlees, P. Jones, R. Julin, S. Juutinen, H. Kankaanpaa, A. Keenan, P. Kuusiniemi, M. Leino, M. Muikku, P. Nieminen, P. Rahkila, J. Uusitalo, K. Eskola, A. Hurstel, M. Huyse, Y. Le Coz, M. B. Smith, P. Van Duppen, and R. Wyss, "*In-beam γ-ray spectroscopy of ^{190}Po: First observation of a low-lying prolate band in Po isotopes.*", *Eur.Phys.J. A* **17** (2003) 167.

[50] D. R. Wiseman, A. N. Andreyev, R. D. Page, M. B. Smith, I. G. Darby, S. Eeckhaudt, T. Grahn, P. T. Greenlees, P. Jones, R. Julin, S. Juutinen, H. Kettunen, M. Leino, A. P. Leppanen, M. Nyman, J. Pakarinen, P. Rahkila, M. Sandzelius, J. Saren, C. Scholey, and J. Uusitalo, "*In-beam gamma-ray spectroscopy of ^{190,197}Po.*", *Eur.Phys.J. A* **34** (2007) 275.

[51] K. Van de Vel, A. N. Andreyev, D. Ackermann, H. J. Boardman, P. Cagarda, J. Gerl, F. P. Hessberger, S. Hofmann, M. Huyse, D. Karlgren, I. Kojouharov, M. Leino, B. Lommel, G. Munzenberg, C. Moore, R. D. Page, S. Saro, P. van Duppen, and R. Wyss, "*Fine structure in a α decay of ^{188,192}Po.*", *Phys.Rev. C* **68** (2003) 054311.

[52] J. Pakarinen, I. G. Darby, S. Eeckhaudt, T. Enqvist, T. Grahn, P. T. Greenlees, V. Hellemans, K. Heyde, F. Johnston-Theasby, P. Jones, R. Julin, S. Juutinen, H. Kettunen, M. Leino, A. P. Leppanen, P. Nieminen, M. Nyman, R. D. Page, P. M. Raddon, P. Rahkila, C. Scholey, J. Uusitalo, and R. Wadsworth, "*Evidence for oblate structure in ^{186}Pb.*", *Phys.Rev. C* **72** (2005) 011304.

[53] J. Pakarinen, V. Hellemans, R. Julin, S. Juutinen, K. Heyde, P. H. Heenen, M. Bender, I. G. Darby, S. Eeckhaudt, T. Enqvist, T. Grahn, P. T. Greenlees, F. Johnston-Theasby, P. Jones, H. Kettunen, M. Leino, A. P. Leppanen, P. Nieminen, M. Nyman, R. D. Page, P. M. Raddon, P. Rahkila, C. Scholey, J. Uusitalo, and R. Wadsworth, "*Investigation of nuclear collectivity in the neutron mid-shell nucleus ^{186}Pb.*", *Phys.Rev. C* **75** (2007) 014302.

[54] R. B. E. Taylor, S. J. Freeman, J. L. Durell, M. J. Leddy, S. D. Robinson, B. J. Varley, J. F. C. Cocks, K. Helariutta, P. Jones, R. Julin, S. Juutinen, H. Kankaanpää, A. Kanto, H. Kettunen, P. Kuusiniemi, M. Leino, M. Muikku, P. Rahkila, A. Savelius, and P. T.

Greenlees, "γ *Decay of Excited States in* ^{198}*Rn Identified using Correlated Radioactive Decay.*", *Phys.Rev. C* **59** (1999) 673.

[55] K. Andgren, B. Cederwall, J. Uusitalo, A. N. Andreyev, S. J. Freeman, P. T. Greenlees, B. Hadinia, U. Jakobsson, A. Johnson, P. M. Jones, D. T. Joss, S. Juutinen, R. Julin, S. Ketelhut, A. Khaplanov, M. Leino, M. Nyman, R. D. Page, P. Rahkila, M. Sandzelius, P. Sapple, J. Saren, C. Scholey, J. Simpson, J. Sorri, J. Thomson, and R. Wyss, "*Excited states in the neutron-deficient nuclei* ^{197,199,201}*Rn.*", *Phys.Rev. C* **77** (2008) 054303.

[56] D. J. Dobson, S. J. Freeman, P. T. Greenlees, A. N. Qadir, S. Juutinen, J. L. Durell, T. Enqvist, P. Jones, R. Julin, A. Keenan, H. Kettunen, P. Kuusiniemi, M. Leino, P. Nieminen, P. Rahkila, S. D. Robinson, J. Uusitalo, and B. J. Varley, "*Low-lying structure of light radon isotopes.*", *Phys. Rev. C* **66** (2002) 064321.

[57] J. F. C. Cocks and the JUROSPHERE Collaboration, "γ*-Ray Spectroscopy of Neutron-Deficient Ra Isotopes.*", *J.Phys.(London) G* **25** (1999) 839.

[58] J. J. Ressler, C. W. Beausang, H. Ai, H. Amro, M. Babilon, J. A. Caggiano, R. F. Casten, G. Gurdal, A. Heinz, R. O. Hughes, E. A. McCutchan, D. A. Meyer, C. Plettner, J. Qian, M. J. S. Sciacchitano, N. J. Thomas, E. Williams, and N. V. Zamfir, "*Isomeric decay of* ^{208}*Ra.*", *Phys.Rev. C* **71** (2005) 014302.

[59] J. J. Ressler, C. W. Beausang, H. Ai, H. Amro, M. A. Caprio, R. F. Casten, A. A. Hecht, S. D. Langdown, E. A. McCutchan, D. A. Meyer, P. H. Regan, M. J. S. Sciacchitano, A. Yamamoto, and N. V. Zamfir, "*Isomer decay tagging in the heavy nuclei:* ^{210}*Ra and* ^{209}*Ra.*", *Phys.Rev. C* **69** (2004) 034331.

[60] F. P. Hessberger, S. Hofmann, I. Kojouharov, and D. Ackermann, "*Decay properties of isomeric states in radium isotopes close to* $N = 126$*.*", *Eur.Phys.J. A* **22** (2004) 253.

[61] P. Van Duppen and M. Huyse, "*Shape coexistence around the Z=82 closed shell probed by* α*-decay.*", *Hyperfine Interactions* **129** (2000) 149.

[62] A. N. Andreyev, M. Huyse, P. Van Duppen, L. Weissman, D. Ackermann, J. Gerl, F. P. Hessberger, S. Hofmann, A. Kleinbohl, G. Munzenberg, S. Reshitko, C. Schlegel, H. Schaffner, P. Cagarda, M. Matos, S. Saro, A. Keenan, C. J. Moore, C. D. O'Leary, R. D. Page, M. J. Taylor, H. Kettunen, M. Leino, A. Lavrentiev, R. Wyss, and

K. Heyde, "*The Discovery of a Prolate-Spherical Shape Triple of Spin 0^+ States in the Atomic Nucleus ^{186}Pb.*", *Nucl.Phys.* **A682** (2001) 482.

[63] K. Van de Vel, A. N. Andreyev, M. Huyse, P. Van Duppen, J. F. C. Cocks, O. Dorvaux, P. T. Greenlees, K. Helariutta, P. Jones, R. Julin, S. Juutinen, H. Kettunen, P. Kuusiniemi, M. Leino, M. Muikku, P. Nieminen, K. Eskola, and R. Wyss, "*Identification of Low-Lying Proton-Based Intruder States in $^{189-193}Pb$.*", *Phys.Rev.* **C65** (2002) 064301.

[64] K. Van de Vel, A. N. Andreyev, D. Ackermann, H. J. Boardman, P. Cagarda, J. Gerl, F. P. Hessberger, S. Hofmann, M. Huyse, D. Karlgren, I. Kojouharov, M. Leino, B. Lommel, G. Munzenberg, C. Moore, R. D. Page, S. Saro, P. van Duppen, and R. Wyss, "*Fine structure in a α decay of $^{188,192}Po$.*", *Phys.Rev. C* **68** (2003) 054311.

[65] A. N. Andreyev, S. Antalic, M. Huyse, P. Van Duppen, D. Ackermann, L. Bianco, D. M. Cullen, I. G. Darby, S. Franchoo, S. Heinz, F. P. Hessberger, S. Hofmann, I. Kojouharov, B. Kindler, A. P. Leppanen, B. Lommel, R. Mann, G. Munzenberg, J. Pakarinen, R. D. Page, J. J. Ressler, S. Saro, B. Streicher, B. Sulignano, J. Thomson, and R. Wyss, "*α decay of the new isotopes $^{193,194}Rn$.*", *Phys.Rev.C* **74** (2006) 064303.

[66] A. N. Andreyev, S. Antalic, D. Ackermann, T. E. Cocolios, V. F. Comas, J. Elseviers, S. Franchoo, S. Heinz, J. A. Heredia, F. P. Hessberger, S. Hofmann, M. Huyse, J. Khuyagbaatar, I. Kojouharov, B. Kindler, B. Lommel, R. Mann, R. D. Page, S. Rinta-Antilla, P. J. Sapple, S. Saro, P. Van Duppen, M. Venhart, and H. V. Watkins, "*α decay of $^{180,181}Pb$.*", *Phys.Rev. C* **80** (2009) 054322.

[67] H. Kettunen, J. Uusitalo, M. Leino, P. Jones, K. Eskola, P. T. Greenlees, K. Helariutta, R. Julin, S. Juutinen, H. Kankaanpää, P. Kuusiniemi, M. Muikku, P. Nieminen, and P. Rahkila, "*α decay studies of the nuclides ^{195}Rn and ^{196}Rn.*", *Phys. Rev. C* **63** (2001) 044315.

[68] J. Uusitalo, S. Eeckhaudt, T. Enqvist, K. Eskola, T. Grahn, P. T. Greenlees, P. Jones, R. Julin, S. Juutinen, H. Kettunen, P. Kuusiniemi, M. Leino, A. P. Leppanen, P. Nieminen, M. Nyman, J. Pakarinen, P. Rahkila, and C. Scholey, "*Alpha-decay studies using the JYFL gas-filled recoil separator RITU.*", *Eur.Phys.J. A* **25** (2005) Supplement 1, 179.

[69] Y. Le Coz, F. Becker, H. Kankaanpaa, W. Korten, E. Mergel, P. A. Butler, J. F. C. Cocks, O. Dorvaux, D. Hawcroft, K. Helariutta, R. D.

Herzberg, M. Houry, H. Hubel, P. Jones, R. Julin, S. Juutinen, H. Kettunen, P. Kuusiniemi, M. Leino, R. Lucas, M. Muikku, P. Nieminen, P. Rahkila, D. Rossbach, A. Savelius, and C. Theisen, "*Evidence of Multiple Shape-Coexistence in* ^{188}*Pb.*", *EPJdirect* **1** (1999) A3, 1–6.

[70] C. W. Beausang, S. A. Forbes, P. Fallon, P. J. Nolan, P. J. Twin, J. N. Mo, J. C. Lisle, M. A. Bentley, J. Simpson, F. A. Beck, D. Curien, G. deFrance, G. Duchêne, and D. Popescu, "*Measurements on prototype Ge and BGO detectors for the Eurogam array.*", *Nucl.Instrum.Methods Phys.Res. A* **313** (1992) 37 – 49.

[71] C. Rossi Alvarez, "*The GASP Array.*", *Nuclear Physics News* **3** (1993) .

[72] F. Beck, "*EUROBALL: Large gamma ray spectrometers through european collaborations.*", *Progress in Particle and Nuclear Physics* **28** (1992) 443.

[73] J. Pakarinen. PhD thesis, University of Jyväskylä, 2005.

[74] G. Duchêne, F. A. Beck, P. J. Twin, G. de France, D. Curien, L. Han, C. W. Beausang, M. A. Bentley, P. J. Nolan, and J. Simpson, "*The Clover: a new generation of composite Ge detectors.*", *Nucl.Instrum.Methods Phys.Res. A* **432** (1999) 90 – 110.

[75] H. Kankaanpää, P. Butler, P. Greenlees, J. Bastin, R. Herzberg, R. Humphreys, G. Jones, P. Jones, R. Julin, A. Keenan, H. Kettunen, M. Leino, L. Miettinen, T. Page, P. Rahkila, C. Scholey, and J. Uusitalo, "*In-beam electron spectrometer used in conjunction with a gas-filled recoil separator.*", *Nucl.Instrum.Methods Phys.Res. A* **534** (2004) 503.

[76] M. Leino, J. Aysto, T. Enqvist, P. Heikkinen, A. Jokinen, M. Nurmia, A. Ostrowski, W. H. Trzaska, J. Uusitalo, K. Eskola, P. Armbruster, and V. Ninov, "*Gas-Filled Recoil Separator for Studies of Heavy Elements.*", *Nucl.Instrum.Methods Phys.Res. B* **99** (1995) 653.

[77] J. Sarén *et al.* to be submitted to Nucl.Instrum.Methods Phys.Res.

[78] R. D. Page, A. N. Andreyev, D. E. Appelbe, P. A. Butler, S. J. Freeman, P. T. Greenlees, R. D. Herzberg, D. G. Jenkins, G. D. Jones, P. Jones, D. T. Joss, R. Julin, H. Kettunen, M. Leino, P. Rahkila, P. H. Regan, J. Simpson, J. Uusitalo, S. M. Vincent, and R. Wadsworth, "*The GREAT spectrometer.*", *Nucl.Instrum.Methods Phys.Res. B* **204** (2003) 634 – 637.

[79] I. Lazarus, E. Appelbe, P. Butler, P. Coleman-Smith, J. Cresswell, S. Freeman, R. Herzberg, I. Hibbert, D. Joss, S. Letts, R. Page, V. Pucknell, P. Regan, J. Sampson, J. Simpson, J. Thornhill, and R. Wadsworth, "*The GREAT triggerless total data readout method.*", *IEEE Trans. Nucl. Sci.* **48** (2001) 567–569.

[80] L. Arnold, R. Baumann, E. Chambit, M. Filliger, C. Fuchs, C. Kieber, D. Klein, P. Medina, C. Parisel, M. Richer, C. Santos, and C. Weber, "*TNT digital pulse processor.*", *IEEE Trans. Nucl. Sci.* **53** (2006) 723.

[81] K. H. Schmidt, R. S. Simon, J. G. Keller, F. P. Hessberger, G. Munzenberg, B. Quint, H. G. Clerc, W. Schwab, U. Gollerthan, and C. C. Sahm, "*Gamma-Spectroscopic Investigations in the Radiative Fusion Reaction* $^{90}Zr + {}^{90}Zr$.", *Phys.Lett.* **B168** (1986) 39.

[82] R. S. Simon, K. H. Schmidt, F. P. Hessberger, S. Hlavac, M. Honusek, G. Munzenberg, H. G. Clerc, U. Gollerthan, and W. Schwab, "*Evidence for Nuclear Shape Coexistence in* ^{180}Hg.", *Z.Phys. A* **325** (1986) 197.

[83] E. S. Paul, P. J. Woods, T. Davinson, R. D. Page, P. J. Sellin, C. W. Beausang, R. M. Clark, R. A. Cunningham, S. A. Forbes, D. B. Fossan, A. Gizon, J. Gizon, K. Hauschild, I. M. Hibbert, A. N. James, D. R. LaFosse, I. Lazarus, H. Schnare, J. Simpson, R. Wadsworth, and M. P. Waring, "*In-Beam* γ*-Ray Spectroscopy Above* ^{100}Sn *using the New Technique of Recoil Decay Tagging.*", *Phys.Rev. C* **51** (1995) 78.

[84] "Jaida - java implementation of aida." Http://java.freehep.org/jaida/.

[85] "Aida - abstract interfaces for data analysis." Http://aida.freehep.org/.

[86] "Root - data analysis framework." Http://root.cern.ch/.

[87] J. F. C. Cocks, M. Muikku, W. Korten, R. Wadsworth, S. Chmel, J. Domscheit, P. T. Greenlees, K. Helariutta, I. Hibbert, M. Houry, D. Jenkins, P. Jones, R. Julin, S. Juutinen, H. Kankaanpaa, H. Kettunen, P. Kuusiniemi, M. Leino, Y. Le Coz, R. Lucas, E. Mergel, R. D. Page, A. Savelius, and W. Trzaska, "*First Observation of Excited States in* ^{184}Pb*: Spectroscopy beyond the neutron mid-shell.*", *Eur.Phys.J. A* **3** (1998) 17.

[88] D. G. Jenkins, M. Muikku, P. T. Greenlees, K. Hauschild, K. Helariutta, P. M. Jones, R. Julin, S. Juutinen, H. Kankaanpaa, N. S. Kelsall, H. Kettunen, P. Kuusiniemi, M. Leino, C. J. Moore, P. Nieminen, C. D. O'Leary, R. D. Page, P. Rakhila, W. Reviol, M. J. Taylor, J. Uusitalo, and R. Wadsworth, "*First Observation of Excited States in* ^{182}Pb.", *Phys.Rev.* **C62** (2000) 021302.

[89] G. Audi, A. H. Wapstra, and C. Thibault, "*The 2003 atomic mass evaluation: (II). Tables, graphs and references.*", *Nuclear Physics A* **729** (2003) 337.

[90] K. S. Toth, J. C. Batchelder, D. M. Moltz, and J. D. Robertson, "*Identification of* ^{180}*Pb.*", *Z.Phys.* **A355** (1996) 225.

[91] K. S. Toth, C. R. Bingham, J. C. Batchelder, L. T. Brown, L. F. Conticchio, C. N. Davids, R. J. Irvine, D. Seweryniak, D. M. Moltz, W. B. Walters, J. Wauters, and E. F. Zganjar, "α*-Decay Rates of* ^{180,182,184}*Pb and the* $Z = 82$ *Shell Closure.*", *Phys.Rev.* **C60** (1999) 011302.

[92] M. Bender. Priv. comm., 2009.

[93] R. R. Rodríguez-Guzmán. Priv. comm., 2009.

[94] J. G. Keller, K. H. Schmidt, F. P. Hessberger, G. Munzenberg, W. Reisdorf, H. G. Clerc, and C. C. Sahm, "*Cold Fusion in Symmetric* ^{90}*Zr-Induced Reactions.*", *Nucl.Phys.* **A452** (1986) 173.

[95] A. N. Andreyev, S. Antalic, D. Ackermann, T. E. Cocolios, V. F. Comas, J. Elseviers, S. Franchoo, S. Heinz, J. A. Heredia, F. P. Hessberger, S. Hofmann, M. Huyse, J. Khuyagbaatar, I. Kojouharov, B. Kindler, B. Lommel, R. Mann, R. D. Page, S. Rinta-Antila, P. J. Sapple, S. Saro, P. Van Duppen, M. Venhart, and H. V. Watkins, "*The new isotope* ^{179}*Pb and* α*-decay properties of* ^{179}*Tl*^{m}.", *J.Phys.(London)* **G37** (2010) 035102.

[96] K. H. Schmidt, C. C. Sahm, K. Pielenz, and H. G. Clerc, "*Some Remarks on the Error Analysis in the Case of Poor Statistics.*", *Z.Phys.* **A316** (1984) 19.

[97] K. H. Schmidt, "*A New Test for Random Events of an Exponential Distribution.*", *Eur.Phys.J. A* **8** (2000) 141.

[98] J. Pakarinen. Priv. comm., 2009.

[99] G. D. Dracoulis, G. J. Lane, A. P. Byrne, A. M. Baxter, T. Kibedi, A. O. Macchiavelli, P. Fallon, and R. M. Clark, "*Isomer bands, E0 transitions, and mixing due to shape coexistence in* $^{188}_{82}Pb_{106}$.", *Phys.Rev. C* **67** (2003) 051301.

[100] A. Dewald, R. Peusquens, B. Saha, P. von Brentano, A. Fitzler, T. Klug, I. Wiedenhöver, M. Carpenter, A. Heinz, R. V. F. Janssens, F. G. Kondev, C. J. Lister, D. Seweryniak, K. Abu Saleem, R. Krücken,

J. R. Cooper, C. J. Barton, K. Zyromski, C. W. Beausang, Z. Wang, P. Petkov, A. M. Oros-Peusquens, U. Garg, and S. Zhu, "*Recoil-gated plunger lifetime measurements in* ^{188}Pb.", *Phys. Rev. C* **68** (2003) 034314.

[101] R. G. Thomas, "*An Analysis of the Energy Levels of the Mirror Nuclei,* $C13$ *and* $N13$.", *Phys. Rev.* **88** (1952) 1109.

[102] J. B. Ehrman, "*On the Displacement of Corresponding Energy Levels of* $C13$ *and* $N13$.", *Phys. Rev.* **81** (1951) 412.

[103] P.-H. Heenen. Priv. comm., 2009.

[104] W. Younes, J. A. Cizewski, H. Q. Jin, L. A. Bernstein, D. P. McNabb, C. N. Davids, R. V. F. Janssens, T. L. Khoo, C. J. Lister, D. J. Blumenthal, M. P. Carpenter, D. Henderson, R. G. Henry, T. Lauritsen, D. T. Nisius, H. T. Penttila, and M. W. Drigert, "*Spectroscopy of* ^{194}Po.", *Phys.Rev.* **C52** (1995) R1723.

[105] K. Helariutta, T. Enqvist, P. Jones, R. Julin, S. Juutinen, P. Jämsen, H. Kankaanpää, P. Kuusiniemi, M. Leino, M. Muikku, M. Piiparinen, A. Savelius, W. H. Trzaska, S. Törmänen, J. Uusitalo, R. G. Allatt, P. A. Butler, P. T. Greenlees, and R. D. Page, "*First Observation of Excited States in* ^{192}Po.", *Phys.Rev. C* **54** (1996) R2799.

[106] K. Helariutta, J. F. C. Cocks, T. Enqvist, P. T. Greenlees, P. Jones, R. Julin, S. Juutinen, P. Jämsen, H. Kankaanpää, H. Kettunen, P. Kuusiniemi, M. Leino, M. Muikku, M. Piiparinen, P. Rahkila, A. Savelius, W. H. Trzaska, S. Törmänen, J. Uusitalo, R. G. Allatt, P. A. Butler, R. D. Page, and M. Kapusta, "*Gamma-Ray Spectroscopy of* $^{192-195}Po$.", *Eur.Phys.J. A* **6** (1999) 289.

[107] H. Kettunen. PhD thesis, University of Jyväskylä, 2003.

[108] P. Jones. PhD thesis, University of Liverpool, 1995.

[109] P. Rahkila http://npg.dl.ac.uk/GREAT/Panu/index.html (2001).

[110] T. Kibédi, T. Burrows, M. Trzhaskovskaya, P. Davidson, and C. N. Jr., "*Evaluation of theoretical conversion coefficients using BrIcc.*", *Nucl.Instrum.Methods Phys.Res. A* **589** (2008) 202.

[111] D. C. Radford, "*ESCL8R and LEVIT8R: Software for interactive graphical analysis of HPGe coincidence data sets.*", *Nucl.Instrum.Methods Phys.Res. A* **361** (1995) 297.

[112] K. Hauschild, A. Lopez-Martens, A. V. Yeremin, O. Dorvaux, A. V. Belozerov, M. L. Chelnokov, V. I. Chepigin, B. Gall, V. A. Gorshkov, M. Guttormsen, P. Jones, A. P. Kabachenko, A. Khouaja, A. C. Larsen, O. N. Malyshev, A. Minkova, H. T. Nyhus, Y. T. Oganessian, D. Pantelica, A. G. Popeko, F. Rotaru, S. Saro, A. V. Shutov, S. Siem, A. I. Svirikhin, and N. U. H. Syed, "*Half-life and excitation energy of the $I^{\pi} = 13 / 2^{+}$ isomer in ^{209}Ra.*", *Phys.Rev. C* **77** (2008) 047305.

[113] F. P. Hessberger, S. Hofmann, G. Munzenberg, A. B. Quint, K. Summerer, and P. Armbruster, "*Observation of Two New Alpha Emitters with Z = 88.*", *Europhys.Lett.* **3** (1987) 895.

[114] T. Kohno, M. Adachi, S. Fukuda, M. Taya, M. Fukuda, H. Taketani, Y. Gono, M. Sugawara, and Y. Ishikawa, "*Level Structure and Electromagnetic Properties in ^{212}Ra.*", *Phys.Rev. C* **33** (1986) 392.

[115] A. E. Stuchbery, G. D. Dracoulis, T. Kibedi, A. P. Byrne, B. Fabricius, A. R. Poletti, G. J. Lane, and A. M. Baxter, "*Spectroscopy and Shell Model Interpretation of High-Spin States in the N = 126 Nucleus ^{214}Ra.*", *Nucl.Phys.* **A548** (1992) 159.

[116] T. Lönnroth. University of jyväskylä department of physics research report no. 4/1981, 1981.

[117] J. R. Novak, C. W. Beausang, N. Amzal, R. F. Casten, G. Cata Danil, J. F. C. Cocks, J. R. Cooper, P. T. Greenlees, F. Hannachi, K. Helariutta, P. Jones, R. Julin, S. Juutinen, H. Kankaanpaa, H. Kettunen, R. Krucken, P. Kuusiniemi, M. Leino, B. Liu, M. Muikku, A. Savelius, T. Socci, J. T. Thomas, N. V. Zamfir, J. Y. Zhang, and S. Frauendorf, "*High-Spin States in ^{205}Rn: A new shears band structure ?.*", *Phys.Rev.* **C59** (1999) R2989.

[118] D. J. Hartley, E. P. Seyfried, W. Reviol, D. G. Sarantites, C. J. Chiara, O. L. Pechenaya, K. Hauschild, A. Lopez-Martens, M. P. Carpenter, R. V. F. Janssens, D. Seweryniak, and S. Zhu, "*Possible shears bands in ^{204}At and ^{206}Fr, and identification of excited states in $^{205,207}Fr$.*", *Phys.Rev. C* **78** (2008) 054319.

[119] M. Leino, J. Uusitalo, R. G. Allatt, P. Armbruster, T. Enqvist, K. Eskola, S. Hofmann, S. Hurskanen, A. Jokinen, V. Ninov, R. D. Page, and W. H. Trzaska, "*Alpha Decay Studies of Neutron-Deficient Radium Isotopes.*", *Z.Phys. A* **355** (1996) 157.

[120] L. Currie, "*Limits for qualitative detection and quantitative determination. Application to radiochemistry.*", *Anal.Chem.* **40** (1968) 586.

[121] L.-E. De Geer, "*Currie detection limits in gamma-ray spectroscopy,.*", *Applied Radiation and Isotopes* **61** (2004) 151.

[122] J. C. Batchelder, K. S. Toth, M. W. Rowe, T. N. Ginter, K. E. Gregorich, V. E. Ninov, F. Q. Guo, J. Powell, X.-J. Xu, and J. Cerny, "*Evidence for the Identification of* ^{178}*Pb.*", in *PROTON-EMITTING NUCLEI: Second International Symposium PROCON 2003*, E. Maglione and F. Soramel, eds., vol. 681, p. 144. AIP Conf. Proc., 2003.

[123] A. N. Andreyev, D. Ackermann, S. Antalic, I. G. Darby, S. Franchoo, F. P. Hessberger, S. Hofmann, M. Huyse, P. Kuusiniemi, B. Lommel, B. Kindler, R. Mann, G. Munzenberg, R. D. Page, S. Saro, B. Sulignano, B. Streicher, K. Van de Vel, P. Van Duppen, and D. R. Wiseman, "*Cross section systematics for the lightest Bi and Po nuclei produced in complete fusion reactions with heavy ions.*", *Phys.Rev. C* **72** (2005) 014612.

[124] Y. H. Pu, K. Morita, M. G. Hies, K. O. Lee, A. Yoshida, T. Nomura, Y. Tagaya, T. Motobayashi, M. Kurokawa, H. Minemura, T. Uchibori, T. Ariga, K. Sueki, and S. A. Shin, "*New* α*-Decaying Neutron-Deficient Isotope* ^{196}*Rn.*", *Z.Phys.* **A357** (1997) 1.

[125] A. Andreyev. Priv. comm., 2007.

[126] M. Leino, J. Uusitalo, R. G. Allatt, P. Armbruster, T. Enqvist, K. Eskola, S. Hofmann, S. Hurskanen, A. Jokinen, V. Ninov, R. D. Page, and W. H. Trzaska, "*Alpha Decay Studies of Neutron-Deficient Radium Isotopes.*", *Z.Phys.* **A355** (1996) 157.

[127] J. Uusitalo, M. Leino, T. Enqvist, K. Eskola, T. Grahn, P. T. Greenlees, P. Jones, R. Julin, S. Juutinen, A. Keenan, H. Kettunen, H. Koivisto, P. Kuusiniemi, A. P. Leppanen, P. Nieminen, J. Pakarinen, P. Rahkila, and C. Scholey, "α *decay studies of very neutron-deficient francium and radium isotopes.*", *Phys.Rev. C* **71** (2005) 024306.

[128] A. Robinson, P. Rahkila, *et al.* Is465 (isolde proposal), evolution of nuclear shape in the light radon isotopes, 2009.

[129] B. Bastin *et al.* Is479 (isolde proposal) shape coexistence measurements in even-even neutron-deficient polonium isotopes by coulomb excitation, using rex-isolde and the ge miniball array., 2009.

[130] T. Grahn, J. Pakarinen, *et al.* Is494 (isolde proposal) measurements of competing structures in neutron-deficient pb isotopes by employing coulomb excitation, 2009.

[131] P. Papadakis, R.-D. Herzberg, J. Pakarinen, P. A. Butler, P. J. Coleman-Smith, J. R. Cresswell, P. T. Greenlees, P. Jones, R. Julin, I. H. Lazarus, S. C. Letts, R. D. Page, E. Parr, P. Peura, V. F. E. Pucknell, P. Rahkila, D. A. Seddon, J. Simpson, J. Sorri, J. Thornhill, and D. Wells, "*Towards combining in-beam gamma-ray and conversion electron spectroscopy.*", in *CAPTURE GAMMA-RAY SPECTROSCOPY AND RELATED TOPICS: Proceedings of the 13th International Symposium on Capture Gamma-Ray Spectroscopy and Related Topics*, J. Jolie, A. Zilges, N. Warr, and A. Blazhev, eds., vol. 1090, p. 14. AIP Conf. Proc., 2009.

[132] J. Pakarinen, A. N. Andreyev, R. Julin, S. Juutinen, S. Antalic, L. Bianco, I. G. Darby, S. Eeckhaudt, T. Grahn, P. T. Greenlees, D. G. Jenkins, P. Jones, P. Joshi, H. Kettunen, M. Leino, A. P. Leppänen, P. Nieminen, M. Nyman, R. D. Page, J. Perkowski, P. M. Raddon, P. Rahkila, D. Rostron, J. Saren, C. Scholey, J. Sorri, and B. Streicher, "*Evidence for prolate structure in light Pb isotopes from in-beam γ-ray spectroscopy of Pb*185.", *Phys. Rev. C* **80** (2009) 031303.